Applied Geochemistry 84 (2017) 387–432

Contents lists available at ScienceDirect

Applied Geochemistry

journal homepage: www.elsevier.com/locate/apgeochem

Invited Review

Molybdenum in natural waters: A review of occurrence, distributions and controls

Pauline L. Smedley [a, *], David G. Kinniburgh [b]

[a] British Geological Survey, Keyworth, Nottinghamshire, NG12 5GG, UK
[b] Formerly British Geological Survey, Wallingford, Oxfordshire, OX10 8BB, UK

ARTICLE INFO

Article history:
Received 3 January 2017
Received in revised form
29 April 2017
Accepted 2 May 2017
Available online 6 May 2017

Editorial handling by Prof. M. Kersten

Keywords:
Groundwater
Redox
Sorption
Molybdate
Anoxia
Speciation

ABSTRACT

Molybdenum is an essential trace element for human, animal and plant health and has played an important part in the evolution of life on earth. Nonetheless, exposure to the element can be harmful and although the evidence for symptoms in humans is sparse, it has been linked with a number of health conditions in animal models. Molybdenum is present in trace quantities (1–10 mg/kg) in most rocks and soils and at concentrations less than, and often orders of magnitude less than, 10 μg/L in most freshwaters. It is the most abundant transition metal in open seawater (10 μg Mo/L) owing to the dominance, and low chemical reactivity, of the molybdate ion (MoO_4^{2-}).

The 2011 WHO Guidelines for Drinking-Water Quality (fourth edition) advised a health-based value of 70 μg/L for Mo but this is no longer promulgated as a formal guideline value as WHO consider such concentrations to be rarely found in drinking water. This is indeed usually the case, but there are instances where currently-used drinking waters do exceed 70 μg Mo/L. We therefore recommend more routine measurement of Mo in water, at least on a reconnaissance scale, in order to improve knowledge on occurrence in water used for potable supply. Where multi-element analytical procedures are already used (e.g. ICP-MS), the marginal cost of adding Mo to the list of elements to be analysed should not be great.

We have reviewed nine areas in the world where high concentrations of Mo in freshwater, and in some cases drinking water, have been found: Argentina, Jordan, Qatar, Ethiopia, UK, USA (three) and Chile. These represent a range of geochemical environments. A common theme of the high-Mo occurrences is (i) oxic, alkaline conditions where, as for seawater, the Mo occurs as the stable molybdate ion; groundwater in oxic, alkaline conditions within volcanogenic sediments can have exceptionally high Mo concentrations (up to hundreds of μg/L) where felsic volcanic ash is present; (ii) anoxic, non-sulphidic waters where Mo can be released to solution by reductive dissolution of Mn and Fe oxides or by release from degradation of organic matter, notably within high-Mo organic-rich muds, black shales or oil shales; or (iii) surface waters or groundwater impacted by metal sulphide mining and/or mineralisation, in particular occurrences of porphyry deposits. Under such conditions, Mo concentrations can reach several tens to several hundreds of μg/L and while not all are otherwise suitable for drinking water, some are.

Much of the basic geochemistry of Mo in oxic natural environments is now quite well understood. Critically, its behaviour is redox-sensitive like its near neighbours in the Periodic Table, W and V. At the near-neutral pH values characteristic of most natural waters, Mo is rather weakly sorbed and formation of Mo minerals is either not indicated or is extremely slow. Molybdenum becomes less mobile when converted to thiomolybdates under the strongly reducing conditions found in some present-day ocean basins (e.g. the Black Sea), fjords, stratified lakes and confined aquifers. This leads to concentrations of around 100 mg Mo/kg or more in black shales and other organic-rich mudstones. However, despite the many studies of these water bodies and the importance of Mo as a palaeoredox indicator, the mechanism of the highly-efficient and diagnostic scavenging of Mo in euxinic (H_2S-rich) waters remains uncertain. Possibilities include the formation of an as yet unidentified Mo-Fe-S mineral or solid solution, or the scavenging by some pre-existing solid such as a sulphide or oxide mineral, or organic matter. The possible role of dispersed and reduced natural organic matter has become more prominent in recent

* Corresponding author.
E-mail address: pls@bgs.ac.uk (P.L. Smedley).

http://dx.doi.org/10.1016/j.apgeochem.2017.05.008

years but this has proven difficult to quantify and the mechanism of binding is poorly understood. Molybdenum isotope studies now play an important role in constraining reaction pathways.

At a more fundamental level, there is a lack of up-to-date thermodynamic and kinetic data for many of the reactions of importance for Mo in the natural environment and this limits the ability of current geochemical models to predict its fate and transport. This is particularly true for the strongly reducing conditions where Mo partitions to the solid phase, leading to the formation of the Mo-rich shales. Even the existence of reduced aqueous Mo species (e.g. in the Mo(V) and Mo(III) oxidation states) in natural waters is uncertain. These uncertainties will only be resolved with focused laboratory experiments using the benefits of modern instrumentation, combined where necessary with supporting molecular dynamics calculations.

The mobility of Mo in aqueous systems has to date received far more attention in the marine than the freshwater setting. The value of Mo speciation as an indicator of redox conditions and of stable-isotopic variations as a tracer, can have more value in the arena of environment and health, and studies of the element's mobility in aqueous systems can be useful for themes varying from radioactive waste disposal, sustainability of unconventional hydrocarbon exploitation and wider surficial pollution.

Contents

1. Introduction

Molybdenum is an essential trace element for human, animal and plant health. It acts as a cofactor for the functioning of a large number of enzymes which catalyse chemical reactions involved in the cycling of N, C, and S (Mendel, 2007; Schwarz et al., 2009). Yet, as with all elements, exposure to high doses of Mo can be detrimental to plant and animal health, including human health (Gupta, 1997; WHO, 2011a). In the context of environmental distributions of Mo, a large literature exists on speciation and mobility in oceanic systems as the element's strong redox control and associated isotopic fractionation are of value in investigating the early Earth's oxygenation, the extent of oceanic anoxic events and their implication for the evolution of life. Rather less attention has been paid to the distributions of Mo in freshwater systems in the context of water supply, environment and human health.

Molybdenum is a transition metal with atomic number 42 and atomic weight of 95.94 g/mol. Estimates of its crustal abundance have been put at around 1.5 mg/kg (Taylor, 1964) or less. Wedepohl (1995) gave an estimate of 1.4 mg/kg for the upper crust and 0.6 mg/kg for the lower crust, although a smaller upper crustal estimate of 0.6 mg/kg has also been given (Hu and Gao, 2008). Molybdenum occurs with coordination numbers from 4 to 8 and in formal oxidation states from -II to VI, although IV, V and VI are the most important in the environment. The variable oxidation states enable Mo to participate in a large number of redox reactions and help explain its crucial evolutionary inclusion in various cofactors. It is strongly chalcophile (sulphur-loving) and has many properties similar to tungsten and vanadium. It occurs naturally in minerals, rocks and soils as well as in aqueous form. It does not occur naturally as the free metal.

There are seven naturally-occurring stable isotopes: ^{92}Mo, ^{94}Mo, ^{95}Mo, ^{96}Mo, ^{97}Mo, ^{98}Mo and ^{100}Mo, the most abundant being ^{98}Mo (24%). As a result of the large mass range (8%) and fairly uniform abundance, combined with advances in instrumentation, many of these can now be resolved. This has led to a new understanding of the role of Mo in the natural environment. ^{99}Mo is also a significant fission product ($t_{½}$ = 66 h) and is used extensively in nuclear medicine to produce ^{99m}Tc for imaging.

Molybdenum is used as a lubricant additive, catalyst, corrosion inhibitor, and component in the manufacture of tungsten, pigments and ceramics. It is a component of steel alloys and welding rods and is added to cast iron and stainless steel for hardness control (Morrison et al., 2006). Historically, molybdenum compounds have been used widely for colorimetric testing in analytical chemistry. Molybdenum is distributed in the environment through industrial and agricultural contamination, for example as a result of fossil-fuel combustion, leaching from fly ash and mobilisation from mine wastes (Morrison and Spangler, 1992; Zhang and Reardon, 2003). It is also used in agriculture to counteract Mo deficiency in crops (WHO, 2011a).

This review focuses on the occurrence and distributions of Mo in natural fresh water (surface water and groundwater) and its environmental, health and water-supply implications. It also draws on the large literature on elemental and isotopic compositions observed in marine systems and explored in palaeoredox studies (Anbar, 2004; Kendall et al., 2017).

In the literature, conventional units for quoting concentrations vary. In freshwaters, units for Mo concentrations tend to be given in μg/L whereas in seawater, concentrations are normally given in μM, and in geochemical modelling, units tend to be in mol/L (M) or mol/kg water (molal). In the text and tables that follow, we have tended to adopt the conventional units and not attempted to convert units to a common format unless direct comparisons between fresh and saline water are being made; 1 μM is approximately 100 μg/L.

2. Molybdenum and its role in human, animal and plant health

2.1. Importance in the evolution of life and the earth's atmosphere

The slow build-up of O_2 in the atmosphere and surface ocean water accelerated about 2.5 Ga ago (the Great Oxygenation Event) and led to the oxidation of pyrite minerals on continents and an increased flux of Mo and U to the oceans (Anbar et al., 2007; Scott et al., 2008). The oxygenation of the deep oceans increased rapidly at the onset of the Phanerozoic about 542 Ma ago and as a result, Mo concentrations increased sharply and consistently to today's levels (Lyons et al., 2014).

It is widely thought that Mo was critical to the early evolution of life in the oceans and that the low concentrations of dissolved Mo in the early anoxic and sulphidic oceans (Parnell and Lindgren, 2016; Scott et al., 2008) delayed evolution during the Mesoproterozoic (1.6–1.0 Ga ago). Recent evidence suggests that this barrier to evolution may not have existed close to continental margins and in freshwater lakes (Parnell et al., 2015). The evolution of the highly-efficient Mo-containing coenzyme, nitrogenase ($N_2(g) \rightarrow NH_3$), enabled a more rapid synthesis of amino acids which in turn led to the faster growth of photosynthetic organisms and eventually a rapid rise of oxygen in the ancient atmosphere and surface waters (Wang, 2012). The earliest nitrogen-fixing bacteria evolved under anoxic conditions, possibly using an Fe-based nitrogenase, but later evolved to be effective under more oxidising conditions (Anbar and Knoll, 2002). This change to an oxic environment also led to a reduction in the concentration of reduced sulphur species and instability of highly insoluble Mo-S-containing minerals, leading to higher dissolved concentrations of Mo. New Mo uptake and storage systems also evolved to make use of the abundant nitrate and sulphate that was present and these persist today in terms of nitrate assimilation facilitated by the Mo-containing enzyme, nitrate reductase ($NO_3^- \rightarrow NO_2^-$), and sulphur detoxification via sulphite oxidase ($SO_3^- \rightarrow SO_4^{2-}$) (George et al., 1989; Hille, 1996).

Molybdenum is biologically inactive unless complexed as a cofactor. It is a cofactor in more than 60 enzymes (Stiefel, 1977,

1996) and it is the redox switching of Mo in these enzymes that plays a fundamental role in global cycling of C, N and S. This role has probably been inherited from the element's long and significant association with the evolution of Earth's atmosphere.

2.2. Human health

Molybdenum is recognised as an essential trace element for human health, with adults having an estimated daily requirement in the range 75–250 μg (National Academy of Sciences, 1989). Four mammalian Mo-dependent enzymes are known, all of them involving a pterin-based Mo cofactor (Moco) in their active site. Sulphite oxidase, xanthine oxidase, aldehyde oxidase and mitochondrial amidoxime-reducing component (mARC) all play roles in human metabolic function. In these enzymes, Mo switches between the two oxidation states, Mo(IV) and Mo(VI). A deficiency of these Mocos in humans has been linked to neurological abnormalities and early childhood death (Food and Nutrition Board, and Institute of Medicine, 2001; Wahl et al., 2010).

High doses of Mo can also be harmful, though evidence of symptoms in humans is limited. The United States Food & Nutrition Board, Institute of Medicine tolerable upper intake level of Mo for adults is given as 2 mg/day (infants 1–3 years: 0.3 mg/day) (Food and Nutrition Board, and Institute of Medicine , 2001)). WHO have given a NOAEL (no observed adverse effect level) of 200 μg/L on the basis of two-year exposure of populations to drinking water at that level. Acute exposure to Mo has been linked to diarrhoea, anaemia and gout, while chronic occupational exposure has been linked to weakness, fatigue, lack of appetite, anorexia, liver dysfunction, joint pain, osteoporosis and tremor (WHO, 2011a). Pneumoconiosis has also been associated with Mo-induced copper deficiency (Expert Group on Vitamins and Minerals, 2003; WHO, 2011a). The toxicity of Mo is a function of its physical and chemical state, the route of exposure, the individual's background health and dietary copper and sulphur concentrations (Expert Group on Vitamins and Minerals, 2003; WHO, 2011a).

No national or international drinking-water standards exist for Mo. The 1993 WHO Guidelines for Drinking-Water Quality (second edition) introduced a health-based guideline value for Mo in drinking water of 70 μg/L, being a third the value of the NOAEL and based on the evidence for health effects from chronic exposure, including animal studies. This value was retained in the third edition of the Guidelines. The 2011 fourth edition continued to advise a health-based value of 70 μg/L (WHO, 2011b), consistent with the toxicological evidence and the essential daily requirement for Mo (Expert Group on Vitamins and Minerals, 2003; WHO, 2011b). However, WHO no longer promulgates a formal guideline value for Mo as they consider such concentrations to be rarely found in drinking water.

The US-EPA's current Lifetime Advisory Level for Mo in drinking water is 40 μg/L. In 2006, the Wisconsin Department of Natural Resources (DNR) adopted a groundwater quality enforcement standard for Mo of 40 μg/L, based on the US-EPA's Advisory Level. This Advisory is currently being reassessed, but on the basis of the available health evidence, the Wisconsin Department of Health Services (DHS) has recommended an interim health advisory level of 90 μg/L in drinking water. This is a concentration that the DHS believe would not result in increased risk of adverse health effects if used at this concentration for a lifetime.

2.3. Animal health

Ruminants are particularly vulnerable to Mo exposure and can suffer from both low and high intakes of Mo. Most animal studies have been carried out on this group. Deficiency has some recognised health consequences: in goats, Mo deficiency has been linked to reduced fertility and increased mortality (Expert Group on Vitamins and Minerals, 2003). However, a larger literature exists on the health impacts of Mo excess. Interaction of Mo with sulphur produced in the rumen results in the formation of thiomolybdates (Clarke and Laurie, 1980; Gould and Kendall, 2011). Tetrathiomolybdate forms two remarkably stable complexes with Cu, namely $Cu_2(HS)_2MoS_4^{2-}$ and $Cu_2S_2MoS_4^{4-}$ as well as a solid, NH_4CuMoS_4 (Helz and Erickson, 2011). These inhibit Cu absorption and the activity of Cu-dependent enzymes and indicate why the Cu/Mo mole ratio in ruminant feed should exceed 2 (Suttle, 1991). Symptoms of molybdenosis (or 'teart') are similar to those of copper deficiency (Shen et al., 2006; Suttle, 1991) and include anaemia, anorexia, diarrhoea, joint abnormalities, osteoporosis and hair discoloration (Expert Group on Vitamins and Minerals, 2003).

Molybdenum-induced copper deficiency in dairy cattle has been reported in the San Joaquin Valley of California, USA (Bradford et al., 1990). In sheep, copper deficiency leads to the neurological condition, swayback. This has long been recognised in the UK, particularly in parts of Somerset and Derbyshire (Thornton and Webb, 1979). Molybdenum-induced copper deficiency in grazing animals in the UK has been found in areas with Mo-enriched soils (Leech and Thornton, 1987).

Shen et al. (2006) described symptoms of a similar condition known as 'shakeback' disease in yaks from the Qing Hai-Tibetan Plateau. Symptoms included emaciation, unsteadiness, shivering backs and reduced appetite (though not hair discoloration). Many of these symptoms are consistent with Mo-induced Cu deficiency. Although the mean Mo content of the soils of the affected area was only 4.85 ± 0.21 mg/kg (dry weight), the mean Cu/Mo ratio in forage was 1.34 ± 0.36 compared to 8.12 ± 1.31 in control areas.

Animal studies using rabbits, rats and mice have also linked high intakes of dietary Mo with weight loss, anorexia, premature deaths and reduced fertility (Expert Group on Vitamins and Minerals, 2003; WHO, 2011a). The toxic effects were seen with administration of Mo(VI) but not with reduced Mo as molybdenite, presumably reflecting the relative bioavailability.

2.4. Plant health and nutrition

The importance of Mo as a micronutrient in plants has been recognised for a long time (Hewitt, 1956). The Mo-dependent enzymes nitrogenase and nitrate reductase catalyse nitrogen fixation and nitrate reduction reactions respectively (Burgess and Lowe, 1996; Hille, 1996; Stiefel, 1996; Wang, 2012). Molybdenum deficiency is most closely associated with legume crops. These are able to fix atmospheric N_2 as biologically available NH_3 in a reaction involving root-nodule *Rhizobium* bacteria, catalysed by nitrogenase. However, both legume and non-legume crops require Mo-bearing nitrate reductase for reduction of nitrate (Adams, 1997). Molybdenum is also important for sulphur metabolism in plants since the oxidation of sulphite to sulphate uses the molybdoenzyme sulphite oxidase. A blue Mo-anthocyanin compound has been suggested to be present in brassicas and may play a role in protecting the plants from Mo toxicity (Hale et al., 2001).

Molybdenum deficiency in plants was first recognised in Australia. As Mo deficiency prevents fixation of N_2, symptoms can be similar to those associated with nitrogen deficiency. Deficiency symptoms include injury to leaves and growing points, though observations vary between plant species (Gupta, 1997). Deficiency may be corrected by application of Mo fertilisers as foliar feeds, or molybdenised P or NPK fertilisers, or by seed treatment with Mo and *Rhizobium* inoculation (Mortvedt, 1997).

Molybdenum toxicity is less common, but has been recorded, at least in laboratory conditions. The most notable manifestation is

yellow-orange chlorosis, with brown tints on young leaves (Gupta, 1997).

The availability of Mo for plant health is a function of both abundance and mobility in soils. Controlling factors include soil pH, amount and crystallinity of metal oxides, and organic matter content. An association has also been found between Mo mobility and waterlogged soils (Gupta, 1997). Molybdenum deficiency is most often associated with acidic soils and sandy soils are more prone than loam or clay soils. Here, deficiency may be due to either smaller quantities of Mo, or more strongly bound Mo, or a combination of the two. Molybdenum mobility is greater in alkaline soils due to reduced binding of molybdate to soil surfaces in alkaline conditions. Molybdenum deficiency may therefore also be treated by liming soil.

3. Analysis for molybdenum

3.1. Water analysis and chemical speciation

Early analyses of Mo in natural waters were usually by colorimetric methods, notably following complexation of reduced Mo with phosphate or more commonly with thiocyanate (Table 1). More precise measurement of the red-orange thiocyanate complex can be obtained by UV-VIS spectrophotometry and a preconcentration step with *iso*-amyl alcohol extraction. This extraction step also removed interferences from tungsten. These methods are not very sensitive, typically having detection limits of a few μg/L. Coprecipitation with manganese dioxide or extracting with a Chelex-100 resin or polyurethane foam column (Ferreira et al., 2003) can also be used to pre-concentrate. If an ionic liquid such as 1-methyl-3-octadecyl-imidazolium bromide (C18mimBr) is used, then a detection limit at the low μg/L level is possible without the need for a solvent extraction step (Pelit et al., 2013).

A variety of instrumental methods has become available with greater sensitivity and these are now commonly used (Table 1). ICP-MS, perhaps following some form of extraction, has the benefit of offering high sensitivity as well as multi-element capability at minimal marginal cost. If a chromatographic column is added to the front, speciation with sensitivity at the ng/L level is possible (Luong et al., 1997). A variety of voltammetric methods are also being developed (Pelit et al., 2013) but are not yet widely used. Other new methods look promising. The catalytic effect of Mo on the oxidation of iodide by hydrogen peroxide to produce iodine which then etches gold nanorods to give a blue-red-coloured solution has recently been developed (Z. Zhang et al., 2015). This method has nM sensitivity and could in principle lead to development of a field-test kit for water testing in areas of suspected high Mo concentrations.

Specialist techniques also exist for specific situations. For example, in-situ determination of sediment porewater Mo concentrations can be obtained by the diffusive gradients in thin films (DGT) technique (Guan et al., 2015; Panther et al., 2013; Shiva et al., 2016) (Fig. 1a). This enables multi-element porewater profiles to be determined. A ZrO_2- or TiO_2-based (Metsorb) sorbent is used to sorb the Mo.

Unlike As and thioarsenate species, the thiomolybdates cannot be measured directly by anion exchange chromatography followed by ICP-MS because they are so strongly retained by the column. However, reverse-phase ion-pair chromatography can resolve the thiomolybdates and opens the potential for their determination with an RP-IPC/ICP-MS system (Vorlicek et al., 2015).

The redox speciation of dissolved Mo is not undertaken routinely but Wang et al. (2009) have developed a method to separate Mo(V) and Mo(VI) by solid-phase separation of the Mo(V)-tartrate complex on a XAD 7HP resin followed by elution with acidic acetone. The method relies on the quantitative separation of the two Mo oxidation states by the resin and does not appear to have been tested thoroughly against synthetic mixtures with known proportions of Mo(V) and Mo(VI).

3.2. Rocks, sediments and soils

Das et al. (2007) have reviewed many methods for the analysis of Mo in rocks, sediments and soils, including the necessary sample extraction and pre-treatment. In many cases, the analytical methods are similar to those for aqueous samples following a pre-treatment to partially or totally dissolve the Mo (Table 2). Fusion of rock samples with sodium hydroxide under oxidising conditions can be used for 'total' analyses. This may be followed by further complexation with dithiol and extraction with an organic solvent. Sometimes the Mo is separated with a Chelex-100 resin to minimise interferences. Microwave-assisted digestion in a pressurised vessel can also be used to aid dissolution. HF is necessary for the total dissolution of silicate rocks.

It is also possible to use non-destructive XRF techniques which do not involve any dissolution (Fig. 1b). This can be done in a variety of ways from a hand-scanner, a semi-automated cm-scale core scanner, a portable bench-top scanner or a fully automated laboratory bench-top system using fused discs. The detection limit with the best of these can be a few mg/kg.

3.3. Molybdenum isotopes

The advent of thermal ionisation mass spectrometry (TIMS) and since the late 1990s, multi-collector inductively coupled plasma mass spectrometry (MC-ICP-MS), have enabled the small but significant natural variation of Mo isotopes to be measured with high precision (Anbar, 2004; Kendall et al., 2017; Wieser et al., 2007; Worsham et al., 2016). Precision on the δ^{98}Mo (^{98}Mo/^{95}Mo) isotopic ratio is typically <0.1‰ (Nägler et al., 2014).

The small fractionation of heavy elements such as Mo means that care has to be taken to minimise analytical artefacts, especially matrix effects (Pietruszka et al., 2006). This usually involves some form of preliminary chemical separation of the Mo (Nagai and Yokoyama, 2014), especially from Fe and Mn. These otherwise produce polyatomic interferences in the mass range 94–97 (Kendall et al., 2017). Separation, often by ion exchange, has to be near-quantitative since some ion-exchange separation processes (notably those involving anion exchange) can themselves lead to isotopic fractionation. Typically, the separation involves both an anion and cation exchange process. Bracketing with standards and spiking with a different element is often used (Anbar, 2004). Double spiking with two Mo isotopes, e.g. ^{97}Mo-^{100}Mo (Siebert et al., 2015), is one of the best ways of correcting for instrumental and mass-dependent fractionation.

Of the seven naturally-occurring isotopes of Mo, ^{95}Mo, ^{97}Mo and ^{98}Mo are most commonly investigated in geochemical studies. These have been reported as the ^{97}Mo/^{95}Mo and/or ^{98}Mo/^{95}Mo mass ratios, although the latter has become more standard (conversion from the former to the latter is achieved by multiplying by 3/2 assuming linear fractionation). The δ^{98}Mo ratio is now the most commonly cited ratio (Anbar and Gordon, 2008; Kendall et al., 2011; Goldberg et al., 2013).

In the developing years of the Mo isotopic technique, there was no internationally-agreed reference standard, although the NIST SRM 3134 standard Mo solution has commonly been used as a *de facto* reference. This lack of unified standard for normalisation has

Table 1
Chemical analysis of molybdenum in aqueous media.

Method[a]	Detection Limit (μg/L)	Usage	Reference
ICP-AES	2	Multi-element	WHO (2011a)
GF-AAS	Not given	Older method, small quantities	WHO (2011a)
ICP-MS	0.06	Multi-element, sensitive, also isotopes	Glass et al. (2013)
UV-VIS spectrophotometry	5	Pre-concentrate with thiocyanate method with tartrate and *iso*-amyl alcohol extraction	Chapelle et al. (1979), p. 95
Pre-concentrate/flame AAS	5	Pre-concentrate with thiocyanate/tartrate and *iso*-amyl alcohol extraction then asprirate	Chapelle et al. (1979), p. 98
GF-AAS	0.072	Uses L'vov platform for atomization	Barałkiewicz and Siepak (1997)
Solid phase (foam) extraction followed by GF-AAS	0.08	Sorption of Mo-SCN complex onto foam followed by GF-AAS of eluted sample	Ferreira et al. (2003)
Solid phase (XAD-7HP) extraction followed by GF-AAS	0.02	Mo(V) and Mo(VI) separation in seawater and other natural waters. However, efficiency of separation not yet adequately demonstrated.	Wang et al. (2009, 2011)
ICP-AES with pre-concentration on activated charcoal	0.4	Mo in steam waters and seawater	Hall et al. (1988)
UV-VIS spectrophotometry	0.04	Based on the effect of Mo(VI) on the kinetics of oxidation of 4-amino-3-hydroxy-naphthalene sulfonic acid (AHNA) by H2O2	Mansouri et al. (2011)
UV-VIS spectrophotometry	20	Complex Mo with 5,7-dibromo-8-hydroxyquinoline (DBHQ). Mo(V) can be masked with tartrate enabling Mo(VI)/Mo(V) speciation.	Ahmed and Haque (2002)
RP-IPC/UV-VIS spectrophotometry	Not given	Molybdate and thiomolybdates with a Dionex system	Vorlicek et al. (2015)
Liquid-liquid extraction/ UV-VIS spectrophotometry	Not given	Complexation with thiocyanate (SCN-) followed by solvent and/or resin extraction	Ghiasvand et al. (2005)
RLS	0.013	Uses influence of Mo in decreasing RLS signal from dibromohydroxyphenylfluorone (DBHPF)-Triton X-100	Chen et al. (2008)
ASV	0.06	Useful dynamic range 0.1–20 μg/L	Ensafi (2002)
Differential pulse polarography	0.2	Used to measure Mo in nitrate growth media	Edmonds (1980)

[a] AAS = atomic absorption spectrometry; ASV = anodic stripping voltammetry; GF-AAS = graphite furnace atomic absorption spectrometry; ICP-AES=Inductively-coupled plasma-atomic emission spectrometry; ICP-MS = inductively coupled plasma-mass spectrometry; RLS = Resonance light scattering; RP-IPC = reverse-phase ion-pair chromatography.

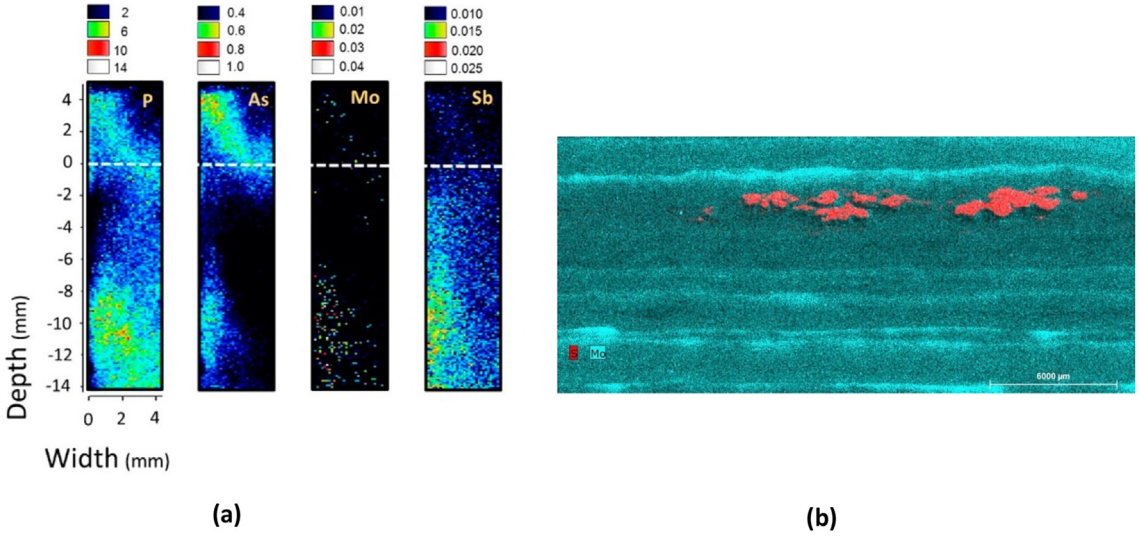

Fig. 1. High-resolution imaging of Mo distributions in the solution and solid phases. (a) 2-dimensional profiles of DGT (diffusive gradient in thin films) fluxes of P, As, Mo and Sb across the sediment-water interface (white dashed line). The legend above each profile gives the flux scale in pg/cm^2/s. Note the high correlation between Mo and P fluxes; (b) an XRF map of Stoer Group black shale showing distributions of Mo and S. Sulphur (red) is restricted to clusters of pyrite. Mo (cyan) occurs in the pyrite alongside S, but is also present in laminae possibly containing organic matter. The total width of the view is 27 mm (from Parnell et al., 2015, Supplementary Data, with permission). (a) is reprinted with permission from Guan et al. (2015): Copyright (2015) American Chemical Society.

been a drawback when comparing datasets from different laboratories, especially as the increased precision of measurements over time has shown significant differences between nominally similar in-house reference materials (Kendall et al., 2017). Nägler et al. (2014) proposed to set the δ^{98}Mo NIST SRM 3134 standard to +0.25‰ so that the canonical values for open seawater of +2.3‰ and for marine Fe-Mn nodules of −0.7‰ could be retained.

Table 2
Chemical analysis of molybdenum in rocks, sediments and soils.

Material	Method[a]	Detection limit (mg/kg)	Comment	Reference
Rock	XRF	3–11	XRF either by hand-held scanner in the field or a mechanised lab-based system. Can also examine whole rock surfaces. Only penetrates the surface by a mm or so.	Dahl et al. (2013b) Wirth et al. (2013)
Soils	XRF	0.2	Wavelength dispersive XRF	Rawlins et al. (2012)
Rocks, minerals	SIMS/EMPA/WDS	<5	Electron microprobe microanalysis based on solid material. Can be rasterised to get an element map	Misch et al. (2016)
Rocks, minerals, soils, sediments	ICP-AES	0.2	First dissolve. Concentrated on activated charcoal. Large dynamic range. Multi-element. Serious Fe and Al interferences necessitate separation. Being superseded by ICP-MS	Hall et al. (1987)
Rocks, minerals, soils, sediments	ICP-MS	not given	First dissolve. Now the most popular approach since multi-elemental analysis possible as well as isotopic determination	e.g. Wirth et al. (2013)
Rocks, minerals, soils, sediments	AAS	0.009–2.2	HF-electrothermal AAS with mild microwave heating and direct introduction of slurry	Campillo et al. (2002)
Rocks, minerals, soils, sediments	UV-VIS spectrophotometry	0.1	First dissolve. Complex with 5,7-dibromo-8-hydroxyquinoline (DBHQ)	Ahmed and Haque (2002)

[a] Abbreviations as in Table 1 except: XRF = X-ray fluorescence; SIMS = secondary-ion mass spectrometry; EMPA = electron microprobe analysis; WDS = wavelength dispersive spectrometry.

4. Distributions in minerals, rocks, sediments and soils

4.1. Minerals

Molybdenum does not occur naturally in its native state but forms minerals in combination with other elements. As a result of its chalcophile behaviour, the principal ore mineral of Mo is molybdenite (MoS_2), a silvery black Mo(IV) mineral. Molybdenite can be produced at high temperatures in the presence of S-bearing solutions but is resistant to formation from aqueous solutions containing Mo(VI) at temperatures below 300 °C (Chappaz et al., 2008; Helz et al., 1996). The δ^{98}Mo of molybdenites (range −1.62 to 2.27‰) cannot be used to distinguish the type of source deposit or its age but can provide some indication of the temperature of formation with the isotopically lightest molybdenites tending to be formed at the highest temperature (Breillat et al., 2016). The mineral is found in some granites (Breillat et al., 2016; e.g. Parnell and Lindgren, 2016) and in association with other trace elements (W, Re, Cu, Sn, Ag, Au, Zn, U, Se V, F) in ore mineralised zones. It does not form in sedimentary diagenesis (Bostick et al., 2003; Dahl et al., 2013a). The layered structure, low coefficient of friction, and stability at high temperatures are responsible for the use of molybdenite as an industrial lubricant. Most of the world's Mo is present in porphyry Cu deposits although there are some notable disseminated porphyry molybdenum deposits, e.g. at Questa (NM), and Henderson and Climax (CO), USA.

Ore minerals undergoing weathering can produce secondary metal molybdates including wulfenite ($PbMoO_4$), ferrimolybdite ($Fe_2(MoO_4)_3.nH_2O$), powellite ($CaMoO_4$), ilsemannite ("molybdenum blue", $Mo_3O_8.nH_2O$), lindgrenite ($Cu_3(MoO_4)_2(OH)_2$) and jordisite (MoS_2) (Table 3). Molybdates are soft and brittle and commonly occur in association with chemically similar tungstate minerals. Secondary Mo-bearing minerals also include limonite ($FeOOH.nH_2O$) and jarosite ($KFe_3(SO_4)_2(OH)_6$). Wulfenite and powellite have been observed to precipitate readily in column experiments simulating mine waste conditions in the presence of Pb and Ca respectively (Conlan et al., 2012). Powellite has also been observed as an authigenic mineral, infilling void spaces and coating grains in aquifer matrices (Pichler and Mozaffari, 2015).

Rutile can contain relatively high concentrations of Mo and this has been implicated in controlling the Mo budget of subducting slabs and arc magmatism. Wilkinson (2015) found contents of 0.8–57.5 mg/kg in rutile from Norwegian eclogites (Table 4).

Many secondary minerals contain Mo either in solid solution or adsorbed to the mineral surfaces. It is often difficult to define the state of Mo in these minerals unambiguously. Helz et al. (2011) proposed that the near-constant concentration of Mo with depth in Rogoznica Lake, Croatia, was consistent with equilibration with a 'new' mineral having the formula, $Fe_5Mo_3S_{14}$. This mineral, or solid solution, has been suggested to account for the distribution of Mo in euxinic basins such as the Black Sea (Helz et al., 2011) and estuarine waters of the Mississippi (Mohajerin et al., 2016).

As will be discussed in detail in Section 6.2.2, Mo is strongly sorbed by many oxide minerals, notably by oxides of Al, Fe and Mn. This accounts for the large contents of Mo found in oxide-rich sediments such as hydrothermal Mn crusts. Goto et al. (2015) reported contents greater than 550 mg/kg in Mn crusts derived from modern hydrothermal vents from a volcanic arc, and Kuhn et al. (2003) reported contents up to nearly 2000 mg/kg in hydrothermal Mn-rich crusts in an active intraoceanic back-arc basin setting (Table 4). The Mo is probably derived from hydrothermal fluids emanating from the associated volcanic rocks rather than from the seawater. This view is supported by the coordination of Mo in the crusts: the Mo tends to be in octahedral coordination suggesting a slightly acidic source (Kuhn et al., 2003) rather than the tetrahedral coordination characteristic of Mo in neutral and alkaline solutions such as seawater (Goto et al., 2015).

Mo-enriched manganese oxides are also found in sulphidic oceanic conditions (Brumsack, 2006). The strong affinity with Mn also explains the relationship between the oxide content of soils and their Mo content (Siebert et al., 2006; Vistoso et al., 2012; Xu et al., 2013). Reductive dissolution of Mn and Fe oxides can release adsorbed Mo and other co-adsorbed elements back into solution (Bennett and Dudas, 2003; Mohajerin et al., 2016; Shimmield and Price, 1986; Smedley and Kinniburgh, 2002). Mo sorbed to $Al(OH)_3$-type minerals is not sensitive to reductive dissolution/desorption.

Molybdenum is found in smaller proportions in feldspars, olivine, biotite, amphibole and magnetite-ilmenite (Voegelin et al., 2014) (Table 4). Calcium carbonate does not adsorb Mo strongly (Goldberg et al., 1996).

4.2. Organic matter

Evidence for the role of organic matter in binding Mo under natural conditions is mostly circumstantial and somewhat controversial. Chappaz et al. (2014) showed that less than 20% of the Mo in nine representative sediment and black shale samples was present in pyrite megacrysts and speculated that the bulk of the remaining matrix Mo was 'non-pyrite' (though it would have included any

Table 3
Molybdenum minerals.

Mineral	Formula	Typical colour	Occurrence
Molybdite	MoO_3	Yellow-green	Secondary, weathering of molybdenite
Ilsemannite	$Mo_3O_8.nH_2O$	Dark green, blue	Secondary, weathering of molybdenite
Molybdenite	MoS_2	Black	Primary high-temperature hydrothermal ore; granites
Jordisite	MoS_2	Black, blue grey	Moderate to low-T hydrothermal
Powellite	$CaMoO_4$	Yellowish brown, blue, green yellow	Contact-metamosomatic, secondary oxidation and authigenic mineral
Wulfenite	$PbMoO_4$	Orange-yellow	Secondary oxidised sulphide minerals, mine wastes. Also with variable W as chillagite
Ferrimolybdite	$Fe_2(MoO_4)_3.7–8H_2O$	Yellow to green	Secondary, weathering of Mo-bearing sulphides
Ferrous molybdate	$FeMoO_4$	Light brown	Secondary, soluble
Manganous molybdate	$MnMoO_4$	Yellow, brown	Secondary, soluble
Lindgrenite	$Cu_3(MoO_4)_2(OH)_2$	Green	Secondary, weathering of sulphide minerals

Table 4
Molybdenum contents of rock-forming minerals.

Mineral	Average (range) mg/kg	Number of analyses	Reference
Pyrite	116 (25–185)	9	Harrison et al. (1973)
ASK-3 Pyrite (SRM)	40		Harrison et al. (1973)
Pyrite, Torridonian black shale	Up to 1000		Parnell et al. (2015)
Pyrite, Cariaco Basin, Venezuela	1100 (891–1239)	3	Chappaz et al. (2014)
Pyrite, Proterozoic Doushantuo Formation, South China	268 (101–473)	18	Li et al. (2010)
Pyrite, Mesozoic Posidonia Shale, Germany	91 (24–250)	22	Chappaz et al. (2014)
Pyrite, Transvaal Supergroup, South Africa	1.86 (0.1–4.9)	24	Ono et al. (2009)
Pyrite, Mount McRae Shale,W. Australia	16 (1–72)	26	Anbar et al. (2007)
Pyrite, black shale	15^m (0.01–5000)	1407	Gregory et al. (2015)
Pyrite, black shale (Cenozoic)	897^m	48	Gregory et al. (2015)
Pyrite, black shale (Neoarchaean)	1.2^m	220	Gregory et al. (2015)
Pyrite, limestone aquifer, FL, USA	<100		Pichler and Mozaffari (2015)
Hydrothermal Mn crusts	667 (115–1548)	14	Kuhn et al. (2003)
Rutile	0.84–57.5		Wilkinson (2015)
Olivine	0.11 (0.07–0.17)	10	Voegelin et al. (2014)
Orthopyroxene	0.29 (0.15–0.44)	9	Voegelin et al. (2014)
Clinopyroxene	0.12 (0.05–0.26)	12	Voegelin et al. (2014)
Biotite	0.67 (0.5–0.95)	10	Voegelin et al. (2014)
Hornblende	0.25 (0.15–0.38)	7	Voegelin et al. (2014)
K feldspar	<0.11	1	Voegelin et al. (2014)
Plagioclase	<0.01	10	Voegelin et al. (2014)
Aragonite/calcite, biologically precipitated	0.04 (0.004–0.12)	15	Voegelin et al. (2009)

SRM: standard reference material; m: median.

very fine-grained pyrite, <10 μm diameter). They pointed out the notable co-variation between Mo and TOC (total organic carbon) in both their samples and in sediments examined in other studies (Algeo and Lyons, 2006; Anbar et al., 2007; Chappaz et al., 2014; Marks et al., 2015; McManus et al., 2006) and inferred some direct, but undefined, involvement of organic matter in the fixation of Mo. Molybdenum has even been suggested as a useful proxy for original organic matter content in sediments (Wilde et al., 2004). Parnell et al. (2015) also noted from XRF mapping of Mo and S in a Stoer Group shale, UK, that some of the Mo appeared to be associated with organic-rich laminae rather than with large amounts of S associated with pyrite crystals (Fig. 1b).

Goodman and Cheshire (1982) demonstrated by EPR that humic material can partially reduce Mo(VI) to Mo(V) and even Mo(III), although such reduction is probably dependent on the overall redox status of the environment from which the organics are derived and is certainly not universal (Gustafsson and Tiberg, 2015). The release of sorbed Mo when organic matter oxidises could be a major source of dissolved Mo in some pore waters (Contreras et al., 1978).

4.3. Rocks

4.3.1. Igneous and metamorphic rocks

The average upper crustal content of Mo is around 0.6–1.5 mg/kg (Hu and Gao, 2008; Taylor, 1964). Igneous and metamorphic rocks have contents in the same range, with average abundance around 1–2 mg/kg. In igneous rocks, Mo contents tend to increase slightly with fractional crystallisation from basaltic to rhyolitic composition on account of the incompatibility of the element in melts (J. Yang et al., 2015). Contents of acidic igneous rocks tend to be in the 2–5 mg/kg range (Table 5).

Molybdenum contents of metamorphic rocks are likely to depend on the lithology of the precursors as well as metamorphic grade. Contents in eclogites (high metamorphic grade with basaltic precursors) have been found in the range 0.189–1.76 mg/kg (Wilkinson, 2015). Crystalline gneisses also have typically small contents of <1 mg/kg (Table 5). Enrichments of Mo can occur in skarns, especially in the contact zones between granitoid bodies and carbonate country rocks, which can be a focus for Mo-bearing hydrothermal assemblages.

4.3.2. Sedimentary rocks

The Mo content of sedimentary rocks depends on lithology and mineralogy and is strongly associated with redox conditions at the time of formation. Abundance is higher in shales and muds than in sandstones and carbonates. Oxic sediments can be relatively enriched where Mn oxides are present. Largest contents are typically found in sediments enriched in organic carbon and sulphur, where syn-sedimentary conditions were euxinic.

Table 5
Molybdenum contents of rocks, sediments and soils.

Rock type	Average (range) mg/kg	Number of analyses	Reference
Continental crust			
Upper continental crust	1.5		Taylor (1964)
Upper continental crust	1.4		Wedepohl (1995)
Upper continental crust	0.6		Hu and Gao (2008)
Lower continental crust	0.6		Wedepohl (1995)
Igneous/metamorphic rocks			
Olivine basalt, Greece	0.83		Voegelin et al. (2014)
Basalt	1.0		BGS (2006); Rahaman et al. (2010); Yang et al. (2015a,b)
Basalt, Massif Central, France	3.6 (2.3–7.7)	12	Voegelin et al. (2012)
Basalt, Mariana Arc	0.79 (0.40–1.3)	19	Freymuth et al. (2015)
Basalt, BHVO-2 (SRM)	3	1	Yang et al. (2015a,b)
Basalt, Iceland	1.3–1.5	6	Yang et al. (2015a,b)
Basaltic andesite, Iceland	2.4–2.7	8	Yang et al. (2015a,b)
Andesite, Iceland	2.7–3.2	3	Yang et al. (2015a,b)
Andesite, Greece	2.57		Voegelin et al. (2014)
Dacite, Greece	4.07		Voegelin et al. (2014)
Dacite, Iceland	3.9	4	Yang et al. (2015a,b)
Rhyolite, Iceland	4.6	2	Yang et al. (2015a,b)
Rhyolite, Iceland	4		Arnórsson and Oskarsson (2007)
Rhyolite, Hekla, Iceland	4.6		Yang et al. (2015a,b)
Rhyolite, Ethiopia	4.58 (0.93–8.69)	10	Rango et al. (2013)
Rhyolitic ash, Argentina	2–6		Smedley et al. (2002)
Granodiorite, GSP-2 (SRM)	2.1	1	Yang et al. (2015a,b)
Granodiorite, CA, USA	0.2		Glass et al. (2013)
Granite, Himalaya	12.1–19.1	2	Siebert et al. (2003)
Granite, Massif Central, France	0.36 (0.26–0.47)	5	Voegelin et al. (2012)
Eclogite, Norway	0.75–1.76		Wilkinson (2015)
Orthogneiss, Massif Central, France	0.09 (0.07–0.19)	7	Voegelin et al. (2012)
Gneiss, Switzerland	0.15–0.28	2	Dahl et al. (2010)
Sediments/sedimentary rocks			
Volcanogenic lake sediment, Ethiopian Rift	2.29–904 (136)	3	Rango et al. (2013)
River sediment, Ethiopian Rift	5.33–5.50 (5.41)	2	Rango et al. (2013)
Loess silts, Argentina	<1–5		Smedley et al. (2005, 2002)
Limestone	0.4		BGS (2006)
Carbonate sand, Bahamas	(0.08–0.18)	5	Romaniello et al. (2016)
Organic-rich carbonate mud, Bahamas	1–28	21	Romaniello et al. (2016)
Dolomite, Switzerland	0.32–0.48	2	Dahl et al. (2010)
Phosphorite, north Jordan	10 (0.5–60)	65	Abed et al. (2016)
Antarctic marine sediment	0.79 (0.41–1.3)	21	Waheed et al. (2001)
Turbidite, off south-west France	0.5–1.3	30	Chaillou et al. (2008)
Holocene fluviolacustrine silt-clay-sand, Inner Mongolia, China	<1–5	12	Smedley et al. (2003)
Siltstone, China	5.5 (1.6–8.1)	4	Wen et al. (2015)
Lake sediments, Castle Lake, CA, USA	7–36		Glass et al. (2013)
Walker Lake seds, NV, USA	9.0–63	5	Domagalski et al. (1990)
Mono Lake seds, CA, USA	33–61	2	Domagalski et al. (1990)
Laminated clays, California margin, NE Pacific	1.00–11.7	68	Zheng et al. (2000b)
Marine deposits, Santa Barbara Basin, off CA, USA	0.7–30		Zheng et al. (2000a)
Shale	3		Och et al. (2013)
Shale	33 (32–34)		Das et al. (2007)
Shale, WI, USA	1.1–1.3	2	Lourigan and Phelps (2013)
Japan Sea marginal ocean basin	0.75–24.4	44	Crusius et al. (1996)
Pakistan margin ocean	0.25–2.67	22	Crusius et al. (1996)
Organic-rich shales			
Ancient organic-rich shale	14.4 (1.13–72.3)	43	Asael et al. (2013)
Black shale	27–316		Brumsack (2006)
Black shale, Cariaco Trench	1100 (891–1240)	3	Chappaz et al. (2014)
Black shale, Torridonian, UK	82 (1.6–232)	20	Parnell et al. (2015)
Black shale, Rove Formation, MN, USA	4–52	40	Kendall et al. (2011)
Black shale, China	8.53 (2.03–20.0)	43	Och et al. (2013)
Black shale, China	16.0 (3.8–52)	27	Wen et al. (2015)
Oil shale, western USA	32 (3.1–93)	9	Harrison et al. (1973)
Oil shale, carbonate rich, Jordan	11.7 (0.93–34.7)	12	Al Kuisi et al. (2015)
Oil shale/carbonate, Jordan	60–173	3	Abed et al. (2009)
Organic-rich sediments (compilation)	6.2^{m} (0.009–496)	187	Dahl et al. (2013b)
Organic-rich mudrock, Three Gorges, China	138 (25–663)	48	Kendall et al. (2015)
Organic rich mud, Tarfaya Basin, off West Africa	6.6 (0.71–30.9)	70	Goldberg et al. (2016)
Organic-rich sediment, Black Sea	33–66		Emerson and Huested (1991)
Euxinic sediment, Black Sea	18.0–44.5	9	Crusius et al. (1996)
Surface sediment, Saanich Inlet, Canada	3–126	16	Crusius et al. (1996)
Surface sediment, Saanich Inlet, Canada	4.4–77	5	Berrang and Grill (1974)
Lake sediments, Eastern Canada	0.95–11		Chappaz et al. (2008)
Sediment (0–800 m bsl) from Cariaco Basin, Venezuela	85 (2–187)	39	Lyons et al. (2003)

(*continued on next page*)

Table 5 (*continued*)

Rock type	Average (range) mg/kg	Number of analyses	Reference
Euxinic sediment, Lake Cadagno, Switzerland	100–130	25	Dahl et al. (2010)
Coal	5 (0.1–10)		Blowes et al. (2004)
Stream sediments			
Stream sediments, England & Wales	<0.5–3.6[a]		Imperial College (1978)
Stream sediments, England & Wales	0.40[m] (<0.1–309)	65,447	Smedley et al. (2014a)
Soils			
Soil	1–2		Jarrell et al. (1980)
Soil	0.03–43		Das et al. (2007)
Topsoil, England	2.2 (0.4–43)	6559	BGS (2006)
Soil, Northern Ireland	<0.1–7.6	6937	Smyth (2007)
Soil, Spain	0.80 (0.32–1.2)	5	Campillo et al. (2002)
Soil, USA	1.2 (0.1–40)		Lourigan and Phelps (2013)
Soil, CA, USA	1.3 (0.1–9.6)	50	Bradford et al. (1996)
Soil, CA, USA	0.2–2.2	10	Glass et al. (2013)
Soil, WI, USA	<1–8.5	664	Stensvold (2012)
Contaminated land			
Sewage-sludge amended soil	8.3		Bettinelli et al. (2000)
Soil, Tungsten mines, Jiangxi, China	10.56–103		Huang and Iskandar (1999)
Porphyry copper tailings, various	11.8–235	Avgs	Seal II (2012)
Pyrite waste, Iberian Belt, Spain	148		Sánchez España et al. (2008)

[a] 10–90th percentiles.
[m] median value.

Average shale Mo contents have been estimated from around 1–3 mg/kg (Och et al., 2013) up to 32–34 mg/kg (Das et al., 2007). Black shales with associated organic and sulphur compounds can have higher values still. Scott and Lyons (2012) related the content of Mo in black shales to the free sulphide present at the time of formation. A bimodal distribution was observed, with black shales containing Mo contents of more than 60 mg/kg, and often in the hundreds, forming under euxinic conditions where free H_2S was present in the ocean bottom waters. Molybdenum contents rarely exceeded 20 mg/kg when sulphide was restricted to porewaters. Such Mo-enriched black shales have been used widely as an indicator of past euxinic conditions (Bostick et al., 2003; Tribovillard et al., 2004) and as a tracer of the evolutionary record of the oceans (Wang, 2012).

BGS (1999) reported contents of Mo up to 70 mg/kg in British black shales, while Parnell et al. (2015) found up to 232 mg/kg in Torridonian black shale of Scotland. Here, the Mo was found to be present in association with both pyrite and organic matter. Molybdenum contents up to 663 mg/kg have been found in organic-rich shales from the Doushantuo Formation, South China (Kendall et al., 2015). Contents up to 1240 mg/kg occur in laminated black shales from the Cariaco Trench off Venezuela (Chappaz et al., 2014; Lyons et al., 2003) (Table 5).

The association of Mo enrichment with lignites and organic-rich black shales has been recognised for a long time as partly responsible for the spatial distribution of Mo-induced Cu-deficiency in cattle, e.g. in South Dakota, USA and England (Thomson et al., 1972).

Oil shales and associated deposits also have relatively large Mo contents. Abed et al. (2009) reported Mo in oil-bearing carbonates from Jordan in the range 60–173 mg/kg; Al Kuisi et al. (2015) reported contents in the range 0.93–34.7 mg/kg (mean 11.7 mg/kg) for similar Jordanian oil shales. The Mo in the Jordanian oil-bearing rocks was thought to be mainly associated with organic matter rather than sulphides (Al Kuisi et al., 2015), though distinguishing between the two on the basis of correlations alone is difficult. Harrison et al. (1973) reported Mo contents up to 93 mg/kg (Table 5). The concentration of Mo in crude oil is low, 0.011–1.4 mg/kg oil in 9 samples, with a range in stable-isotope compositions (δ^{98}Mo) similar to that of major rivers (Ventura et al., 2015).

Relatively large Mo contents are also found in ironstones and phosphorites, although such rock types are uncommon. The Mo content of phosphorite from northern Jordan has been reported as 0.5–60 mg/kg (mean 10 mg/kg) (Abed et al., 2016).

In contrast, Mo contents of limestone are typically <1 mg/kg (Table 5). Primary carbonates, such as those from the Bahamas carbonate platform, normally contain <0.2 mg Mo/kg (Romaniello et al., 2016). However, in organic-rich carbonate muds, a range up to 28 mg/kg was found, considered to be sourced from cyanobacterial microbial mats and local terrestrial and aquatic plants. Here, H_2S was concluded to be important in the generation of thiomolybdates with consequent loss to the solid phase (Romaniello et al., 2016).

4.3.3. Unconsolidated sediments

Unconsolidated sediments have similarly variable Mo contents depending on grainsize, mineralogy and mode of formation. As with indurated equivalents, contents are greater in fine-grained and organic-rich and/or sulphide-rich deposits.

Molybdenum contents of cores from the Japan Sea oceanic margin, deposited under oxic conditions, have been recorded in the range 0.75–24.4 mg/kg (Crusius et al., 1996). Highest values were found in horizons bearing Mn oxides. Pakistan ocean margin sediments had a range of 0.25–2.67 mg/kg (Table 5).

Zheng et al. (2000b) reported contents of 1–23.7 mg/kg in fine-grained laminated California margin sediments; Zheng et al. (2000a) found contents up to 30 mg/kg in the Santa Barbara Basin. Goldberg et al. (2016) reported contents in organic-rich muds off West Africa in the range 0.71–30.9 mg/kg. In sulphidic marine sediments, a large number of studies have established that contents can rise substantially higher: values up to 190 mg/kg have been found in the Cariaco Basin, off Venezuela by Lyons et al. (2003); Berrang and Grill (1974) found up to 80 mg/kg in sulphidic sediments from Saanich Inlet off Canada while contents up to 126 mg/kg were found there by Crusius et al. (1996). Emerson and Huested (1991) reported contents up to 66 mg/kg and Crusius et al. (1996) up to 44.5 mg/kg for sulphidic sediments from the Black Sea (Table 5).

Sulphidic lake sediments below the meromictic Lake Cadagno, Switzerland, have Mo contents in the range 100–130 mg/kg; Mo was found to correlate positively with solid-phase organic carbon

and sulphide content, but not with sediment Fe or Mn contents (Dahl et al., 2010).

Long-range atmospheric deposition from smelting and coal combustion can have a significant impact on lake sediment Mo contents: sediments from 3 lacustrine lakes in Quebec, Eastern Canada, were up to 3–16 times higher than their source lithogenic composition (Chappaz et al., 2012, 2008).

Relative enrichment in Mo is also a feature of volcanogenic sediments. For example, Rango et al. (2013) found a range of 2.29–904 mg/kg Mo in Quaternary lacustrine silt, clay, and sand deposits with a component of rhyolitic volcanic ash in the Ethiopian Rift Valley (Table 5).

Stream sediments typically have Mo contents around 10 mg/kg or less, depending on the component mineralogy. In England & Wales, values in the <0.5–3.6 mg/kg (10–90th percentiles) have been reported (Imperial College, 1978). Highest values occur where the stream sediments are derived from Carboniferous argillaceous deposits, including marine black shale. Increased Mo values are also a feature of sediments derived from English Jurassic shales.

From the British Geological Survey's G-BASE (unpublished) dataset of stream sediment samples, Mo analyses from England & Wales have an observed range of <0.1–309 mg/kg (n = 65,447) with a median of 0.4 mg/kg (10th–90th percentile range <0.1–2.9 mg/kg). Of the analysed samples, 99% had Mo contents <10 mg/kg. As with data from Imperial College (1978), relative highs are seen in sediments from Carboniferous black shales. Greater abundance (>20 mg/kg) is also found in sediments derived from granites of south-west Scotland and from Cambro-Ordovician shales and volcanic tuffs in North Wales. Data for 5874 samples of stream sediments in Northern Ireland give a range of 0.1–86 mg/kg with a mean of 1.2 mg/kg (10th–90th percentile range 0.3–6.7 mg/kg) (Lister et al., 2007).

4.3.4. Soils

Non-contaminated soils typically have Mo contents <10 mg/kg. Top soils from the Humber-Trent area of England have Mo contents in the range 0.4–43 mg/kg (6559 samples) with a median of 2.2 mg/kg (BGS, 2006). BGS (2006) noted relatively high median values in soils from the Carboniferous Limestone, Coal Measures and Cretaceous ironstones and clays, and lowest median values in soils on the red-bed Triassic Sherwood Sandstone and Mercia Mudstone, as well as Chalk. Relatively large Mo contents were also found in top soils around the urban centres of northern England (Sheffield, Leeds and Bradford, Sunderland-Newcastle) and can be attributed to inputs from historic coal burning (Rawlins et al., 2012). The median Mo content of 5670 topsoils (0–15 cm depth) systematically sampled from England & Wales was 1.2 mg/kg with a 10th–90th percentile range of 0.62–2.3 mg/kg (Rawlins et al., 2012).

Of 25,673 deep-soil analyses in the British Geological Survey database for Humber-Trent region of England, the observed range in Mo was <0.6–885 mg/kg with a median of 1.4 mg/kg. Highest values were present above the Namurian Millstone Grit, as for top soils. As a general rule, contents are lower in the deeper soils than topsoils. The highest value, 885 mg/kg, was considered to have been contaminated with industrial waste (BGS, 2006).

Soils in Northern Ireland have Mo contents of <0.1–7.6 mg/kg with a mean of 0.97 mg/kg, median of 0.88 mg/kg and a 10th–90th percentile range of 0.29–1.6 mg/kg (n = 6937) (Smyth, 2007).

Anomalous quantities of Mo can be found in soils in industrial and mining/mineralisation settings. In the Deilmann Tailings Management Facility, Saskatchewan, Canada, the Mo in uranium mill tailings was characterised by EXAFS and found to be in the form of $NiMoO_4$ and $CaMoO_4$, as well as molybdate adsorbed onto ferrihydrite (Essilfie-Dughan et al., 2011). Contents up to 103 mg/kg were found in soil close to tungsten mining operations in Jiangxi, China (Huang and Iskandar, 1999) (Table 5).

5. Distributions in aqueous systems

5.1. Rainfall

Sub-μg/L quantities of Mo are expected in rainwater. Neal et al. (1994) reported an average value for Mo in rainwater from Wales of 0.17 μg/L. Agusa et al. (2006) found concentrations of 0.07–0.14 μg/L in rainwater from Hanoi, Vietnam (Table 6). Care should be taken with interpretation of rainwater concentrations because of the commonly significant contribution of particulate matter.

5.2. Seawater and estuaries

While Mo is present in trace quantities in most sediments and soils, it is the most abundant transition metal in the oceans, with a concentration in open (oxic) water of ca. 10 μg/L (or 107 nM) (Table 6). The salinity-normalised concentration is essentially constant in all open-ocean waters (Collier, 1985; Emerson and Huested, 1991; Mohajerin et al., 2016). Despite the requirement of organisms for Mo, the marine abundance is greater than required in biological functions and concentrations in seawater are therefore not significantly affected by biological activity or biological cycling (Dellwig et al., 2007).

Rivers supply most of the Mo to the oceans, up to 22,000 tonnes Mo/year, mainly by the weathering of continental material (Archer and Vance, 2008; McManus et al., 2006; Rahaman et al., 2010). In open marine water, Mo occurs as the molybdate oxyanion ($Mo(VI)O_4^{2-}$) whose stability means that the element behaves conservatively. Molybdenum has a long residence time in the oceans, probably ca. 400 ky (Miller et al., 2011) but possibly as long as 800 ky (Firdaus et al., 2008), some orders of magnitude greater than ocean mixing times (Bruland et al., 2014; Rahaman et al., 2010). Hence, it has been estimated that the ocean circulates some 300 times before the Mo is finally lost to the sediments (Kendall et al., 2017).

In contrast, concentrations of Mo in euxinic aqueous conditions are much lower as Mo is sequestered by sulphides, FeS or thiomolybdates (Vorlicek and Helz, 2002), and possibly to a lesser extent by organic-rich phases. In the Black Sea, concentrations diminish from 3.8 μg/L at the ocean surface to 0.28 μg/L in sulphidic conditions below the chemocline. Vertical profiles in the Black Sea and other euxinic basins show distinct negative correlations between the concentrations of dissolved Mo and dissolved sulphide, illustrating the loss of dissolved Mo and the low solubility of Mo-S compounds below the permanent chemocline (Brumsack, 2006; Neubert et al., 2008). Helz et al. (2011) proposed that the near-total removal of Mo from deep Black Sea waters is due to the serendipitous combination of relatively low pH (ca. pH 7) and high dissolved H_2S concentration (1–10 μg/L; 10–100 μM).

Concentrations in estuarine waters can vary over a range up to and in excess of values observed in seawater, but salinity-normalised concentrations in non-polluted waters largely show near-conservative behaviour (Mohajerin et al., 2016). Scheiderich et al. (2010) found slightly non-conservative behaviour in parts of Chesapeake Bay reflecting the small loss of Mo to the sediments. The range of Mo in estuarine waters from Terrebonne Bay, Mississippi, USA was found to be 0.87–5.37 μg/L. A study of the mixing behaviour of Mo in the Elbe, Rhine and Weser estuaries also indicated that it behaved mostly conservatively with only small deviations at mid-salinities (Schneider et al., 2016). A range of Mo of 0.1–8.6 μg/L was reported for five Indian estuaries by Rahaman et al. (2010), and Archer and Vance (2008) found a range of 0.46–11.2 μg/L in the English River Itchen (Table 6).

Table 6
Molybdenum in rain and surface water.

Water type	Average (range) μg/L	Number	Reference
Rainwater			
Rainwater, upland Wales	0.17	205	Neal et al. (1994)
Rainwater, Hanoi, Vietnam	0.10 (0.07–0.14)	2	Agusa et al. (2006)
Rainwater, Kofu, Japan	0.15 (0.1–0.2)	7	Kawakubo et al. (2001)
Streamwater			
World streams	0.5[a]		Reimann and de Caritat (1998)
Streams, Wales	<9 (<9–200)	13,337	BGS (1999)
Streams, England & Wales	0.57[a] (<0.05–230)	10,822	Johnson et al. (2005)
Upland (baseflow), Wales	0.20[a] (0–14.7)	67	Neal et al. (1998)
Upland (stormflow), Wales	0.36[a] (0–11.2)	67	Neal et al. (1998)
Upland streams, Clyde, Glasgow	0.069[a] (<0.02–8.1)	1702	Smedley et al. (2017)
Streamwater, Northern Ireland	0.43 (<0.02–28)	3063	Ander (2009)
European streamwater	<0.1–10.1 (0.22[a])	807	Salminen (2005)
Rivers			
World rivers	0.42		Gaillardet et al. (2014)
World rivers	1.21 (0.11–8.63)		Linnik and Ignatenko (2015)
Rivers, China	5.0–14.4		Zhao et al. (1990)
Rivers, India	2.36 (0.22–8.63)		Rahaman et al. (2010)
Rivers, France	0.05–2.15		Elbaz-Poulichet et al. (2006)
River Tweed, England	0.39 (0–4.2)	119	Neal and Robson (2000)
River Wear, England	1.46 (0.20–10.3)	55	Neal and Robson (2000)
River Swale, England	0.61 (0–5.00)	172	Neal and Robson (2000)
River Nidd, England	0.78 (0–4.32)	184	Neal and Robson (2000)
River Ure, England	0.51 (0–3.0)	180	Neal and Robson (2000)
River Ouse, England	0.95 (0–4.47)	144	Neal and Robson (2000)
River Derwent, England	0.90 (0–26)	173	Neal and Robson (2000)
River Wharfe, England	0.72 (0–4.92)	192	Neal and Robson (2000)
River Aire, England	23.5 (0.32–70.3)	196	Neal and Robson (2000)
River Calder, England	4.70 (0.57–19.7)	176	Neal and Robson (2000)
River Don, England	8.88 (0.70–20.1)	180	Neal and Robson (2000)
River Trent, England	5.05 (1.75–9.80)	153	Neal and Robson (2000)
River Great Ouse, England	3.34 (1.1–40.2)	58	Neal and Robson (2000)
River Thames, Oxford, England	2.85 (0.5–10.0)	108	Neal and Robson (2000)
River Thames, Oxford, England	2.80 (0.91–9.60)		Neal et al. (2000b)
River Clyde, Scotland	0.059[a] (<0.02–0.691)	60	Smedley et al. (2017)
River Clyde urban, Scotland	0.84[a] (0.071–214)		Smedley et al. (2017)
Two streams, Massif Central, France	0.19 (0.19–0.81)	12	Voegelin et al. (2012)
River Vardar, Macedonia/Greece	0.31 (0.03–0.81)	27	Popov et al. (2014)
Chao Phraya River, Thailand	0.31–0.47		Dalai et al. (2005)
Bhaluhi River, Nawalparasi, Nepal	0.29 (0.096–0.38)	8	Diwakar et al. (2015)
Mississippi River, USA	1.25	2	Mohajerin et al. (2016)
Carson River, Sierra Nevada, USA	5.20–30.5		Johannesson et al. (2000)
Sacramento River, CA, USA	<0.03–3.4	320	Alpers et al. (2000); Taylor et al. (2012)
Animas River, CO, USA	0.03–0.25	7	Rodriguez-Freire et al. (2016)
Lakes			
Esthwaite Water, England	0.1 (0.069–0.162)	32	CEH (unpublished, 2007)
Windermere (N), England	0.09 (0.048–0.15)	32	CEH (unpublished, 2007)
Windermere (S), England	0.096 (0.05–0.157)	32	CEH (unpublished, 2007)
Lake Greifensee, Switzerland	0.31–0.48		Magyar et al. (1993)
Castle Lake, California, USA	0.19–0.38		Glass et al. (2013)
Oxic water, Fayetteville Green Lake, NY, USA	16.0 (11.3–18.3)	26	Havig et al. (2015)
Euxinic bottom water, Fayetteville Green Lake, NY, USA	1.73 (0.97–3.85)	25	Havig et al. (2015)
Oxic water, Lake Cadagno, Switzerland	0.69–1.43	15	Dahl et al. (2010)
Euxinic bottom water, Lake Cadagno, Switzerland	0.17–0.84	15	Dahl et al. (2010)
Lake Hoare, McMurdo, Antarctica	0.48–4.13	4	N. Yang et al. (2015)
Lake Fryxell, McMurdo, Antarctica	0.34–2.45	4	N. Yang et al. (2015)
Headwater lakes, Québec, Canada	0.03 (0.01–0.18)	30	Chappaz et al. (2008)
Walker Lake, Sierra Nevada, USA	1.2–334		Johannesson et al. (2000); Domagalski et al. (1990)
San Joaquin Valley lakes, CA, USA	2850 (138–23,700)		Bradford et al. (1990)
Great Salt Lake, UT, USA	4.9–30.4	7	Domagalski et al. (1990)
Salton Sea, CA, USA	37.0		N. Yang et al. (2015)
Mono Lake, CA, USA	49.2–85	7	Domagalski et al. (1990)
Estuaries			
Estuary, River Clyde, Scotland	1.70[a] (<2.5–6.4)	7	Smedley et al. (2017)
Estuary, River Tamar, England	1.44–8.63	7	Khan and Berg (1989)
Estuary, River Itchen, England	0.46–11.2		Archer and Vance (2008)
Estuary, Wadden Sea, Germany	2.9–15		Dellwig et al. (2007)
Estuaries, Elbe, Rhine and Weser			Schneider et al. (2016)
Estuary, Mississippi, USA	0.87–5.37	22	Mohajerin et al. (2016)
Estuary, Chao Phraya, Thailand	0.31–11.2		Dalai et al. (2005)
Estuaries, India	0.1–8.6		Rahaman et al. (2010)

Table 6 (*continued*)

Water type	Average (range) μg/L	Number	Reference
Seawater			
Open water, oxic	9.3–10.4		Firdaus et al. (2008); Bruland et al. (2014); Sohrin et al. (1987)
Euxinic, Black Sea	0.67–3.74	19	Nägler et al. (2011)
Euxinic, Baltic Sea	1.82–3.26	7	Nägler et al. (2011)
Mine/mineralisation-impacted			
Acid mine pit lakes, Iberian Belt, Spain	10	22	Sánchez España et al. (2008)
Landfill leachate, WI, USA	1.28–16	4	Lourigan and Phelps (2013)
Coal-ash leachate, WI, USA	1650–16,700	4	Lourigan and Phelps (2013)
Water impacted by coal by-products, landfill, Pines, IN, USA	8.11 (7–123)	79	ENSR (2007)
Red River Valley, NM, USA	<7[a] (<0.5–210)		Nordstrom (2015)

[a] Median. *: 10th, 90th percentile values.

Estuary waters of the Wadden Sea off north-west Germany have shown periodic Mo depletion consistent with development of oxygen-depleted zones and/or breakdown of phytoplankton blooms, with associated fixation to mineral surfaces (Dellwig et al., 2007). Subsequent release of Mo was attributed to a breakdown of organic matter, in some cases resulting in concentrations in excess of those in open seawater (Table 6).

5.3. Rivers and streams

Reimann and de Caritat (1998) quoted a median Mo concentration in streamwaters worldwide of 0.5 μg/L. Estimates for world rivers have been given as around 0.42 μg/L (Gaillardet et al., 2014) and 0.11–8.63 (mean 1.21 μg/L) (Linnik and Ignatenko, 2015) (Table 6). Rivers from China have a reported range up to 20 μg/L (Zhao et al., 1990) and from India up to 8.6 μg/L (Rahaman et al., 2010). The Rivers Marne and Seine of France have values in the range 0.05–2.15 μg/L.

British rivers are broadly comparable with these compositions. Neal and Robson (2000) reported median values from 18 sites in eastern England of mostly <1 μg/L, but with higher medians (3–10 μg/L) in the Rivers Calder, Don, Trent, Great Ouse and Thames. Neal et al. (2000b) reported a mean Mo concentration of 2.80 μg/L for the River Thames (Oxfordshire) (Table 6). The highest median value reported by Neal and Robson (2000) (20.7 μg/L) was obtained for samples from the River Aire in Yorkshire (maximum observed concentration 70.3 μg/L; Table 6). The river flows through an urban and industrial catchment and water at the sampling point, downstream of the city of Leeds, has been impacted by industrial contamination including coal-mine drainage (Neal and Davies, 2003). Before recent rehabilitation measures, the River Aire was one of the most polluted rivers in Britain. Nonetheless, only one sample from the Neal and Robson (2000) dataset had a Mo concentration greater than 70 μg/L. The river water samples showed evidence of strong seasonal variability, with highest concentrations occurring during summer months when river flow is lowest and least diluted by storm water (Smedley et al., 2014a).

Neal et al. (2000a) suggested that Mo in the River Great Ouse in Bedfordshire, southern England (Table 6) may be derived from contamination from the car components industry at Bedford. The highest reported maximum value for the site was 1590 μg/L but this was anomalous and the next highest observed concentration was 9.6 μg/L. The authors also found occasionally large Mo contents in the particulate fraction of river-water samples from this area.

In Wales, median Mo values for streamwaters from acid upland catchments with indurated Palaeozoic bedrocks were 0.20 μg/L in baseflow and 0.36 μg/L in stormflow conditions (Neal et al., 1998). In Northern Ireland, streamwaters above indurated bedrocks gave a range of <0.02–28 μg/L with a mean of 0.43 μg/L and a 10th to 90th percentile range of 0.03–0.93 μg/L (3063 samples) (Ander, 2009).

First-order British streams recorded in the British Geological Survey's G-BASE dataset from 2007 (BGS, 2006) had an observed Mo concentration range of <0.05–230 μg/L with a median of 0.57 μg/L and mean of 1.33 μg/L (10,822 samples) (Table 6). Only 12 samples (0.1%) had concentrations greater than 70 μg/L. Most samples derive from central-eastern England, where concentrations are largely in the range 0.06–2.7 μg/L (10–90th percentile range) (BGS, 2006). Particularly low concentrations (<1 μg/L) typified streams draining Mesozoic limestones. Comparable ranges of Mo concentrations (<1.5 μg/L) are also seen in English public-supply (drinking) water sourced from surface waters (Smedley et al., 2014b).

Consistent with the river observations of Neal and Robson (2000), relatively high Mo concentrations have been found in streamwaters forming tributaries of the River Aire in northern England. Streams close to two coal-fired power stations located along the river itself had concentrations of 230 μg/L and 152 μg/L, likely associated with contamination from coal and fly ash (BGS, 2006).

Concentrations up to 32 μg/L are recorded in streams close to the Parys Mountain mineral mine in North Wales, a well-documented area of sulphide mineralisation (BGS, 1999). The Mo range for streams and rivers in the urban Clyde catchment of Scotland is also large, 0.07–214 μg/L (Table 6), higher values in the urban area of Glasgow reflecting inputs from urban and mine-drainage sources (Smedley et al., 2017) (see Section 7.5).

In the USA, values in the range 0.03–0.25 μg/L were found in the Animas River, CO (Rodriguez-Freire et al., 2016). A value of 1.25 μg/L was reported for the Mississippi River, MS (Mohajerin et al., 2016). The Sacramento River, downstream of the Iron Mountain Superfund site, CA, USA, has a reported Mo range of 0.03–3.4 μg/L (Alpers et al., 2000; Taylor et al., 2012), values which do not show obvious signs of water contamination.

5.4. Lakes

A large range of Mo concentrations is seen in lake waters, depending on ambient redox, pH and salinity variations. Measured concentrations of Mo in lake waters from upland Cumbria in north-west England are universally low (<0.2 μg/L) (Smedley et al., 2014a from CEH unpublished data, 2007) (Table 6). Magyar et al. (1993) also reported low concentrations, in the range 0.31–0.48 μg/L, in lakewater from Greifensee, Switzerland.

Some large lakes showing vertical stratification in redox conditions display large variations in dissolved Mo concentration, being high under oxic conditions and diminishing to low or undetectable values under anoxic and especially euxinic conditions. Stratification has been documented in the Fayetteville Green Lake, NY, USA (Havig et al., 2015) where observed concentrations lie in the range 11.3–18.3 μg/L in the oxic zone to (Section 7.6; Table 6)

and 0.97–3.85 μg/L in the euxinic zone below. A similar trend but with smaller concentrations was seen in lakewater from Lake Cadagno, Switzerland where the range was 1.17–1.43 μg/L in the shallow oxic zone and 0.35–0.84 μg/L in the euxinic bottom waters (Dahl et al., 2010). The profiles indicate that dissolved Mo is being removed in the water column rather than below the sediment-water interface (Dahl et al., 2010). Concentrations in Castle Lake, CA, USA, where in summer bottom waters become suboxic, lie in the range 0.19–0.38 μg/L. Increases in relation to dissolution of Mn and Fe oxides were noted (Glass et al., 2013).

Variations in concentration are also observed with increasing salinity, with some high concentrations observed in the terminal alkaline lakes of western USA. Walker Lake, a terminal lake in the Great Basin, NV, USA, has a salinity of some 13 g/L. Oxic conditions occur in the lake profile down to the sediment-water interface (albeit with lake stratification in the summer months) (Domagalski et al., 1990). Under the ambient oxic and alkaline conditions in the main lake body, Mo concentrations behave conservatively and increase in response to evaporation. Concentrations up to 330 μg/L have been reported (Table 6) (Domagalski et al., 1990; Johannesson et al., 2000). In lakes of the San Joaquin Valley, CA, USA, also impacted by evaporation, concentrations in the range 138–23,700 μg/L (mean 2850 μg/L) have been reported (Bradford et al., 1990). The lakewaters have correspondingly high concentrations of U and V. Concentrations in the alkaline saline Mono Lake, CA, have been reported in the range 49.2–85 μg/L (Domagalski et al., 1990). Below the lake's chemocline at some 15 m depth, anoxic bottom waters and underlying sediments have Fe-, Mn- and SO_4-reducing conditions. Molybdenum in the anoxic bottom waters and sediments has been sequestered with sulphides (probably FeS). Hypersaline waters of the Great Salt Lake, UT, have recorded Mo concentrations of 4.9–30.4 μg/L, decreasing with depth in response to a chemocline at 7.5 m depth (Domagalski et al., 1990). Strongly reducing bottom waters and sediments below the chemocline sustain sulphide production and immobilisation of Mo. Molybdenum concentrations in the saline lakes of the Salton Sea, CA have been reported at around 37 μg/L (Table 6) (N. Yang et al., 2015).

5.5. Porewater

Marine and fresh porewaters demonstrate a comparable variability in Mo concentrations as a function of redox conditions, pH and mineralogy. The variations can be notable in unconsolidated sediments because of the large solid-solution ratios and potential abundance of organic matter to drive conditions from oxic to anoxic and possibly sulphidic. In marine porewaters, oxic conditions favour the stabilisation of molybdate and concentrations are commonly similar to those seen in the open ocean. In superficial (<40 cm) porewaters from continental margin sediments off Washington, USA, Morford et al. (2005) found concentrations of around 10 μg/L, consistent with overlying oxic seawater compositions. However, in mildly reducing porewaters, concentrations increased to around 24 μg/L with associated increases in dissolved Mn, denoting likely origin from dissolution of Mn oxides. Similar increased concentrations were also found under Mn- reducing conditions in shallow marine porewaters of Boston Harbour, USA (up to around 12.5 μg/L) (Morford et al., 2007) and off the coast of France (around 20 μg/L or more) (Chaillou et al., 2008). Enhanced Mo concentrations in Mn-reducing conditions have also been noted in marine porewaters by several other authors (Dalai et al., 2005; Scott and Lyons, 2012; Shimmield and Price, 1986). Tidal-flat porewaters of the Wadden Sea also had concentrations up to around 15 μg/ (Beck et al., 2008) (Table 7). These increases were inferred to be due to reductive dissolution of/desorption from either Mn or Fe oxides.

Under sulphate-reducing conditions, porewater concentrations in both Boston Harbour and the Wadden Sea diminish significantly (<2 μg/L) (Beck et al., 2008; Morford et al., 2007). Similar reductions in Mo concentration were observed in sulphidic porewaters below the Terrebone Bay Estuary, MS, USA (Mohajerin et al., 2016) (Table 7).

Similar increases in Mo concentration below the sediment-water interface have also been noted in fresh porewaters. In oxic porewaters below a lake in eastern Canada, Chappaz et al. (2008) noted increased concentrations at 1–2 cm depth below the sediment-water interface. From association with dissolved Fe, they inferred an origin from dissolution of Fe oxides. Concentrations in the porewaters were small: 0.3 μg/L or less (Table 7).

5.6. Groundwater

Concentrations of Mo in groundwater are typically of the order of a few μg/L or less, although higher concentrations can occur in some hydrogeological conditions. Concentrations are strongly influenced by groundwater pH and redox status. Reported concentrations of Mo in groundwater from Great Britain have a 10^{th}–90^{th} percentile range of 0.035–1.80 μg/L with a median of 0.20 μg/L (mean 0.87 μg/L) (Smedley et al., 2014b). The observed range was <0.02–89.2 μg/L (1735 samples) but 82% of samples had concentrations <1 μg/L, with only two observations greater than the WHO health-based value of 70 μg/L. Relatively low concentrations have been found in groundwater from granitic terrain where pH conditions are mildly acidic (Smedley et al., 2014b).

Several studies of Mo in groundwater from European aquifers indicate concentrations of a few μg/L to a few tens of μg/L (Table 7). As examples, groundwaters from Neogene, Plio-Quaternary and Cretaceous aquifers in Belgium, Bulgaria and the Czech Republic respectively, all have reported Mo concentrations <10 μg/L (Coetsiers and Walraevens, 2009; Machkova et al., 2009; Paces et al., 2009).

In the USA, a summary of analyses produced by the United States Geological Survey's National Water-Quality Assessment Program (NAWQA) for the period 1992–2003 found a range of Mo concentrations in groundwater of 0.13–4.9 μg/L (10^{th}–90^{th} percentile range) with an observed maximum of 4700 μg/L and median of 1.0 μg/L (n = 3063) (Ayotte et al., 2011). Some of the highest concentrations were found in groundwater from unconsolidated sand and gravel and glacial sand and gravel aquifers (Fig. 2). Relatively high values were a feature of shallow glacial unconsolidated aquifers in Illinois and Indiana as well as Basin & Range basin-fill aquifers in western Nevada. In both types of unconsolidated aquifer, Mo concentrations were broadly higher in groundwaters with pH > 7 than with pH < 7, whether in oxic or anoxic conditions (Ayotte et al., 2011). Groundwater from springs in carbonate/volcanic aquifers of the southern Great Basin, USA, had concentrations up to 25 μg/L (Hodge et al., 1996) (Table 7).

In some aquifers, concentrations of Mo are observed to increase down the groundwater flow gradient as aquifers become confined below poorly-permeable overlying strata and aquifer redox conditions change from oxic to anoxic (but non-sulphidic). The magnitude of the changes may be small. Downgradient increases in concentration are seen in the English East Midlands Triassic Sandstone aquifer and the Yorkshire Chalk aquifer (Smedley et al., 2014b) where step changes in dissolved Mo concentrations coincide with confinement and the onset of Fe- and Mn- reducing conditions. In the Triassic Sandstone, Mo concentrations increase from typically <1 μg/L in the oxic groundwater in the unconfined section, to values around 4 μg/L in the Fe-reducing confined aquifer (Smedley and Edmunds, 2002). Further downgradient, a deep

Table 7
Molybdenum in groundwater (including porewater).

Aquifer/region	Average (range) µg/L	Number	Reference
Various			
Various, USA	1.0[a] (0.13–4.9[b])	3063	Ayotte et al. (2011)
Springs, carbonate/volcanic aquifers, southern Great Basin, USA	10.1 (6.33–24.9)	23	Hodge et al. (1996)
Basalt, non-geothermal	<1		Arnórsson and Ívarsson (1985)
Quaternary/Cretaceous aquifers, Portugal	0.45 (<0.1–13.2)	144	Condesso de Melo and Marques da Silva (2009)
Neogene, Flanders, Belgium	0.46 (<0.1–8.3)	40	Coetsiers and Walraevens (2009)
Plio-Quaternary, Bulgaria	1 (0.1–8)	18	Machkova et al. (2009)
Cretaceous carbonates, Czech Republic	<2 (<2–6.2)	104	Paces et al. (2009)
Proterozoic shallow groundwater, Burkina Faso (dug wells)	<0.1[a] (<0.1–0.41)	9	Smedley et al. (2007)
Oxic, alkaline aquifers			
Quaternary loess, Córdoba, Argentina	85.4 (0.97–7900)	60	Nicolli et al. (1989)
Quaternary loess, La Pampa, Argentina	2.70–990	114	Smedley et al. (2002)
Quaternary loess, Burruyacú Basin, Argentina	19.3 (0.5–90.1)	74	Nicolli et al. (2008)
Quaternary loess, Salí River Basin, Tucumán, Argentina	39.7 (0.2–727)	86	Nicolli et al. (2012b)
Santa Fe, Esperanza, Argentina	59.7[a] (43.6–69.8)		Nicolli et al. (2012a)
Santa Fe, Argentina	31.8[a] (30–635)		Nicolli et al. (2012a)
Rio Dulce, Santiago del Estero, Argentina	20.0[a] (5.4–1907)	40	Bhattacharya et al. (2006)
Rhyolite/volcanogenic sediment, Rift Valley, Ethiopia	0.53–446	25	Rango et al. (2010)
Rhyolite/volcanogenic sediment, Rift Valley, Ethiopia	22.9 (0.50–103)	117	BGS (unpublished, 2014)
Rhyolite/sediment, Rift Valley, Ethiopia	10.9 (0.11–78.3)	42	Reimann et al. (2003)
Palaeogene carbonate, Great Northern Basin, Qatar	26.9 (1.0–103)	205	Kuiper et al. (2015)
Amu Darya Delta, Aral Sea Basin, Uzbekistan	1.4–237	30	Schettler et al. (2013)
Reducing aquifers			
Upper Cretaceous limestone (oil shale), north Jordan	4–650		Al Kuisi et al. (2015)
Glacial till/Ordovician–Silurian dolomite, WI, USA	10.9–145	24	Lourigan and Phelps (2013)
Lithia, FL, USA	645 (0.3–4740)	58	Pichler et al. (2017)
Aquia aquifer, MD, USA	1–143		Vallee (2009)
Holocene alluvial aquifers, Cambodia	1.41 (<0.5–70.8)	94	Feldman et al. (2007)
Gia Lam alluvial aquifer, Hanoi, Vietnam	1.18 (0.16–6.69)	11	Agusa et al. (2006)
Thanh Tri alluvial aquifer, Hanoi, Vietnam	1.58 (0.23–5.25)	14	Agusa et al. (2006)
Holocene alluvial/deltaic aquifer, Lakshmipur, Bangladesh	8.15 (<0.1–20.0)	59	BGS and DPHE (2001)
Holocene alluvial aquifer, Faridpur, Bangladesh	<0.1–20.5	59	BGS and DPHE (2001)
Holocene alluvial aquifer, Ch. Nawabganj, Bangladesh	1.23 (0.13–9.77)	69	BGS and DPHE (2001)
Pleistocene aquifer, Lakshmipur, Bangladesh	<0.1–2.89	22	BGS and DPHE (2001)
Pleistocene aquifer, Faridpur, Bangladesh	1.49 (0.26–2.15)	5	BGS and DPHE (2001)
Pleistocene aquifer, Ch. Nawabganj, Bangladesh	0.35 (0.14–0.61)	20	BGS and DPHE (2001)
Holocene alluvial aquifers, Datong, China	0.1–269	91	Guo and Wang (2005)
Holocene fluviolacustrine aquifer, Huhhot Basin, China (<100 m depth)	1.9[a] (<0.1–63)	59	Smedley et al. (2003)
Quaternary fluviolacustrine aquifer, Huhhot Basin, China (>100 m depth)	1.6[a] (<0.1–14)	14	Smedley et al. (2003)
Holocene aquifer, Upper Bhaluhi River, Nawalparasi, Nepal	0.096–5.28 (1.54)	25	Diwakar et al. (2015)
Holocene aquifer, Middle Bhaluhi River, Nawalparasi, Nepal	0.38–22.4 (7.20)	37	Diwakar et al. (2015)
Holocene aquifer, Lower Bhaluhi River, Nawalparasi, Nepal	1.54 (0.096–3.74)	11	Diwakar et al. (2015)
Sulphate-reducing, Pannonian basin, Hungary/Romania	<0.5–20.7	35	Rowland et al. (2011)
Methanogenic, Pannonian basin, Hungary/Romania	0.9–120	15	Rowland et al. (2011)
Sulphidic porewater, Lake Cadagno, Switzerland	2.0–313	17	Dahl et al. (2010)
Marine porewaters			
Santa Barbara Basin, off CA, USA	0.96–11.5		Zheng et al. (2000a)
Boston Harbour, USA, manganous	1.9–12.5		Morford et al. (2007)
Boston Harbour, USA sulphidic	0.67–1.25		Morford et al. (2007)
Tidal flats, Wadden Sea, Germany	<2–15		Beck et al. (2008)
Marine porewater, off France	5–20	39	Chaillou et al. (2008)
Estuarine porewater, Terrebonne Bay, USA	0.06–4.3		Mohajerin et al. (2016)
Fresh porewaters			
Oxic/anoxic lakes, eastern Canada	<0.1–0.27		Chappaz et al. (2008)
Geothermal groundwaters			
Basalt, Iceland	1–70		Arnórsson and Ívarsson (1985)
Geothermal springs, North West Territories, Canada	<0.1–30	41	Hall et al. (1988)
Hotsprings, Rift Valley, Ethiopia	21.6 (9.74–34.6)	7	Reimann et al. (2003)
Thermal groundwater, Pannonian Basin, Hungary/Romania	<0.5–6.8	7	Rowland et al. (2011)
Mining/mineralised aquifers/areas			
Acidic pyrite mine leachate, Iberian Belt, Spain	10,400		Sánchez España et al. (2008)
Minewater (ilsemannite), Idaho Springs, CO, USA	5,320,000[c]	1	Horton and Laney (1916)
Miduk Copper Complex, Iran	179 (0.70–1175)	42	Kargar et al. (2011)
Spence Porphyry Copper Deposit, Chile	79.0 (2–475)	50	Leybourne and Cameron (2008)
Massive sulphide deposits, eastern Canada	0.7–56		Leybourne (1998)
Uronai porphyry copper deposit, Russia	up to 420	390	Balandis et al. (2005)
Antamina copper deposit, Peru	10–13,900	16	Skierszkan et al. (2016)
Uranium mine tailings, CO, USA	4800		Morrison et al. (2006)
Proterozoic aquifer, Burkina Faso (boreholes)	0.78[a] (<0.1–76.3)	36	Smedley et al. (2007)

(*continued on next page*)

Table 7 (*continued*)

Aquifer/region	Average (range) μg/L	Number	Reference
Coal ash waste, Pines, IN, USA	12.8 (0.7–162)	94	ENSR (2007)
Massive sulphide, New Brunswick, Canada	0.5–19		Nordstrom (2015)
Red River Valley, NM, USA	<7[a] (<7–18)		Nordstrom (2015)

[a] Median.
[b] :10th, 90th percentile values.
[c] Includes colloidal.

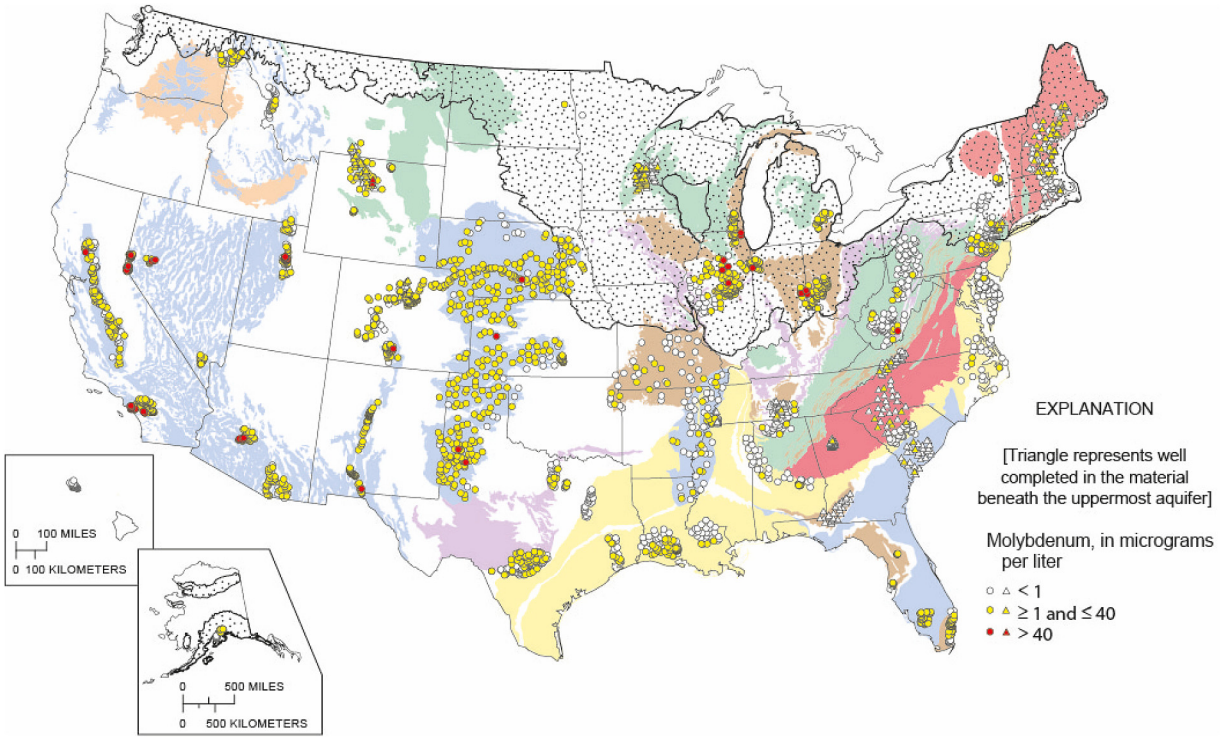

Fig. 2. Map of molybdenum distributions in groundwater from the USA. Stipple denotes distribution of glacial unconsolidated sand and gravel aquifers (Ayotte et al., 2011, with permission). Also available at http://pubs.usgs.gov/sir/2011/5059.

saline part of the confined aquifer (ca. 50 km downgradient of the outcrop edge) is subject to more strongly reducing conditions with evidence of sulphate reduction (Smedley and Edmunds, 2002). Here, Mo concentrations fall to ≤1 μg/L. In the Yorkshire Chalk aquifer, oxic waters from the unconfined aquifer have uniformly low concentrations of <0.4 μg/L but increase to typically 1–4 μg/L beyond the redox boundary where Fe- and Mn-reducing conditions occur. The trends were attributed to mobilisation of Mo in response to release from Fe and/or Mn oxides via reductive dissolution, and immobilisation under sulphate-reducing conditions by co-precipitation with/sorption to newly forming metal sulphides.

Downgradient changes in Mo concentration coincident with redox transformations have also been observed in the Aquia aquifer of Maryland, USA. Vallee (2009) found concentrations down to 1 μg/L in unconfined conditions within the aquifer, increasing along two groundwater flowlines, and reaching a maximum of 143 μg/L in Fe-reducing groundwaters. The trend was linked mainly to release by reductive dissolution of Fe oxides. Further downgradient in one of the flowlines, concentrations fell due to immobilisation of Mo with precipitating sulphide minerals.

Many anoxic groundwaters have elevated concentrations of dissolved Mo, though values much above the WHO health-based value (70 μg/L) are unusual. Groundwater from a Quaternary aquifer in the Pannonian Basin of Hungary and Romania has a reported range of <0.5–20.7 μg/L (n = 35) in sulphate-reducing conditions but a range of 0.9–120 μg/L (n = 15) in more strongly reducing methanogenic conditions (Rowland et al., 2011). The variation was taken to be due to the amounts of organic carbon in the system, with production of sulphide in active sulphate-reducing aquifer conditions and, in areas with high organic carbon contents, rapid exhaustion of sulphate and onset of methanogenic conditions. The authors' investigation concerned the distribution of As. The concentrations of dissolved As were lowest in sulphate-reducing conditions, with As removed from solution along with precipitating sulphide minerals. The trends for dissolved Mo were coupled with As and suggest similar controlling processes.

Guo and Wang (2005) found Mo ranges in five zones of the Quaternary aquifers of the Datong Basin, Shanxi, northern China: Zone I: 0.1–12.2 μg/L (mean 2.9 μg/L), Zone II: 0.1–6.7 μg/L (mean 2.6 μg/L); Zone III: 3.6–269 μg/L (mean 28.7 μg/L); Zone IV: 0.1–79.6 μg/L (mean 8.2 μg/L), and Zone V: 0.4–8.3 μg/L (mean 2.4 μg/L). Zone I occurred along the margins of the Basin, Zone II between recharge and discharge zones, Zone III was the discharge area with the aquifer being semi-confined, Zone IV was the anoxic discharge zone where low concentrations of SO_4 denoted sulphate-reducing conditions and Zone V was an alluvial fan on the margins of the Basin. Highest Mo (and As) concentrations occurred under mildly (Fe- and Mn-) reducing conditions in the lower parts of the

basin. Some observations in Zones III and IV of the Datong Basin exceed the WHO health-based value for Mo.

Diwakar et al. (2015) found concentrations up to 22 μg/L in shallow groundwaters from the Holocene alluvial aquifers of the catchment of the Bhaluhi River, Nawalparasi, Nepal. Concentrations were highest in the middle reach of the catchment, coincident with the highest groundwater As concentrations and the most reducing conditions. Holocene reducing fluviolacustrine aquifers in the Huhhot Basin of China showed a Mo concentration range of <0.1–63 μg/L (Smedley et al., 2003), with highest concentrations in the low-lying part of the basin where anoxic groundwater conditions prevailed.

In Bangladesh, elevated Mo concentrations (up to 21 μg/L) were found in groundwater from shallow (<150 m) Holocene aquifers under strongly reducing conditions; these groundwaters displayed positive correlations between dissolved Mo and As (BGS and DPHE, 2001) (Table 7).

High Mo concentrations are a feature of groundwater from Upper Cretaceous aquifers interconnected with overlying oil-shale deposits in northern Jordan. A Mo range of 4–650 μg/L has been described by Al Kuisi et al. (2015) (Section 7.2). Affected groundwaters are largely anoxic with the likely origin of the Mo being from oil shales.

Around the town of Caledonia just south of Milwaukee, WI, USA, high concentrations of Mo have also been reported in a number of private water wells that abstract anoxic groundwater from both an Ordovician-Silurian aquifer and an overlying Quaternary till/alluvial aquifer (Hensel et al., 2015). Some wells had concentrations >40 μg/L (Section 7.7).

Some of the highest concentrations of Mo occur under oxic, alkaline conditions. In such conditions, Mo tends to behave near conservatively (Hodge et al., 1996), its concentration depending on availability of Mo in the aquifer solids. This is well-demonstrated by the distributions in groundwaters from the Chaco-Pampean Plain of Argentina. In Córdoba Province, Nicolli et al. (1989) reported groundwater Mo concentrations in the range 0.97–7900 μg/L with a mean of 85.4 μg/L. In the Salí River Basin, Tucumán, Nicolli et al. (2012b) reported concentrations of 0.2–727 μg/L with a mean of 39.7 μg/L and median of 7 μg/L. In Santiago Del Estero Province, groundwater Mo concentrations in the range 5.4–1907 (median 20.0 μg/L) have been reported (Bhattacharya et al., 2006). In La Pampa Province, Smedley et al. (2002) found Mo concentrations in pumped groundwaters in the range 2.7–990 μg/L, with a median of 61.5 μg/L (n = 114) (Table 7). In these, origins of Mo have been linked to the presence of rhyolitic ash within the loess silt-sand deposits and the maintenance in soluble form by the oxic and alkaline conditions.

In the Ethiopian Rift Valley, sedimentary aquifers with intermixed rhyolitic ash also have some high-Mo groundwaters. Rango et al. (2010) reported concentrations in the range 0.53–446 μg/L in parts of the Ethiopian Rift Valley; a range of 0.50–103 μg/L was also reported for groundwater from rhyolitic/volcanogenic sedimentary rocks from the same area (BGS unpublished data).

Concentrations of Mo up to 237 μg/L have also been found in unconfined groundwater from the Amu Darya Delta, Aral Sea Basin of Uzbekistan (Table 7). Here, high concentrations were in largely oxic groundwater with pH 6.8–8.7, conditions under which molybdate is stable in solution. The association with saline groundwater suggests that increasing Mo concentrations are also likely to have been impacted by evaporation (Schettler et al., 2013).

5.7. Geothermal water

Some enrichments in Mo concentrations are apparent in geothermal waters. Enrichment of Mo, along with other elements (Mn, Co, Ni, Zn and Cd), occurs in some geothermal springs in basaltic areas suggesting that the basaltic rocks are a source of these elements. Arnórsson and Ívarsson (1985) reported Mo concentrations up to 70 μg/L in groundwater from basaltic rocks in Iceland (Table 7). Non-thermal waters had low concentrations. Hall et al. (1988) reported Mo concentrations in the range <0.1–30 μg/L in geothermal springs from granite in Canada (Table 7). Reimann et al. (2003) found concentrations up to 35 μg/L in geothermal springs from rhyolitic areas of the Ethiopian Rift Valley (Table 7). However, Rowland et al. (2011) found comparatively low concentrations, in the range <0.5–6.8 μg/L, in thermal groundwater from the Pannonian Basin of Hungary and Romania.

5.8. Water impacted by mining and mineralisation

Especially high concentrations of Mo can be found in surface water and groundwater in areas with accumulations of metal sulphide minerals. Occurrences in solution have been particularly noted in association with porphyry copper and porphyry molybdenum deposits, the former being the more common. Oxidation reactions of e.g. molybdenite, can release molybdate, sulphate and acid to solution:

$$2MoS_2 + 9O_2 + 6H_2O \rightarrow 2MoO_4^{2-} + 4SO_4^{2-} + 12H^+$$

Though this reaction is unlikely to be a main control on acidity in the presence of more abundant Fe sulphides. The acidity of the resultant solution will in any case control the solubility and mobility of Mo in a self-limiting way since a lowering of pH will increase Mo sorption (Section 6.1.2). The overall impact will therefore depend on the pH-buffering provided by the mineralogy of the host rock and will be greatest when the acidity produced by the above reaction is neutralised by associated host minerals. Under very acidic conditions (e.g. pH < 3.5), ferrihydrite and other iron oxides will begin to dissolve, releasing sorbed Mo.

Perhaps the largest number of studies on mineralisation/mining impacted waters derives from North America. Morrison et al. (2006) reported Mo concentrations of 4800 μg/L mobilised by oxidation reactions at a uranium tailings site in Colorado. In the area around the Climax molybdenum mine, Kaback and Runnels (1980) indicated that Mo concentrations in Tenmile Creek were usually in the range 90–100 μg/L and in Blue River (*sic*), 160–535 μg/L, depending on the amount of dilution by the nearby Dillon reservoir. Ludington and Plumlee (2009) suggested that the relatively low concentrations of Mo compared to other trace elements in the mine waters there reflected the element's oxyanion behaviour and its preferential sorption to metal oxides at near-neutral and slightly acidic pH. Nordstrom (2015) noted that concentrations of metals in surface waters and groundwaters in mineralised areas were potentially orders of magnitude lower in natural acid drainage compared to acid mine drainage impacted by mining excavations. In the Red River Valley of New Mexico, USA, naturally acidic surface waters (pH 2.4–4.4) had Mo concentrations in the range <0.5–210 μg/L (Table 6). Naturally acidic groundwaters from the region (pH 2.99–4.0) had much lower Mo concentrations: <7–18 μg/L (Table 7) (Nordstrom, 2015). Relatively low concentrations (<0.5–19 μg/L) were also found in groundwaters from massive sulphide deposits in New Brunswick, Canada. This is likely due to the lack of oxidation under non-mined conditions as supported by the observed low SO_4 concentrations (Nordstrom, 2015), though the mobility of molybdate under acidic conditions may be an additional factor.

Elsewhere, documentation of mining- and mineralisation-related Mo mobility is much more limited and cases more dispersed. Groundwater from boreholes close to the Miduk Copper

Complex of Iran, enriched in chalcopyrite and other metal sulphide minerals, shows Mo concentrations in the range 0.70–1175 μg/L (mean 179 μg/L). The highest concentration observed was closest to the copper mine tailings dam (Kargar et al., 2011).

Concentrations of Mo up to 420 μg/L have been recorded in groundwaters from the Uronai porphyry copper deposit of Russia (Balandis et al., 2005) and concentrations up to 475 μg/L were found in groundwaters from the vicinity of the Spence porphyry copper deposit in Chile (Leybourne and Cameron, 2008) (Section 7.9). Antamina Cu-Zn-Mo mine, Peru, has recorded Mo concentrations in mine drainage of 10–13,900 μg/L, in waters that are mostly alkaline (pH 2.2–8.4, median 7.9) (Skierszkan et al., 2016). Sánchez España et al. (2008) found Mo concentrations of 10,400 μg/L in highly acidic (pH 0.61–0.82) leachates from waste piles at a pyrite mine in Huelva, Spain.

Smedley et al. (2007) found Mo concentrations of <0.1–76.3 μg/L in borehole water from sulphide-mineralised Proterozoic metamorphic rocks in northern Burkina Faso. Molybdenum concentrations were highest in zones with mineralised veins and Mo correlated well with dissolved As (as As(V)), suggesting both are released into solution via oxidation of sulphide minerals.

5.9. Global distributions in groundwater and surface water

A map of the global distributions of documented occurrences of high-Mo fresh water (groundwater and surface water) is shown in Fig. 3. Aside from ore-mineralised areas, distributions of Mo in groundwater are sporadic but some common features emerge. A number are associated with oxic alkaline conditions (Chaco-Pampean Plain, Argentina; Ethiopian Rift Valley; Qatar; San Joaquin Valley, USA; Aral Sea Basin, Uzbekistan). Some, though not all, have intermixed felsic volcanic ash (Argentina, Ethiopian Rift Valley) which potentially contributes an enriched and labile Mo source. Most are aquifers composed of young sediments, typically Quaternary, which may contain ready sources of newly-formed and reactive minerals compared to older indurated rocks with more structured mineral assemblages and longer groundwater flow histories.

Concentrations of Mo in oxic aquifers are also related to climate as many of the high-Mo groundwater terrains documented are in arid areas. A similar observation was made for Mo in groundwater of the USA (Ayotte et al., 2011). Aridity may be associated with paucity of vegetation and in turn paucity of organic matter to drive redox reactions. Hence, oxic conditions tend to prevail. In some arid groundwater environments, oxic conditions can persist for long distances downgradient in confined aquifers if there is a lack of organic carbon or other electron donors available to change the ambient redox conditions (Robertson, 1989). In many of these aquifers, groundwaters are also saline and evaporation may be an additional factor determining the high concentrations observed. Similar processes control the mobilisation of Mo in alkaline, saline, terminal lakes (e.g. Mono Lake, San Joaquin Valley lakes, Walker Lake, all in USA).

In the oxic alkaline aquifers documented, a common association between Mo and other anions and oxyanions (e.g. As, HCO_3, F, Cr, V, U) is observed and expected (Ayotte et al., 2011; Kuiper et al., 2015; Nicolli et al., 1989; Smedley et al., 2002). This is in line with the sorption affinity of anionic species in alkaline conditions (Section 6.2.2).

High Mo concentrations are also a feature of a number of anoxic aquifers. Hints at this have been seen from rising Mo concentrations as groundwater flows downgradient from oxic to anoxic sections of aquifers. High Mo concentrations in anoxic conditions characterise the Quaternary alluvial or fluviolacustrine aquifers in Datong, China and the Palaeocene Aquia aquifer, MD, USA (Fig. 3). Molybdenum concentrations generally do not appear to reach such high concentrations in most of the Quaternary (Holocene) high-As alluvial and deltaic aquifers of south Asia (Bangladesh, Cambodia, Vietnam, Nepal, other parts of the Yellow River Plain of China). Here, concentrations are elevated but values in the range tens of μg/

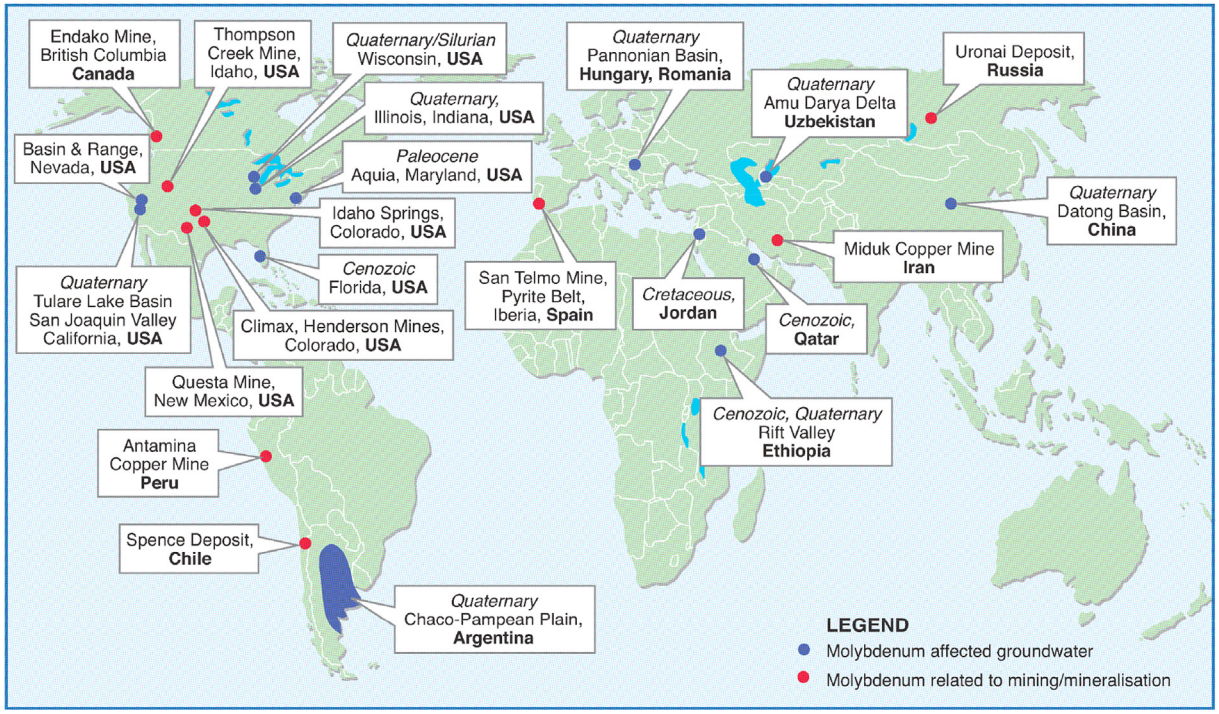

Fig. 3. Global distribution of areas with high-molybdenum groundwater or surface water (Mo > 70 μg/L), including those related to metal mining and/or mineralisation (see text for data sources).

L appear typical (Table 7). In such aquifers, increasing Mo concentrations tend to be a feature of Fe- and Mn-reducing (non-sulphidic) conditions. Under sulphidic conditions, concentrations are lower, with loss of Mo to the solid phase.

Some high-Mo groundwaters appear to be associated with the occurrence of organic-rich shales (black shales, oil shales). Examples include northern Jordan and Wisconsin, USA. Here, release of Mo from the solid (sulphide/organic) phase via an oxidation reaction would seem to be the main process. The Cretaceous was a particular period of enhanced marine black shale formation, linked to global warm temperatures and large-scale ocean anoxia (Goldberg et al., 2016), in turn probably linked to increased ocean primary productivity (Vorlicek et al., 2004). The Carboniferous was similarly linked to large-scale emplacement of organic-rich shales.

In the USA, high-Mo groundwaters have been observed under both oxic and anoxic conditions. The concentrations have associations with groundwater pH, being greater under alkaline conditions (pH > 7), regardless of whether oxic or anoxic (Ayotte et al., 2011).

The ore-mineralised areas of the world have some of the largest concentrations of dissolved Mo observed. The principal Mo mining regions of the world include the USA, Chile, Canada and Russia (Fig. 3); the principal mined mineral is molybdenite. Porphyry copper and molybdenum deposits are the chief locations with Mo mineralisation and these provide around 95% of the world Mo supply (Seal II, 2012). Porphyry deposits are found mostly in areas of active or past volcanism, in association with intermediate to felsic intrusions. The deposits occur chiefly in veins and stockworks (Dold and Fontboté, 2001). Occurrences of porphyry copper are typically of low grade (0.44% Cu in 2008) and large extent (Seal II, 2012). Ore minerals present in the structures include pyrite, chalcopyrite, bornite, molybdenite and gold. Spatial extent is made significantly larger by the haloes of hydrothermal mineralisation that occur around the primary source. Sericitic to argillic alteration in these zones can reduce the acid-neutralising capacity of the rocks (Seal II, 2012) which may have an impact on the mobility of Mo in the ore zones. Porphyry deposits are concentrated along the western USA (North American Cordillera), the Andean Chain, Caribbean, Appalachian, Alpine-Tethyan, Urals, south-west Pacific and Tasman regions, as well as more dispersed occurrences.

The world map (Fig. 3) shows locations of only a small proportion of the global occurrences of porphyry deposits but indicates where documented cases of associated high-Mo water occur. Doubtless, other porphyry deposits, and indeed other occurrences of sulphide mineralisation, will be accompanied by some occurrences of high-Mo water, but without drivers for monitoring (e.g. international standards for Mo in drinking water), they may not be recognised unless picked up incidentally by multi-element analytical techniques.

6. Chemical controls

6.1. Aqueous speciation

Molybdenum has a very complex chemistry. It can occur in a range of oxidation states and forms a large number of complexes with cations, anions and organic ligands. Mo(VI) is the dominant oxidation state in most oxygenated natural waters but more reduced states can exist under extreme low pH/Eh conditions and in the protected environments of minerals, natural organic matter and biological macromolecules such as enzymes.

Under oxic conditions, dissolved Mo is dominated by the relatively unreactive tetrahedral $Mo(VI)O_4^{2-}$ ion. Protonated forms, $HMoO_4^-$ and H_2MoO_4, are found at pH < 5 though even here, $HMoO_4^-$ is rarely dominant. A range of polynuclear species consisting of linked MoO_6 octahedra can occur at pH < 6 and high Mo concentrations (Cruywagen, 1999). These are typically formed when alkaline molybdate solutions are acidified. A wide range of metal molybdates such as $CaMoO_4$ are also quite stable both in solution and in the solid phase. $MgMoO_4$ could be a major Mo soluble species in seawater for example. Molybdenum also interacts strongly with solid surfaces including minerals and organic matter, but this tends to be favoured by low pH or strongly reducing conditions.

Understanding the many interactions of Mo in the natural environment is a daunting challenge. One approach is to attempt to model them using geochemical models. There is now an abundance of high-quality geochemical modelling software available (Blanc et al., 2012) but a limitation remains the quality of the associated thermodynamic databases and the difficulty and cost of characterising and quantifying natural materials in a way that is appropriate for modelling. Much of the cautionary advice given by Grauer (1997) 20 years ago is still relevant today. The precipitation and dissolution of minerals is always kinetically-based on some timescale. Molybdenite (MoS_2) is notably reluctant to form even when it should from a thermodynamic point of view and yet some sort of Mo-S precipitation is the key to the behaviour of Mo in sulphur-rich waters. Most natural materials are not pure compounds (i.e. they are solid solutions) and many are sufficiently fine-grained to have significant adsorbed phases. This is particularly important for trace metals, including Mo, which are often not sufficiently abundant to form pure minerals but which can be bound to the less-demanding environment found at a surface.

6.1.1. Thermodynamic databases

Building and maintaining relevant thermodynamic databases (TDBs), especially comprehensive and internally consistent ones, is a skilled and demanding task that usually only attracts significant funding when associated with high-profile investigations such as performance assessment (Voigt et al., 2007). Some publicly-available databases are listed in Table 8. These are all available in Phreeqc format, reflecting the popularity of the Phreeqc geochemical modelling software and the clarity and flexibility of the associated database format (Parkhurst and Appelo, 2013). Some other large databases (LLNL and NAGRA/PSI) include Mo but only have a single aqueous Mo species defined.

The OECD Nuclear Energy Agency (NEA) and IUPAC have undertaken a series of reviews of thermodynamic data over the last several decades. The NEA TDB project is currently (November 2016) reviewing Mo. Molybdenum has attracted such attention because it is a corrosion product of high-performance stainless steels. It is now included in the ThermoChimie (Giffaut et al., 2014), PSI/Nagra and HATCHES (Baston et al., 1988) databases although the amount of modern, high-quality Mo data relevant to natural waters is still limited. Much of the primary data being used dates back to the 1970s and before. Molybdenum is not included in some important databases, e.g. THEREDA (https://www.thereda.de/en/thereda-projekt).

Inclusion in a database does not guarantee correctness or completeness. The propagation of errors due to database parameter uncertainty is unknown for Mo but a study of U using Monte Carlo simulation has shown that it can be large (Denison and Garnier-Laplace, 2005).

Many of the solid phases in the databases are of dubious significance when it comes to modelling low-temperature environments, particularly when considering relatively short timescales. For example, many silicate minerals do not form readily at low temperatures and even some simple oxides (e.g. haematite) only form over long timescales. In terms of Mo, minerals such as molybdite (MoO_3(s)), molybdenite (MoS_2(s)): the principal Mo-ore mineral, tugarinovite (MoO_2(s)) and molybdenum metal (Mo(s)),

Table 8
Sources of thermodynamic data for molybdenum species in natural systems in various publicly-available thermodynamic databases.

Source of database	Filename and date of database	Aqueous redox states Included	Comment	Link*
ThermoChimie	ThermoChimie_PHREEQC_eDH_v9b0.dat (10 Aug 2015)	Mo(III), Mo(VI)	Actively maintained by ANDRA/RWM. Related versions use different activity models. 10 aqueous Mo species including polynuclear species. No thio, chloro or phospho or aqueous metal-Mo species. 16 Mo minerals, mostly metal molybdates plus Mo, MoO_3, MoS_2 and MoS_3. Fully documented and referenced database.	[a]
JAEA	100331c2.tdb (2012)	Mo(III), Mo(VI)	Maintained by Japanese Atomic Energy Agency. 7 aqueous species including polynuclear; no thio, chloro or phospho species. 5 solids consisting of Mo, MoO_2 and metal molybdates.	[b]
PSI/NAGRA	PSINA_110615_DAV_s.dat (2015)	Mo(VI)	MoO_4^{2-} is the only aqueous species defined. Includes 3 Mo solids (Mo, MoO_2 and MoO_3).	[c]
LLNL	llnl.dat	Mo(VI)	Based on thermos.com.V8.R6.230 version (1992) from the Lawrence Livermore National Laboratory EQ3/EQ6 database. MoO_4^{2-} is the only aqueous species defined. Includes just 2 solids (Mo and $MoSe_2$).	[d]
MINTEQ	minteq.v4.dat	Mo(VI)	Originally developed by the USEPA in 1990. Contains a wide variety of organic ligands and trace metals including 9 aqueous Mo species and 22 Mo solids, mostly metal molybdates plus MoS_2 and MoO_3.	[d]
SIT	sit.dat	Mo(III), Mo(VI)	The SIT (Specific ion Interaction Theory) version of ThermoChimie (see above).	[d]
HATCHES	PCHatches.dat, Version 20 (15 Jul 2013)	Mo(III), Mo(V), Mo(VI)	Developed by Amec Foster Wheeler for the UK NDA. Fairly comprehensive. 24 aqueous Mo species and 27 Mo solids. Includes some thio, chloro, phospho, metal and polynuclear Mo species. Also reduction to Mo(V) and Mo(III) though primary data old and questionable. $MoO_2Cl_2.H_2O$(s) species needs checking.	[e]
Thermoddem	phreeqc_thermoddemv1.10_11dec2014.dat	Mo(VI)	Developed by BRGM. MoO_4^{2-} and $HMoO_4^-$ are the only aqueous species defined. No minerals.	[f]
RES^{3}T HZDR	Interactive only	Mo(VI)	The Rossendorf Expert System for Surface and Sorption thermodynamics - a sorption database which includes metadata for Mo sorption on a variety of minerals. Data sources fully referenced.	[g]

* [a] https:/www.thermochimie-tdb.com/; [b] http://geo-iso.jaea.go.jp/tdb_e/pre_de_e/100331_e.html; [c] https://www.psi.ch/les/database; [d] http://wwwbrr.cr.usgs.gov/projects/GWC_coupled/phreeqc/; [e] http:/www.HATCHES-database.com/; [f] http://thermoddem.brgm.fr/; [g] https://www.hzdr.de/db/RES3T.queryData. Retrieved Nov-Dec 2016. For links to other databases, including proprietary ones, see the THEREDA site (https://www.thereda.de/en/links/35-thermodynamische-datenbanken).

are usually only formed under rather extreme non-surface conditions, e.g. subsurface hydrothermal or volcanic. Molybdenite, is not believed to be formed in the low-temperature environments characteristic of most freshwater bodies for kinetic reasons (Helz et al., 1996; Mohajerin et al., 2016). Supersaturation by 10^9 has been shown to occur even after leaving MoS_2-supersaturated solutions to age for 40 days (Vorlicek et al., 2004). Lack of evidence for precipitation of MoS_2 is also supported from x-ray spectrographic investigations of S-rich sediments (Dahl et al., 2013a). On the other hand, MoS_2(s) has been found to be produced in a matter of days by the sulphate-reducing bacterium *Desulfovibrio desulfuricans* in both suspended cell systems and immobilised cell systems (Tucker et al., 1998, 1997). This process needs further characterisation in terms of the underlying geochemical parameters – concentrations, Eh, pH, SIs. Zheng et al. (2000a) suggested that at least about 100 μM sulphide was needed for some kind of authigenic Mo-S precipitation but only 0.1 μM sulphide was required for some kind of Mo-Fe-S precipitation to occur. They found that a ready supply of organic C was also critical.

These Mo-containing minerals will tend to dissolve ('weather') when exposed to near-surface environments. The rate at which these weathering reactions occur is largely unknown and poorly quantified although MoS_2 is known to be strongly hydrophobic and so oxidises more readily when exposed directly to air than in equivalent air-equilibrated aqueous conditions (Greber et al., 2015). Larger O_2 concentrations lead to more rapid oxidation. An O_2 concentration of at least 72 ± 20 ppmv is required to initiate oxidation.

A disappointing feature of all the existing databases is the general lack of inclusion of phases that would account for the reduction of Mo concentrations in euxinic (sulphidic) environments, a key feature of the geochemistry of Mo. Of the databases listed in Table 8, only the HATCHES database includes the reduction of Mo(VI) to Mo(V); ThermoChimie and HATCHES also include reduction to Mo(III). HATCHES is the only one of these databases to include thio species (Mo(VI) not Mo(V)).

The databases also ignore the role of Fe in this process. Both FeS(s) (Helz et al., 2004) and pyrite (FeS_2(s)) as well as zero-valent sulphur in polysulphides, dissolved elemental sulphur and organic macromolecules have been implicated in the uptake of Mo by solids (Vorlicek et al., 2004). Sub-micron-sized FeS, pyrite and greigite (Fe_3S_4) particles have been measured in anoxic waters (Cutter and Kluckhohn, 1999). Dissolved S(0) is difficult to measure and tends to be metastable with respect to sulphide and sulphate (Helz, 2014). While some pyrite is undoubtedly formed as a secondary mineral at low temperatures and coprecipitates some Mo, this process has not yet been sufficiently well-characterised over a broad range of conditions to be incorporated into the databases. We explore (Section 6.2) the impact that a proposed putative $Fe_5Mo_3S_{14}$ phase (Helz et al., 2011) could have on speciation but again this has not yet been incorporated in any of the above-mentioned databases and seems unlikely to account for all of the relevant observations.

Characterising the geochemical environment in terms of the amounts and nature of the various solid phases present can also be challenging. Where geochemical gradients are large and timescales relatively short, such as at redox boundaries, various poorly-ordered and thermodynamically-unstable phases may be formed and can play an important role in determining the behaviour of trace elements such as Mo. These solids tend to be appreciably more soluble than their well-crystallised counterparts.

These transitory (in a geological sense) phases often have high specific surface areas and so sorption reactions can be important, especially for trace elements. This in turn requires associated 'sorption databases' (Brendler et al., 2003). The mechanism leading to the accumulation of Mo in black shales over geologic timescales might depend on a completely different set of reactions (Bostick

et al., 2003).

At a more fundamental level, there are challenges relating to the activity models used and how the activity coefficients are defined. This applies particularly to saline environments where ionic interactions are greatest (Pitzer vs Specific Ion Interaction Theory models) and where the databases are less well-developed. Measurements are also often restricted to temperatures around 25 °C and the behaviour away from this is correspondingly poorly understood.

In the absence of measured thermodynamic data, it may be necessary to estimate values of missing data and various approaches for doing this have been adopted usually based on LFERs (Linear Free Energy Relationships). The absence of thermodynamic data for a species does not imply that such a species is unimportant!

6.1.2. Oxic conditions

Molybdenum(VI) is the stable oxidation state under oxic conditions. It forms various protonated species depending on pH, total Mo concentration and ionic strength. Even for relatively simple systems, there can be quite large differences in the calculated speciation depending on the database used (Fig. 4). There is universal agreement that under oxidising conditions, the molybdate ($Mo(VI)O_4^{2-}$) ion dominates above pH 5–6 but at lower pH values and at relatively high Mo concentrations, polynuclear species dominate. This involves a change in Mo coordination number from 4 (tetrahedral) to 6 (octahedral). The precise set of polynuclear species formed is still a matter of debate but potentiometric, UV-spectrophotometric and ^{95}Mo NMR data suggest species mainly with 6–8 Mo atoms. Under very acidic conditions (pH < 2) and high Mo concentrations, clusters with 13, 18, 19 or more Mo atoms may form (Cruywagen et al., 2002). Under even more acidic conditions (pH ≤ 0), depolymerisation occurs and the MoO_2^{2+} species is again formed (Stiefel, 1977).

Polynuclear species are only formed at relatively high concentrations of Mo, normally above about 10^{-4} mol/kg water (Fig. 4). This is reflected in all four of the databases examined. The primary data for some of the most important experiments studying the formation of polynuclear species were acquired at high ionic strengths (up to 3 M) and the reported stability quotients were conditional on these conditions. Some databases have attempted to correct the data to log K values at zero ionic strength, others have not. Clearly, it is best if corrections are made and guidelines for doing this have been given (Grenthe et al., 2013).

Below pH 6 and for low Mo concentrations, two protonated forms are found, notably $HMoO_4^-$ and H_2MoO_4. H_2MoO_4 is sometimes written as MoO_3 but is perhaps more correctly written as $MoO_3(3H_2O)$ from a structural point of view (Oyerinde et al., 2008). $HMoO_4^-$ is not usually a dominant species, as indicated by the predominance diagrams prepared from both the ThermoChimie and HATCHES databases. This is because there is a change of geometry going from tetrahedral $HMoO_4^-$ to octahedral $MoO_3(3H_2O)$, which means that the usual step rule for the difference between successive dissociation constants of polyprotic acids (Δ log K~ 5) is no longer followed. Below pH 3, the species $MoO_2OH(3H_2O)^+$ has been suggested (Cruywagen and Heyns, 1987; Cruywagen, 1999; Cruywagen et al., 2002). All of these species equilibrate rapidly, i.e. within the time of mixing.

In summary, since most oxic natural waters have a pH greater than 6 and Mo concentrations orders of magnitude less than that

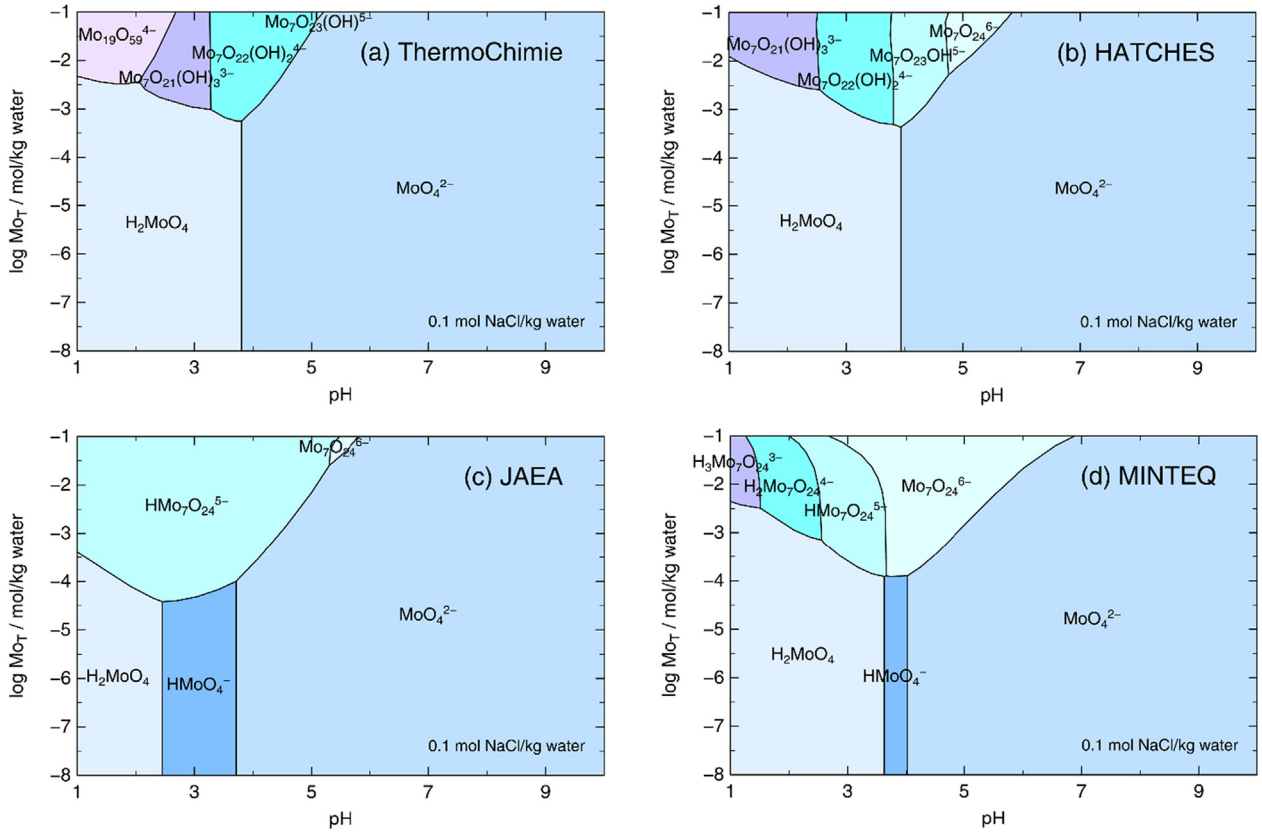

Fig. 4. Predominance diagrams showing the dominant species in the Mo-H_2O system calculated using four different databases (Table 8). Aside from the different naming conventions used for the same species, the diagrams show a considerable variation in the dominant set of polynuclear species present at high Mo concentrations and low pH. The importance of the intermediate $HMoO_4^-$ species also varies between databases.

required for polynuclear species formation, MoO_4^{2-} is expected to be the dominant solution species in all such waters. It may be complexed to a minor extent with other ions such as Ca^{2+} and Mg^{2+}. Under mildly acidic conditions, protonated species may occur, but their concentration is expected to be very low because these are precisely the conditions under which adsorption to minerals and organic matter is strongest (Section 6.2.2). Only in exceptional circumstances, as with acidic drainage from near Mo-rich mines and ore bodies, are the more exotic polynuclear species likely to be found.

6.1.3. Suboxic and anoxic conditions

'Blue waters' were first recognised by Native Americans near Idaho Springs, CO, USA (Müller and Serain, 2000; Liu et al., 2003). A sample of dark, greenish blue, highly acidic drainage emanating from a mine tunnel in the area was analysed by R. C. Wells in 1916 and found to contain approximately 5 g/L Mo (Campbell, 1923; Clarke, 1924; Horton and Laney, 1916). This probably consisted predominantly of colloidal ilsemannite ($Mo_3O_8.nH_2O$) – some lack of transparency of the water was also reported – resulting from the partial oxidation of molybdenite (MoS_2). Given the circumstances, the presence of at least some dissolved heteropolymolybdates also remains a strong possibility.

Deep "molybdenum blue" solutions can be produced readily in the laboratory by the reduction of acid molybdate solutions with $SnCl_2$ or dithionite, resulting in the slow formation of giant wheel-shaped Mo_{154} anionic clusters containing both Mo(VI) and Mo(V) (Gouzerh and Che, 2006; Nakamura et al., 2015). The deep blue colour reflects the large number of delocalised electrons. Mo also readily forms mixed metal polyoxomolybdates (POMs) as well as reduced heteropolymolybdate complexes containing P, Si, V and W. The blue reduced heteropolymolybdate complexes, first discovered by the Swedish chemist Scheele in 1778, are well-known for their role in the classical analysis of P (as $PMo_{12}O_{40}^{3-}$), Si, As and Ge. A yellow Mo(V) complex is formed when MoO_4^{2-} is mixed with thiocyanate (SCN^-); this has also been used to analyse Mo. Addition of tartrate/$TiCl_3$ rapidly reduces Mo(VI) to Mo(V) (Spence and Heydanek, 1967).

The thermodynamic literature on reduced Mo oxidation states in aqueous systems is sparse and the primary data often date back more than 50 years. While the reduced Mo(V) species MoO^{3+}, $Mo_2O_3^{4+}$ and $Mo_2O_4^{2+}$ are believed to exist, at least under laboratory conditions (Mitchell, 1966), their presence under environmental conditions is much less certain and the corresponding thermodynamic data are not widely accepted. Of the databases listed in Table 8, the HATCHES database is the only one that includes data for the MoO_4^{2-} - > MoO_2^+ reduction reaction. The variation of Mo speciation with redox can be explored using the existing databases although from what has been said above, these do not yet capture all of the important processes and may even be misleading.

The ease with which the reduction of different oxidation states can occur varies with species and gives rise to a sequence of changes sometimes referred to as the 'redox ladder'. At pH 8 and at trace concentrations, the ease of reduction for the most probable reactions follows the approximate sequence: $O_2 > NO_3^- > MnO_2(s) > Cr(VI) \sim Se(VI) > Fe(III) > \sim V(V) > As(V) > U(VI) > SO_4^{2-} \sim Mo(VI) > CO_2 > H_2O$. This sequence varies with pH and concentration but broadly follows the sequence seen in reduced ('gley') soils, stratified lakes and oceans, and confined aquifers as the water 'ages'. It suggests that Mo reduction from Mo(VI) to Mo(V) requires strongly reducing conditions similar to those required for sulphate reduction. Groundwaters containing dissolved $CH_4(g)$ and even $H_2(g)$ are not uncommon. Eh values of less than 0 V at near-neutral pH are quite common. Given that highly reducing conditions do exist naturally, surprisingly few studies have attempted to identify whether the Mo(VI) - > Mo(V) reduction reaction actually takes place in natural waters.

Some field and laboratory evidence suggests that Mo(VI) may be transiently reduced to Mo(V) by sulphate-reducing bacteria, leading ultimately to the formation of $MoS_2(s)$ (Wang et al., 2011). The protonated Mo(V) species is known to form a dimer readily at high concentrations in the laboratory (Spence and Heydanek, 1967) and has been speculated to do so under natural conditions (Dahl et al., 2013a). Wang et al. (2011) used their Mo(V)/Mo(VI) separation technique to speciate Mo in some sediment porewaters and showed that Mo(V) was often detected although it was only ever a minor proportion of the total Mo, normally <10% (Wang et al., 2011). However, their speciation scheme relies on the quantitative separation of Mo(V) and Mo(VI) species on a resin – only the Mo(V) is retained – and more work is required to demonstrate that this is always the case. It could also be that the Mo(V) is associated with natural dissolved organics such as fulvic acid. Therefore, the unambiguous presence of 'free' Mo(V) species in natural waters is difficult to sustain at present.

Fig. 5 shows the calculated change in speciation with the progressive reduction of $O_2(g)$ fugacity in a Mo-S-H_2O system under conditions where the concentration of polynuclear species would be expected to be minimal. This figure is based on the HATCHES database. If Mo(V) species are excluded, then free MoO_4^{2-} dominates over the whole range of conditions except when sulphide species begin to dominate the S speciation and polysulphides form (Kendall et al., 2017).

Calculations of the redox speciation of Mo (Fig. 5) show that the inclusion of the Mo(VI) → Mo(V) reduction reaction has a large impact on the calculated speciation in reduced systems. The reduced MoO_2^+ species dominates the speciation in strongly anoxic conditions. This is important since its inclusion will have a large effect on the activity of the MoO_4^{2-} species with a knock-on effect on the interpretation all other species that depend on the MoO_4^{2-} activity. Vlek and Lindsay (1977) also included data for MoO_2^+ formation based on the data of Titley (1963) but they used a much lower log K value (19.85 cf. 26.46) and the experiments and data analysis of Titley are unconvincing. Reddy et al. (1990) did not include this reaction in their review and most modern studies have not considered it (Erickson and Helz, 2000; Chappaz et al., 2008; Helz et al., 2014; N. Yang et al., 2015). Mohajerin et al. (2016) do discuss the reduction of Mo(VI) in some detail and suggest that, at least for the Titley data, inclusion of MoO_2^+ is likely to be an artefact of data analysis since the paper ignored the formation of polynuclear species where they are expected to exist and managed to produce Mo(V) without adding a reducing agent. Our conclusion is that the available data for MoO_2^+ are not yet of sufficient quality to merit inclusion in thermodynamic databases.

The HATCHES database also includes data for the formation of $Mo(V)O^{3+}$, $Mo(V)OCl_3$ and Mo^{3+} species although there are no data for the hydrolysis of Mo^{3+} (Wang et al., 2010). None of these species is as critical as MoO_2^+ since they only become significant under quite acidic conditions and low Eh. For most natural waters, they can be safely ignored.

Reduction of Mo(VI) in the presence of other ligands, both inorganic and organic (Wang et al., 2009), is more feasible but in an experimental study of the formation of Mo(VI) polysulphides by UV-VIS spectrophotometry, Erickson and Helz (2000) did not find any evidence for the reduction of Mo(VI) species by sulphide over 60 days.

Under reducing conditions characteristic of some natural waters, a wide range of aqueous complexes with S are formed, albeit with Mo still assumed to be in the Mo(VI) oxidation state. This includes a series of thiomolybdates in which S^{2-} replaces the O^{2-} in $Mo(VI)O_4^{2-}$ in a stepwise manner all the way to tetrathiomolybdate,

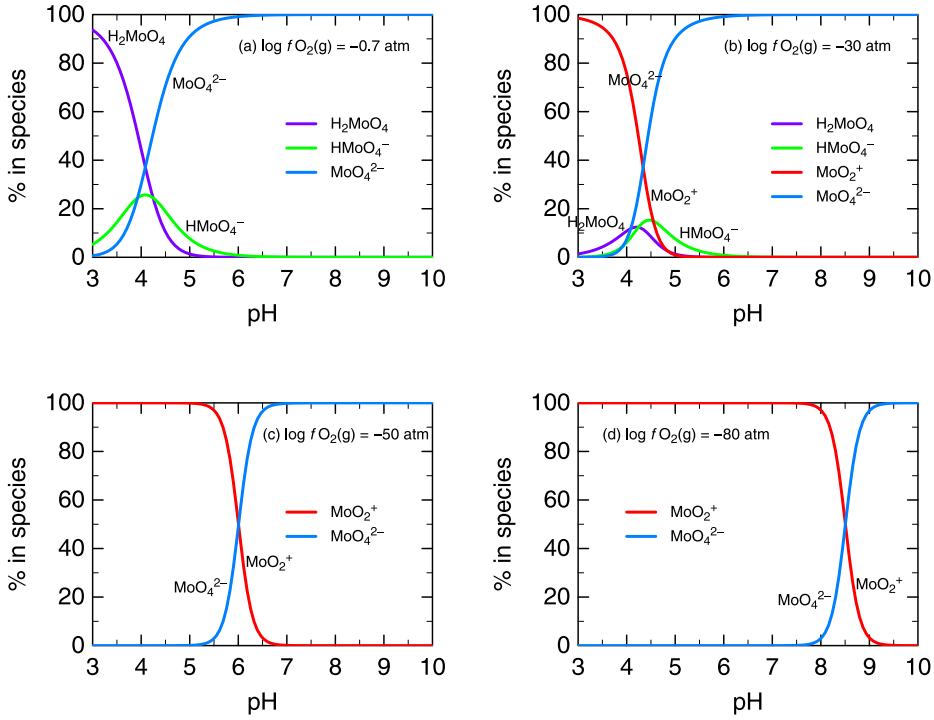

Fig. 5. Calculated variation in the aqueous speciation of molybdenum based on data from the HATCHES thermodynamic database including the reaction for the contentious reduction of MoO_4^{2-} to MoO_2^+. The redox status is controlled by equilibration with an atmosphere of increasingly low oxygen fugacity (a)–(d). This varies from (a) −0.7 atm (near atmospheric) to (d) −80 atm (strongly anoxic), a range that spans much of the stability domain of water. The total Mo concentration is 10^{-4} mol/kg water in all cases and the background solution contained 0.01 mol NaCl/kg water. No solids were allowed to precipitate. Note that reduction of $Mo(VI)O_4^{2-}$ to $Mo(V)O_2^+$ is most significant at lower pHs but eventually dominates the speciation over much of the pH range at log fO_2(g) = −80 atm (d).

$Mo(VI)S_4^{2-}$. The transformation to tetrathiomolybdate is believed to take place in four increasingly slow steps: $MoO_4^{2-} \rightarrow MoO_3S^{2-}$ (~5 h), $MoO_3S^{2-} \rightarrow MoO_2S_2^{2-}$ (50 h), $MoO_2S_2^{2-} \rightarrow MoOS_3^{2-}$ (60 d) and $MoOS_3^{2-} \rightarrow MoS_4^{2-}$ (1.5 yr) (Dahl et al., 2010). This ligand-exchange process involves S derived from H_2S and O loss to H_2O. The final conversion of $MoOS_3^{2-}$ to MoS_4^{2-} may be very slow because it involves an intermediate ligand-induced reduction reaction with polysulphides (Vorlicek et al., 2004). The first three steps are thought to be sufficiently fast to allow complete equilibration in natural waters but the final conversion of $MoOS_3^{2-}$ to MoS_4^{2-} occurs over a sufficiently long timescale that complete equilibration within the water column may not always be achieved, e.g. in seasonally or sporadically-disturbed euxinic basins such as the Baltic Sea (Nägler et al., 2011). The conversion can be catalysed by H^+ and NH_4^+. Erickson and Helz (2000) suggested that when the concentration of sulphide was slowly being increased, a sharp increase in the rate of conversion occurred at a dissolved H_2S(aq) concentration of approximately 11 μM, creating a type of geochemical 'switch'. Later, Helz et al. (2011) suggested that the H_2S(aq) concentration alone is not so critical and that the pH and concentration of reactive Fe also plays a part (Helz et al., 2014). In the presence of large concentrations of Fe^{2+}, soluble iron-containing thiomolybdates can also form and so reduce tetrathiomolybdate activity.

Removal of thiomolybdates by binding to various minerals including FeS (Helz et al., 2004), pyrite (e.g. Bostick et al., 2003; Vorlicek et al., 2004) and unspecified Mo-(Fe)-S phases (Dahl et al., 2013a) has been demonstrated or suggested. The thiomolybdates also react with natural organic matter (Anbar et al., 2007; McManus et al., 2006; Parnell et al., 2015). In other words, the thiomolybdates are relatively reactive. The replacement of O by S lengthens and weakens the bond to the central Mo atom. It is this formation of thiomolybdates that leads to the dramatic reduction of Mo concentrations in strongly reducing natural waters (Scott and Lyons, 2012) and it is the lack of such formation in oxic waters that accounts for the remarkably unreactive ('conservative') nature of Mo in most seawater.

In the presence of S and anoxic conditions, a variety of sulphur ligands will exist and these can play an important role in the speciation of many trace metals (Wang and Tessier, 2009), including Mo (Azrieli-Tal et al., 2014). Low pH favours the formation of polysulphides and in euxinic basins such as the Black Sea, the pH is lowered to less than pH 8 by extensive microbial sulphate reduction, decomposition of organic matter and CO_2 release, thereby favouring the formation of polysulphides. Many of the sulphur species are sensitive to pH in the pH 7–8 range.

There are a number of reports of bacteria, including sulphate-reducing bacteria (SRBs), reducing Mo(VI) and even producing molybdenum blue in laboratory situations (Biswas et al., 2009; Shukor et al., 2010; Tucker et al., 1998, 1997). Molybdenum can be reduced by dead cells and result in Fe-free, Mo(IV)-sulphide compounds with molecular structures similar to Mo enzymes (Dahl et al., 2016).

6.2. Molybdenum minerals and surface reactions

6.2.1. Minerals

Molybdenum, W, U, V and Cr are all redox-sensitive elements that form highly insoluble minerals under certain reducing conditions. U, V and Cr form insoluble oxides and hydroxides – and are therefore very sensitive to pH. Molybdenum is most insoluble when it forms a Mo-S mineral and so is also sensitive to H_2S concentrations.

Pyrite invariably contains measurable amounts of Mo as a solid

solution (Table 4) and was originally thought to be the main host for Mo binding in euxinic conditions. However, while the content of Mo in some pyrites can be high (0.5–5.8%), the relatively low abundance of pyrite in euxinic muds and shales means that it probably accounts for <20% of the total Mo in sediments (Chappaz et al., 2014). Harrison et al. (1973) found much lower Mo contents in pyrite extracted from the Green River Formation Oil Shales of Wyoming, Utah and Colorado, USA, ranging between 25 and 185 mg/kg (mean 116 mg/kg or 0.0116%). The range of Mo contents in pyrite shows some relation with age of rock formation, being higher in younger formations (Gregory et al., 2015) (Table 4). As pyrite recrystallises over time, impurities including Mo tend to be ejected and the pyrite becomes purer. In a detailed laser-ablation study of pyrite from 114 black shales, Gregory et al. (2015) found that Mo was significantly depleted in Archean pyrite and enriched in Cenozoic pyrite, with a minor enrichment in the Proterozoic through to Mesozoic. A simple analysis based on age alone is complicated by the secular increase of Mo in ocean water over time, as well as variable ocean redox status over space and time which would, for example, have altered the supply of Mo-bearing Mn particles to the bottom waters. It is therefore unclear whether the variations are due to primary supply or to post-depositional effects. Texture is also significant, for example, framboidal pyrite tends to contain larger quantities than microcrystalline pyrite (Gregory et al., 2015).

As a result and contrary to early expectations, there is now overwhelming evidence from analysis of sediments in euxinic basins that neither molybdenite nor its amorphous polymorph, nor even pyrite are the predominant sinks for Mo in these sediments (Dahl et al., 2013a). The precise mechanisms involved remain unknown but it appears that Mo could be immobilised in some form of Fe-Mo-S structure. Helz et al. (2011) proposed a putative Mo(VI) mineral with stoichiometry $Fe_5Mo_3S_{14}$ whereas Dahl et al. (2013a), using EXAFS (extended x-ray absorption fine structure) and XANES (x-ray absorption near-edge structure), suggest a structure more akin to the Mo-Fe-S structure found in nitrogenase enzymes, with Mo locally reduced to the very O_2-sensitive Mo(IV) state. They suggest that a possible pathway is via initial formation of Mo(VI)-thiomolybdates, with the reduction of the $Mo(VI)OS_3^{2-}$ species to form Mo(IV)-polysulphide species. This is aided by metastable, zero-valent dissolved sulphur (S_8) which is invariably found in euxinic waters. These highly reactive thiomolybdates could then be scavenged by amorphous FeS to end up within a Mo-Fe-S compound. The role of organic matter in this scenario remains unclear even though the Mo content of black shales often correlates better with organic matter content than with Fe content. It may be that the final scavenging of the Mo(IV)-polysulphide species is by organic matter (Wirth et al., 2013).

Molybdate, like phosphate, also forms many relatively insoluble metal molybdates of which probably the most important are powellite ($CaMoO_4$) and magnesium molybdate ($MgMoO_4$), minerals normally associated with hydrothermal environments. Seawater is undersaturated with respect to powellite by three orders of magnitude (Helz et al., 1996). Powellite has been observed in sediment cores from a limestone aquifer (Pichler and Mozaffari, 2015) and might be expected where Mo concentrations could be particularly high, as in weathered spent oil-shale deposits (Essington and Huntington, 1990). Similar considerations apply to the yellowish mineral, molybdite (MoO_3). Its significance is likely to be restricted to environments where the ore is exposed to weathering. The solubility product of $MgMoO_4$ in the current Thermochimie database (−0.64) needs confirmation as it is seven orders of magnitude greater than that given for $CaMoO_4$ (−7.90) and an order of magnitude greater than that in the minteq.v4.dat database (−1.85).

Compared with pyrite, molybdenite is resistant to bacterial attack, bioleaching being relatively slow (Olson and Clark, 2008). Microorganisms can apparently be poisoned by the released Mo unless this is subsequently sequestered by, for example, iron oxide (Dold and Fontboté, 2001; Ehrlich, 1996).

6.2.2. Sorption

All fine-grained minerals can provide surfaces for sorption reactions and this becomes increasingly important for trace elements such as Mo which are present at low concentrations and where solubility products for pure Mo minerals are less likely to be achieved. Ion exchange is not important for Mo binding in the environment because permanently-charged clays such as smectites are negatively charged and will repel negatively-charged MoO_4^{2-} ions, leading to a small amount of 'negative adsorption'. Also, ion exchange which is based on a smeared-out surface charge, is not sufficiently selective for trace ions to compete with major ions such as HCO_3^-.

There have been many laboratory studies of the sorption of Mo by various minerals and natural organic matter. These provide a basis for understanding the sorption behaviour of Mo in more complex natural environments: waters, sediments and soils, and are summarised in Table 9. Most studies have concentrated on the sorption or uptake of Mo but the reverse is also true: if conditions change appreciably then desorption can occur, e.g. as a result of an increase in pH. Under more extreme conditions, the solid involved might dissolve and release some or all of its scavenged Mo, e.g. by reductive dissolution of Mn (Chaillou et al., 2008) or Fe oxides (Bennett and Dudas, 2003; Chappaz et al., 2008; Smedley et al., 2014a), or in the case of organic matter, by degradation.

6.2.3. Oxides

Enrichments of Mo in oxic sediments are often attributed to adsorption onto Fe and Mn oxides (Kaback and Runnells, 1980; Barling and Anbar, 2004; Chappaz et al., 2008; Goldberg, 2009). The less visible aluminium oxides and hydroxides are also likely to be significant given their abundance and proven importance for phosphate binding (Slomp et al., 1996). The affinity of sorption to Fe and Al oxides in soils has been demonstrated by the positive correlation of Mo with both extractable Fe, e.g. Karimian and Cox (1978) and Al (e.g. Barrow, 1970). Studies with pure oxides have also demonstrated this. Aluminium oxides and hydroxides are known to bind Mo (Jones, 1957; Reisenauer et al., 1962; Goldberg and Sposito, 1984; Goldberg et al., 1996). Gustafsson and Tiberg (2015) found from EXAFS and XANES evidence that $Al(OH)_3$-type compounds, possibly allophane, were important for the binding of Mo in a soil from a strongly acidic, organic-rich Bs horizon of a podzol with abundant oxalate-extractable Al.

The characteristics of this sorption are now quite well understood. Adsorption of molybdate to Fe and Al oxides increases with decreasing pH but sometimes exhibits a weak maximum at pH around 4–5 (Goldberg et al., 1998, 1996; Gustafsson, 2003). This makes Mo binding by oxides particularly important in acid soils and can even limit the plant-availability of the metal as in some Australian soils (Brennan et al., 2004). Many oxides tend to dissolve below pH 3–4, limiting sorption in very acidic systems such as in acid mine drainage. Sorption is considerably reduced under pH-neutral and alkaline conditions such that there is little sorption above pH 8 (Goldberg et al., 1996; Harita et al., 2005; Xu et al., 2013; Gustafsson and Tiberg, 2015). This general behaviour applies to all oxides: adsorption to Mn (Balistrieri and Chao, 1990) and Ti (Xu et al., 2013) oxides also decrease with increasing pH. The surface chemistry of Mn oxides is probably the most variable and least well-understood of the common oxides – the point of zero charge (pzc) can vary from pH 1.5 to 7.3 depending on its crystalline form

Table 9
Laboratory studies that have investigated the binding of molybdenum by various minerals and natural organic matter.

Material	Method	Comment	Reference
Iron oxides			
Ferrihydrite ($Fe_2O_3.1.8H_2O$)	pH dependence	pH 1–10. Sharp decline in sorption at pH > 8	Jones (1957)
Goethite (α-FeOOH)	Isotherms at constant pH, electrophoresis, Bowden	Max at pH 3.5, sorption related to surface area for difft minerals	McKenzie (1983)
Ferrihydrite ($Fe_2O_3.1.8H_2O$)	Competitive sorption	At pH 6.5 and 0.1 M $NaClO_4$, selectivity was P > As=Se(IV) >Si > Mo > SO_4>Se(VI)	Ryden et al. (1987)
Goethite (α-FeOOH)	Pressure jump, kinetics, Triple Layer	pH 2–8, 0.01, 0.05, 0.10 M $NaNO_3$. Kinetics in <1 s. Two steps: ion pair formation (fast) then ligand exchange (slow)	Zhang and Sparks (1989)
Ferrihydrite ($Fe_2O_3.1.8H_2O$)	Triple layer model	pH 7: P > Si > Mo > F > SO_4. Binuclear inner-sphere complexes	Balistrieri and Chao (1990)
Ferrihydrite ($Fe_2O_3.1.8H_2O$)	Langmuir	Max at pH 4–5, 2.4 μmol/m^2	Bibak and Borggard (1994)
Goethite (α-FeOOH)	Langmuir	Max at pH 4–5, 3.6 μmol/m^2	Bibak and Borggard (1994)
Ferrihydrite ($Fe_2O_3.1.8H_2O$)	EXAFS	After high temperature annealing, Mo at the surface inhibits crystal growth	Zhao et al. (1994)
Ferrihydrite, hematite, goethite	Electrophoresis, Constant Capacitance	pH 3–11, max pH 4–5, low sorption above pH 8, constant ionic strength	Goldberg et al. (1996)
Goethite (α-FeOOH)	Competitive sorption, electrophoresis, CC model	pzc (iep) = 8.7, Mo, As, P sorption pH 2–11.5. Also Mo + P competition	Manning and Goldberg (1996)
Goethite (α-FeOOH)	Isotherms	%sorbed-pH plots at 1.25 g solid/L and 25 g/L, pH 2–10.5, two initial Mo concs, little ionic strength dependence	Goldberg and Forster (1998)
Goethite (α-FeOOH)	CD-MUSIC model	Measured H^+-MoO_4^{2-} exchange ratio. Also SEO_3^{2-}, CrO_4^{2-}, WO_4^{2-}, SeO_4^{2-} and SO_4^{2-}	Rietra et al. (1999)
Ferrihydrite ($Fe_2O_3.1.8H_2O$), goethite (α-FeOOH)	DLM, CD-MUSIC models	pH 3–10, WO_4^{2-} > MoO_4^{2-}. Also P sorption, P-Mo, As-Mo and P-W competition. Two monodentate complexes fitted both models	Gustafsson (2003)
Goethite (α-FeOOH)	Desorption kinetics, DOM, SEM, XRD	Dissolved organic matter (DOM) slows down diffusion of Mo into and out of oxide	Lang and Kaupenjohann (2003)
Akaganeite (β-FeOOH)	Kinetics, Freundlich	Fitted 2nd-order kinetic model	Lazaridis et al. (2003)
Goethite (α-FeOOH)	Competition, CD-MUSIC	W and P competitors, Si and SO_4 not	Xu et al. (2006a)
Goethite (α-FeOOH)	Electrophoresis, Thiomolybdate, Langmuir	pzc = 8.8, 44 m^2/g. pH 3–10. 0–50 μM Mo. Selectivity MoS_4^{2-} > MoO_4^{2-}. P always competes strongly, Si and SO_4 do not. Two monodentate surface complexes	Xu et al. (2006b)
Ferrihydrite ($Fe_2O_3.1.8H_2O$)	Kinetics, Langmuir	0-1300 min, near equilibrium in 1 h. Mo and V sorption measured separately and in competition with P pH 4–9. V > P & V > Mo	Brinza et al. (2008)
Ferrihydrite ($Fe_2O_3.1.8H_2O$)	Raman, ATR-FTIR, Triple layer model	pH 3.5–11.5. Compared with amorphous $Al(OH)_3$ which was greater on a wt basis. Inner sphere complexes for pH < 9.5	Goldberg et al. (2008)
Ferrihydrite, goethite, hematite and magnetite	$\delta^{98/95}$Mo, solid/solution ratio, surface area, Langmuir	Sorption at pH 6.9–8.0 leads to preferential uptake of lighter isotopes (Δ^{98}Mo 1.0–1.3‰) which is greater at pH 8.0 than pH 6.9. Ferrihydrite > goethite > hematite ≫ magnetite (wt basis) and hematite > ferrihydrite = goethite (area basis)	Goldberg et al. (2009)
Goethite (α-FeOOH)	XANES	pH 4–7. 60 m^2/g. 9 samples analysed	Arai (2010)
Ferrihydrite ($Fe_2O_3.1.8H_2O$), hematite, goethite	EXAFS	pH 4–9. 0.01 & 0.7 M $NaNO_3$. Kds shown	Kashiwabara et al. (2011)
Magnetite	Electrophoresis, kinetics, Triple Layer model, Langmuir, Freundlich	Magnetite is supported by zeolite (clinoptilolite). Pzc(iep) = 4.0. Ionic strength has little effect. Pseudo 2nd order kinetics. P competes, SO_4 does not. Sorption increases with temperature (4–40 °C)	Verbinnen et al. (2012)
Ferrihydrite ($Fe_2O_3.1.8H_2O$)	XANES/EXAFS, CD-MUSIC model	Fitted pH 3–10 adsorption edges in 0.01 M $NaNO_3$ with 50 μM Mo and 0.3, 1 and 3 mM Fe. Also competition from addition of 200 μM P	Gustafsson and Tiberg (2015)
Mixture of synthetic (Fe^{2+}/Fe^{3+} iron oxides)	XPS, TEM, magnetic properties	Ferromagnetic property aids coagulation during treatment of Mo-rich water	Ma et al. (2015)
Ferrihydrite ($Fe_2O_3.1.8H_2O$)	Electrophoresis, competition	$CaCl_2$ reduced sorption slightly. SO_4 and Si had no effect. P and HA reduced sorption	Zhang et al. (2015)
Ferrihydrite ($Fe_2O_3.1.8H_2O$)	XRD, Raman, TEM, EXAFS/XANES, logistic kinetics	Age ferrihydrite (270 m^2/g) at pH ~10 & 75 °C for up to 96 h transforms to mostly hematite (14 m^2/g) and irreversibly incorporates sorbed Mo as octahedral Mo replacing structural Fe^{3+}	Das et al. (2016)
Aluminium oxides			
Boehmite (α-AlOOH)	pH dependence, XRD	pH 3.8–10. Sharp decline in sorption at pH > 7. Crystalline Al molybdate formed at c. pH 5	Jones (1957)
Alumina	^{95}Mo NMR	pH 5.45–8.0: polymolybdates decompose within minutes of coming into contact with alumina	Luthra and Cheng (1987)
Alumina (γ-Al_2O_3)	^{95}Mo and ^{31}P NMR	Sorption of various molybdophosphates to make a catalyst	Cheng and Luthra (1988)
Alumina (γ-Al_2O_3)	temperature	pH 3.0–8.5, 10–55 °C	Spanos et al. (1990)
Al_2O_3 (synthetic)	Langmuir	Max at pH 4–5, 1.8 μmol/m^2	Bibak and Borggard (1994)
$Al(OH)_3$ (amorphous), gibbsite ($Al(OH)_3$), alumina	Electrophoresis, Constant Capacitance	Sorption pH 2–11, max pH 5. Material specific surface areas 210, 56 and 103 m^2/g, resp. pzcs	Goldberg et al. (1996)
Gibbsite (α-$Al(OH)_3$)	Competitive sorption, electrophoresis, CC model	pzc (iep) = 9.8, Mo, As, P sorption pH 3–11. Also Mo + P competition	Manning and Goldberg (1996)
Alumina (γ-Al_2O_3)	Freundlich, SRS	Mo-SO_4, Mo-Se(VI), Mo-Se(IV) competition	Wu et al. (2002)
γ-alumina		NTA and EDTA ligands reduced Mo sorption but increased Ni sorption	Al-Dalama et al. (2005)
$Al(OH)_3$ (amorphous)			Goldberg et al. (2008)

(*continued on next page*)

Table 9 (*continued*)

Material	Method	Comment	Reference
	Raman, ATR-FTIR, Triple Layer model	pH 3.5–11.5. Fe oxide compared with amorphous $Al(OH)_3$ which was greater on wt basis. Outer-sphere complexes at pH > 8	
Gibbsite	FTIR, CD-MUSIC model	pH 4, 6, 8. Inner-sphere. Bidentate corner-sharing complex. Mo-O 17.3 nm	Miedaner et al. (2011)
Zn-Al-SO_4 layered double hydroxide		LDHs may be useful for removing Mo in water treatment (pH 7–8). Much less efficient than for As. Possible $ZnMoO_4$ precipitation	Ardau et al. (2012)
$Al(OH)_3$ (amorphous)	XANES, EXAFS	Spectral data	Gustafsson and Tiberg (2015)
Manganese oxides			
Birnessite	Isotherms at constant pH	Max at pH < 1.5	McKenzie (1983)
MnO_2	Triple layer model	Mo ≥ P > Si > F > SO_4. Monodentate inner-sphere	Balistrieri and Chao (1990)
Birnessite	$\delta^{97/95}$Mo	$\delta^{97/95}$Mo (dissolved-adsorbed) = 1.9–1.6 ‰ from 1 to 50 °C.	Wasylenki et al. (2008)
Mn_3O_4	Freundlich	pH 1–6.5	Zhao et al. (2010)
δ-MnO_2	EXAFS/XANES	pH 8. Spectral data with log Kd vs pH plot for I = 0.01 and 0.7 M $NaNO_3$	Kashiwabara et al. (2011)
Birnessite	EXAFS, $\delta^{97/95}$Mo, DFT	Mainly spectral and isotopic data. Mo is polynuclear on the birnessite surface at high loadings	Wasylenki et al. (2011)
Birnessite	Kinetics, competitive sorption, FTIR, XRD, Freundlich, Langmuir	pzc = 7.3, pH 4–7. Competitive effect was Se(IV) > Se(VI) > P	Matern and Mansfeldt (2015)
Titanium oxides			
Titania	Adsorption, titration, electrophoresis	At pH 7.3 and about 2.3 wt% MoO_3, the surface is completely covered. Lower pH leads to multilayers	Spanos et al. (1992)
Titania (TiO_2)	CD-MUSIC model	Potentiometric titrations, H^+-MoO_4^{2-} titration, adsorption vs pH data. Mono- and bidentate surface complexes. At high concn and pH < 5.5, $Mo_7O_{23}(OH)^{5-}$ bound	Bourikas et al. (2001)
Anatase (TiO_2)	Temperature, Langmuir	Mo sorption decreases with increasing temperature	Saripalli et al. (2002)
Sulphides			
Pyrite (FeS_2)	XANES/EXAFS, Langmuir	41.7 m^2/g. Sorption decreases with increasing ionic strength and sulphide	Bostick et al. (2003)
Pyrite	Thiomolybdate, Langmuir	pH 3–10. Selectivity MoS_4^{2-} > MoO_4^{2-}. P always competes strongly, Si and SO_4 do not	Xu et al. (2006a)
Covellite (CuS)	CD-MUSIC model	Used iPhreeqc to fit zeta (ζ) potential-pH curves	Nduna et al. (2014)
Pyrite (FeS_2)	EXAFS, Langmuir	MoO_4^{2-}, MoS_4^{2-} and 2MPA sorption, pH 4.8–7.7. 2MPA > MoO_4^{2-}. Mo-S distance increases. Mo(VI)→Mo(IV) reduction during MoS_4^{2-} sorption but not MoO_4^{2-} sorption	Freund et al. (2016)
Natural organic matter			
Humic acid		Max at pH 3.5	Bibak and Borggard (1994)
Fulvic acid	XANES/EXAFS, SHM	Mo binding by Suwannee River FA through carboxylate groups (although thiols may also be important)	Gustafsson and Tiberg (2015)

(Healy et al., 1966). 'Natural birnessites' have hexagonal symmetry (not the triclinic symmetry of some birnessites), significant negative structural charge (Villalobos et al., 2003) and at pH 8 are negatively-charged (Balistrieri and Murray, 1982).

In laboratory studies, Balistrieri and Chao (1990) observed that at pH 7, the relative affinity of adsorption on MnO_2 followed the order molybdate > phosphate > silicate > fluoride > sulphate. Matern and Mansfeldt (2015) found the sequence: selenite > selenate > phosphate > sulphate for the effectiveness of displacement of Mo from birnessite. Molybdate has been found to have a lower affinity for hydrous ferric oxide compared to other oxyanions such as phosphate, arsenate, vanadate and tungstate (Gustafsson, 2003; Harita et al., 2005; Kashiwabara et al., 2013). Not surprisingly, phosphate competes with molybdate for sorption sites (Brinza et al., 2008; Gustafsson, 2003; Xu et al., 2006a). In the natural environment, Mo is readily captured by Mn oxyhydroxides and is often concentrated at the sediment-water interface (Bertine and Turekian, 1973; Calvert and Pedersen, 1993; Crusius et al., 1996; Erickson and Helz, 2000; Zheng et al., 2000a). Molybdate also sorbs to clays at low pH, in the order montmorillonite > illite > kaolinite, in line with their specific surface areas (Goldberg et al., 1996). This binding by clays probably occurs via exposed Al-O bonds at the edges.

Using sub-millimetre element mapping by XRF of marine ferromanganese oxides, Kashiwabara et al. (2013) found that Mo and W were bound more strongly to ferrihydrite than to δ-MnO_2 and that W binding to ferrihydrite was stronger than Mo, reflecting the difference between inner-sphere (ferrihydrite) and outer-sphere surface complexes (δ-MnO_2).

6.2.4. Sulphides

The presence of sulphide minerals in sediments is characteristic of deposition under strongly anoxic conditions. The most common authigenic iron sulphide minerals are pyrite (FeS_2) and its metastable precursors, mackinawite (FeS) and a poorly-ordered FeS mineral (Davison, 1991). Ore minerals such as galena (PbS) and sphalerite (ZnS) may be found in mineralised areas. The surfaces of these minerals provide plenty of opportunity for binding chalcophilic Mo.

There is also the possibility of Mo being incorporated into the bulk structure as a solid solution. It can be difficult to separate sorption from the formation of a solid solution especially from scavenging-type data alone. Additional information such as the behaviour of co-ions and the relative stoichiometry of their uptake/release, the reversibility and kinetics of the reaction, modelling as well as modern spectroscopic methods (Das et al., 2016) are needed for this. The difference is particularly difficult to distinguish when minerals are being freshly formed, e.g. at redox fronts. Experience from oxides, e.g. Ca^{2+} bound to Al gel (Kinniburgh et al., 1975), has shown that trace uptake on freshly-precipitated gels can be similar to that when the ions are co-precipitated together, i.e. coprecipitation can be largely by adsorption. This can change with time, loading, and the degree to which the adsorbed ions fit comfortably into the bulk structure (Prieto et al., 2013). Adsorption can merge

into surface precipitation at very high loadings.

Sorption of Mo by various S-containing minerals has been studied quite extensively. Conversion of molybdate to thiomolybdates has been found to favour the reaction. In strongly reducing environments, sorption of thiomolybdates to sulphide minerals, particularly amorphous FeS and pyrite, is likely to be more important than sorption to oxides. Both molybdate (MoO_4^{2-}) and tetrathiomolybdate (MoS_4^{2-}) are sorbed by pyrite (FeS_2) with sorption is greatest under acid conditions (pH 4 to 5), as seen with oxides and clays (Freund et al., 2016). MoS_4^{2-} tends to be slightly less strongly sorbed than (MoO_4^{2-}) especially at high pH (ca. pH 9). P-Mo competition is likely to reduce Mo sorption somewhat both on oxides and sulphide minerals (Xu et al., 2006b). Competition from sulphate and silicate are likely to be negligible.

Bostick et al. (2003) showed that molybdate was readily desorbed from pyrite at pH 9 whereas tetrathiomolybdate was not and suggested that molybdate formed labile outer-sphere surface complexes with pyrite whereas tetrathiomolybdate formed stronger inner-sphere complexes. This lack of reversibility in tetrathiomolybdate desorption may reflect the relatively large change in Mo coordination on sorption – Mo-Fe-S cubane-type clusters were proposed – and may be partly responsible for the enrichment of Mo in anoxic marine environments.

6.2.5. Organic matter

There is increasing evidence that natural organic matter could play an important, possibly even dominant, role in the binding of Mo in many soils and sediments. However, this evidence is almost entirely circumstantial as it is difficult to separate and quantify Mo-organic interactions under field conditions. The evidence comes from the strong correlations between organic matter and Mo in soils and sediments (Section 4.2), from selective extractions (Dold and Fontboté, 2001; Siebert et al., 2015), from experimental studies of the binding of Mo by natural organics, from XANES/EXAFS studies (Dahl et al., 2016) and from direct observation (Parnell et al., 2016). Indeed, Wichard et al. (2009) suggest that the strong binding of Mo to organic matter in top soils plays an important part in preventing Mo from leaching and thereby enables it to play its vital role in the accumulation and utilisation of soil N. Siebert et al. (2015) suggested that organic matter may be more important for Mo binding in Icelandic soils than Fe and Mn oxides.

Mo(VI) appears to be sorbed to some extent by most forms of natural organic matter, ranging from living and dead cellular material in sulphide-rich, reducing environments (Dahl et al., 2016), fresh seaweed (Bertoni et al., 2015) and humic-like materials (Albéric et al., 2000; Bibak and Borggard, 1994; Gustafsson and Tiberg, 2015; Linnik and Ignatenko, 2015; Wichard et al., 2009). While interesting, many of these studies are based on unnaturally low pH and/or high Mo loadings.

Often it is not possible to implicate organic matter directly in Mo binding because of its dispersed nature and the relatively low binding density expected. It is even harder to rule it out. There is more scope for organic matter to invoke binding in S-rich reducing environments (Helz et al., 1996; Marie et al., 2015) and there is now laboratory evidence to support this (Dahl et al., 2016). Overall, it appears that Mo can bind to natural organic matter but it does not appear to be particularly strong or selective except perhaps under sulphide-rich conditions. The balance between Mo scavenging by organic matter versus formation of a Mo-Fe-S mineral under euxinic conditions is presently much debated.

6.2.6. Models and surface speciation

Many attempts have been made to model Mo sequestration by minerals and natural organic matter particularly in terms of surface (sorption) reactions. These have employed the classical adsorption isotherms with their varying complexity and demands: Langmuir, Freundlich, Constant Capacitance (CC), Bowden, Diffuse Layer (DLM), Triple Layer (TLM), MUSIC/CD-MUSIC, WHAM/Model VI/SHM/Model VII, NICA-Donnan and Ligand Charge Distribution (LCD) (Table 9). Other approaches could be explored (solid solutions, surface precipitation and kinetic models) but mostly have not been. All models attempt to relate the amount of a substance bound to a surface to its concentration or activity in solution.

In practice, the simplest approach that fits the observed data has often been used. The frequent use of the Langmuir isotherm stands out, particularly for the all-important binding of Mo to sulphide minerals, but the fitted parameters show little consistency (Freund et al., 2016). Fitting of the Langmuir isotherm to experimental data is rather undemanding – it can fit most adsorption data reasonably well, but since it does not deal with electrostatic interactions explicitly, its scope is rather limited and it is not normally formulated to consider competition from other ions, even H^+/OH^-.

The increased availability of bright and tunable x-ray sources from synchrotrons has enabled the use of XANES (x-ray absorption near edge structure) and EXAFS (extended x-ray absorption fine structure) techniques to study the coordination of metals in solids and solutions. These techniques have been applied to Mo solids and adsorbed Mo and provide information on the oxidation state of the Mo (XANES) as well as bond lengths and nearest-neighbour distances (EXAFS) (Table 10).

The proposed mode of binding of molybdate to oxides has varied by mineral and author. An inner-sphere binding mechanism has been postulated for molybdate sorption onto goethite, ferrihydrite, montmorillonite and γ-Al_2O_3 (Goldberg et al., 1998, 1996; Xu et al., 2013) whereas adsorption to Al oxides and kaolinite (Goldberg et al., 2008) and ferrihydrite (Kashiwabara et al., 2013) has been attributed to an outer-sphere complex. Inner-sphere complexes form when the sorbed ions bind directly to the surface without an intervening layer of water molecules. Outer-sphere binding implies that a layer of water molecules – part of the ion's hydration sphere – is retained between the ion and the surface, meaning that the binding is predominantly electrostatic and implicitly less selective than with inner-sphere complexes. This distinction can provide some insight into the mechanism of binding, its strength and selectivity and can guide the way that surface complexation models are formulated. Under some conditions, a proposed structure can be inferred experimentally from estimated interatomic bond distances and coordination numbers. Wasylenki et al. (2011) used EXAFS to characterise the molecular structure of Mo sorbed to birnessite (MnO_2). They found that adsorbed Mo was probably present as an inner-sphere polymolybdate complex containing Mo in distorted octahedral coordination with multiple oxo bridging ligands linking the Mo atoms together.

XANES can provide information about the oxidation state of sorbed ions as well as their symmetry and coordination. For example, using XANES, Gustaffson and Tiberg (2015) showed that the sorbed Mo(VI) coordination was tetrahedral as in molybdate. In contrast, the Mo bound to an organic-rich acid soil was in a distorted octahedral coordination. The XANES spectra showed that the Mo(VI) had not been reduced to Mo(V) on sorption. Goldberg et al. (2008), using ATR-FTIR (attenuated total reflectance-Fourier transform infrared) spectroscopy, suggested that pH played a major part in determining the surface coordination for amorphous Fe and Al oxides – Mo forming mainly inner-sphere surface complexes at low pH but mainly outer-sphere complexes at pH > 5. Arai (2010) also used the XANES spectra to infer that a tetrahedral inner-sphere complexing was formed on goethite at near-neutral pH but that under acidic conditions, an inner-sphere complex formed in a mixed tetrahedral/octahedral arrangement.

The oxidation state of adsorbed MoO_4^{2-} sorbed on pyrite

Table 10
Oxidation state and coordination of molybdenum in or on various materials based on X-ray spectroscopy.

Material	Interpretation	Reference
Various inorganic solids ($Na_2MoO_4.2H_2O$, MoO_2Cl_2, MoO_3, MoO_2) and hydrothermal solutions	XANES/EXAFS shows distorted octahedral coordination for Mo(VI) in MoO_3 whereas Mo(IV) in MoO_2 is only slightly distorted. Sodium molybdate tetrahedral in solid and solution. No Mo-Cl complexes in near neutral solutions	Borg et al. (2012)
Goethite (α-FeOOH)	XANES showed that Mo(VI) changed from inner-sphere tetrahedral coordination to octahedral coordination with decreasing pH. Possible surface polymerisation	Arai (2010)
Iron oxides	Ferrihydrite: tetrahedral outer-sphere complex as in solution; goethite and hematite: mixed tetrahedral and octahedral inner sphere complexes	Kashiwabara et al. (2011)
Birnessite	Mo is polynuclear on the birnessite surface in distorted octahedral coordination with O	Wasylenki et al. (2011)
δ-MnO_2 and two ferromanganese oxides	Distorted octahedral inner sphere complexes. Sorption by natural FeMn oxides similar to Mn oxide not Fe oxide	Kashiwabara et al. (2011)
Pyrite (FeS_2)	MoO_4^{2-} sorption is bidentate whereas MoS_4^{2-} sorption is tridentate (face sharing) with a Mo-Fe-S cubane structure	Bostick et al. (2003)
Fulvic acid	Mo binding by carboxylate groups	Gustafsson and Tiberg (2015)
Live/dead cells of SRB, lake sediment	Live and dead SRB cells/Lake Cadagno sediment in sulphide-rich environment showed Mo oxidation state between 4 (MoS_2) and 6 (thiomolybdate). 2–4 Mo-S (and 1–2 Mo-O) ligands similar to that in Moco enzymes but lower than in MoS_2	Dahl et al. (2016)
Lake Cadagno sediments	Oxidation state falls into two groups: (i) 4.1–4.5 where Mo-S ligands dominate (but differ from MoS_2 and MoS_4^{2-}) and have a cubane-like structure; (ii) 5.3–5.5 where there is a mixture of Mo-S and Mo-O ligands. Stable over time when buried	Dahl et al. (2013a)
Black shale (Utica)	EXAFS showed that Mo is bound to 2–2.5 O atoms at a distance of 1.71–1.72 Å, to S at 2.41–2.43 Å and to Mo at 3.18–3.20 Å suggesting presence of an organic Mo species and molybdenite (MoS_2) created following thermal maturation and remobilization. Mean oxidation state (XANES) of Mo was 4.9–5.4.	Ardakani et al. (2016)

measured by XANES was about 5.5, as for pure molybdate standards, and contrasts with that of adsorbed MoS_4^{2-} which was 4 (Freund et al., 2016). EXAFS also showed that the Mo-S internuclear distances remained unchanged upon MoO_4^{2-} adsorption in contrast to MoS_4^{2-} sorption where it lengthened slightly. Freund et al. (2016) found that Mo was only reduced when it was adsorbed by pyrite as MoS_4^{2-} (not as MoO_4^{2-}), supporting the ligand-induced reduction described by Vorlicek et al. (2004).

The relatively similar redox potentials of Mo(IV), Mo(V) and Mo(VI) redox couples leads to small redox steps and may be a contributory factor accounting for the importance of the Moco and FeMoco cofactors in enzymes. The Moco enzymes have Mo at the active centre coordinated via S to one or two pterin ligands and usually one or two oxo groups depending on the oxidation stat of the Mo centre (Kendall et al., 2017). The coordination of Mo with natural organics is largely unknown but if it is important, it is likely to be dominated by humic-type compounds because of their abundance and heterogeneity. Given the importance of S-containing moieties – thiols, siderophores (Bellenger et al., 2008) – in binding Mo in cellular material, it is likely that these will also play an important role in humics even though their abundance may be substantially less than carboxylic functional groups (Gustafsson and Tiberg, 2015). The S and redox status of the environment is therefore likely to be an important factor in determining the importance of humics in binding Mo (Section 6.2.5).

Techniques such as XANES/EXAFS are important in that they provide an independent insight into surface coordination which can be used to constrain those chemical speciation models that are based on assumed molecular surface structures, e.g. CD-MUSIC. Although these x-ray techniques currently require rather high Mo loadings (in environmental terms), and so may involve some degree of surface polymerisation, this should become less of a problem as more intense light sources are built and detection limits lowered.

6.3. Predominance diagrams

Predominance diagrams show the predominant species for a given element in a system as a function of two variables, often pH versus some measure of redox status (pe, Eh, log $f\,O_2$(g)). They are useful for providing a quick oversight into the most important processes taking place in complex systems. They often are limited to dissolved and mineral species but can include solid solution and adsorbed species. Their appearance depends on the database used including log Ks and the species selected for inclusion. Indeed, predominance diagrams can be used to rapidly assess the significance of these choices.

Fig. 6 shows a set of eight predominance diagrams for the Mo-S-Fe-Al-H_2O system. The system has been chosen to reflect some of the major processes taking place in natural waters, including seawater, in so far as these have been captured in existing thermodynamic databases. The diagrams have been calculated using a full chemical speciation using Phreeqc/PhreePlot (Kinniburgh and Cooper, 2004; Parkhurst and Appelo, 2013) combined with the ThermoChimie database. Mo(V) species have not been included. The database has been supplemented with some additional data for adsorption onto hydrous ferric oxide (HFO) and gibbsite surfaces as well as a putative $FeMo_{0.6}S_{2.8}$ species (equivalent to $Fe_5Mo_3S_{14}$). Only the most 'labile' solid species have been considered which means for example that molybdenite (MoS_2) and pyrite (FeS_2) were not considered, whereas FeS(am) and $FeMo_{0.6}S_{2.8}$ were. Adsorption by Mn oxides and organic matter has not been considered because the corresponding databases are not available.

Total concentrations of all elements were maintained across the calculation domain and are the same for each diagram. These were (in mol/kg water): Mo (5e-8), S (28e-3), Fe (27.8e-3), Al (50e-3), Na and Cl (c. 0.5). The calculated Mo speciation and dissolved S concentrations are very sensitive to the excess S present after FeS(am) has precipitated and to the stability of the $FeMo_{0.6}S_{2.8}$ phase. We found that we had to increase the log K for the $FeMo_{0.6}S_{2.8}$ phase from −8.3 (Helz et al., 2011) to −10 to obtain reasonable Mo uptake and dissolved S concentrations. This may reflect the slightly different systems considered, e.g. we included the $NaMoO_4^-$ species which reduces the MoO_4^{2-} activity whereas Helz et al. (2011) did not. Mohajerin et al. (2016) also suggested that this Fe-Mo-S compound may contain reduced Mo rather than Mo(VI).

Despite the obvious oversimplifications in such an analysis, the diagrams highlight some broad points: (i) under oxic conditions, Fe^{3+} is present mostly as HFO solid and this is an important control on Mo concentrations while it is stable (HFO dissolves under very

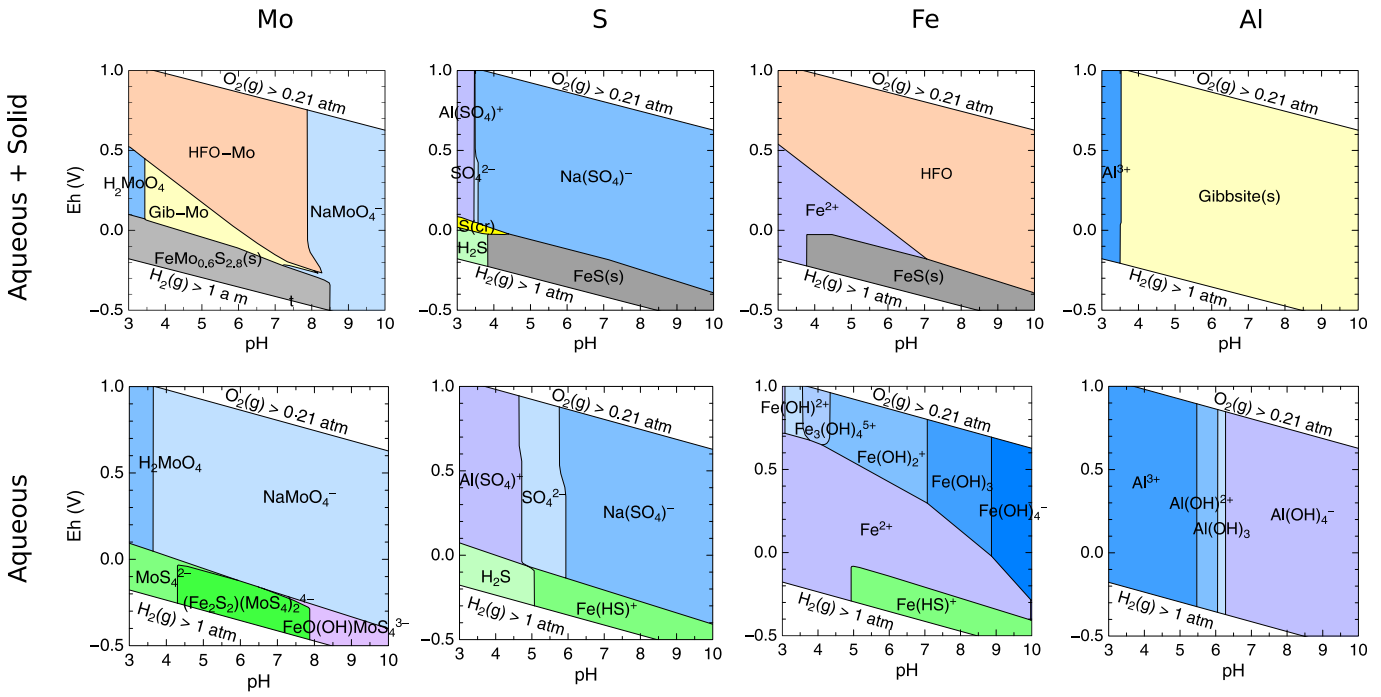

Fig. 6. Eight Eh-pH diagrams showing the predominant species for the same Mo-S-Fe-Al-O-H system. The system contains aqueous, mineral and adsorbed species. The upper row is when all species are considered including solid and adsorbed species while the lower row only includes the dissolved species found in the upper row. All calculations are based on the ThermoChimie database supplemented with additional data (see text). HFO-Mo and Gib-Mo are Mo adsorbed by HFO and Gibbsite, respectively.

acid and strongly reducing conditions); (ii) gibbsite is not sensitive to reductive dissolution and so is important as an adsorber when the HFO has dissolved; (iii) under strongly reducing conditions, FeS(am) becomes the main repository of Fe and S and the co-existing $FeMo_{0.6}S_{2.8}$ phase controls the dissolved Mo concentration; (iv) at high pH, even under strongly reducing conditions, dissolved Mo concentrations rise because sorption is low and the $FeMo_{0.6}S_{2.8}$ phase becomes unstable. The relative stability of FeS and Mo-Fe-S solid phases is critical to the fate of Mo.

An alternative view of Mo in the same system is to contour the Mo concentration against the same two 'master' variables (Fig. 7). This figure shows that Mo remains essentially completely dissolved above pH 8.5 – thereby accounting for its very conservative behaviour in seawater. Its concentration decreases gradually with increasing acidity under oxic conditions, and very abruptly at low Eh. This difference reflects the continuous variation in sorbed amount in contrast with the step change that occurs when a Mo mineral is formed. Calculated dissolved concentrations in the pH 8–Eh −0.2 V region, broadly characteristic of euxinic basins, show a large variation with only a small change in pH or Eh.

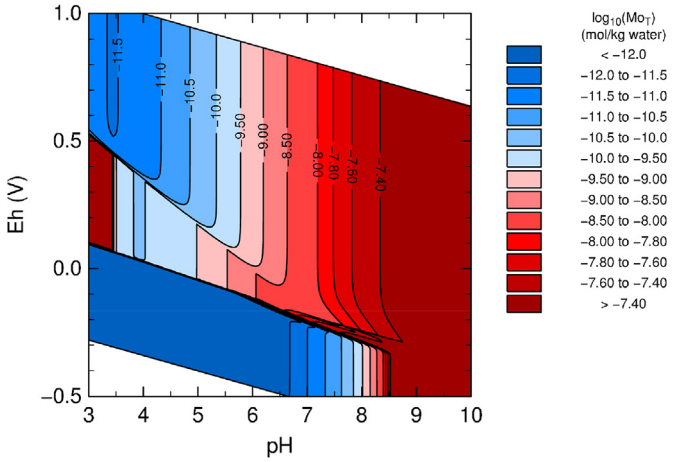

Fig. 7. Contour diagram showing the variation in dissolved Mo concentration as a function of Eh and pH for the same system as shown in Fig. 6. The high Mo concentrations (dark reds) reflect the broad range of conditions under which little or no mineral precipitation or adsorption takes place reflecting the highly conservative behaviour of Mo at high pH. In contrast, concentrations reduce somewhat due to sorption under oxic and not too acidic conditions. They then diminish dramatically at very low Ehs and neutral to low pH, due to the formation of a $FeMo_{0.6}S_{2.8}$ solid phase.

6.4. Isotopic variation

The isotopic variation of Mo in sediments and seawater has been used extensively in studies of palaeoredox conditions and the evolution of ocean anoxia and oxidative weathering over geological time. It has recently been reviewed in detail by Kendall et al. (2017). The value of Mo isotopes for such studies arises from the large mass range of the stable Mo isotopes, together with their redox sensitivity. These provide scope for fractionation of the stable-isotopic composition as a result of phase changes occurring during precipitation/dissolution and sorption/desorption reactions. In the environment, these reactions are largely redox- and pH-controlled, but probably not strongly mediated by microbial activity as Mo is not widely used as a terminal electron acceptor or donor in microbial respiration (Anbar, 2004).

Fractionation occurs when preferential removal of some (e.g. lighter) isotopes occurs. The isotopic composition is not changed when near-complete removal of dissolved Mo occurs, e.g. under euxinic conditions (Archer and Vance, 2008; Dahl et al., 2010; Goldberg and Humayun, 2016; Neubert et al., 2008; Noordmann et al., 2015; Romaniello et al., 2016). Conservation of mass means that if the solid phase becomes relatively light (depleted), the aqueous phase must become relatively heavy (enriched) and *vice versa*. The δ^{98}Mo isotopic ratio of present-day seawater is

remarkably homogeneous at about 2.3‰ (Barling et al., 2001; Goldberg et al., 2016; Neubert et al., 2008), as a result of the relatively large Mo concentration, long oceanic residence times and extensive mixing. This enriched composition has been attributed to the partial removal of Mo from seawater by adsorption of Mo onto Mn oxides in oxic conditions (Goto et al., 2015; Wasylenki et al., 2011), or more generally, to sorption by ferromanganese oxides and clays (Noordmann et al., 2015). This explains why the ocean is the isotopically heaviest Mo reservoir on Earth (Kendall et al., 2017).

Fig. 8 shows the range of δ^{98}Mo isotopic compositions observed in aqueous and solid media. Most investigations have been carried out in the marine context. Laboratory studies have shown that the lighter ^{95}Mo isotope is preferentially adsorbed by minerals compared to ^{97}Mo, with a fractionation of about 2‰ (Goldberg et al., 2009; Noordmann et al., 2015). This offset is similar to that between seawater and natural marine ferromanganese oxides (Barling and Anbar, 2004). Fractionation is greatest when there is a large change in the structure of the sorbed ion, e.g. a change from tetrahedral to distorted octahedral coordination such as occurs when MoO_4^{2-} is adsorbed to MnO_2 (Kashiwabara et al., 2011). Much smaller isotopic fractionations have been observed when there is no change in coordination, as with ferrihydrite (Goldberg et al., 2009; Kashiwabara et al., 2011). Where marine sediments are isotopically heavier (up to +1.5‰), this could suggest formation under a reducing, possibly continental margin, environment (Siebert et al., 2006).

In Mn- or Fe-reducing conditions where Mo is released from sediment via Fe or Mn oxide dissolution or desorption, ^{95}Mo should be preferentially released to the porewater (Goldberg et al., 2012). However, the picture is complicated by the possible resorption of Mo by other adsorbents (Fe oxides and organic matter). As a result, the isotopic compositional range of anoxic sediments is relatively large (Fig. 8). It is also dependent on factors including the Fe and Mn oxide abundance and crystallinity and dissolved sulphide concentration (Goldberg et al., 2012). It has been suggested that the isotopic signature of lake sediments is complicated further by the anthropogenic inputs of Mo as a result of smelting or combustion of oil or coal (Chappaz et al., 2012).

Mass fractionation should also occur in the sequential conversion of molybdate to tetrathiomolybdate (Kendall et al., 2017). Such fractionation is observed in low-sulphide sediments (Goldberg et al., 2016), but the effect is muted or absent in strongly euxinic conditions because of the quantitative removal of Mo to the solid phase. This is observed in both marine and meromictic lake settings (e.g. Black Sea, Lake Cadagno, Kyllaren Fjord) (Dahl et al., 2010; Nägler et al., 2011; Neubert et al., 2008; Noordmann et al., 2015). As a result, the Mo isotopic signature of euxinic sediments should largely reflect that of seawater. Meromictic lakes show a range of isotopic compositions from oxic (light) to euxinic (heavy) (Fig. 8).

Adsorption of Mo may at least partially account for the heavy δ^{98}Mo signature of Mo in some acid mine drainage (Skierszkan et al., 2016) (Fig. 8). Similar reasoning applies to the heavy Mo signature of the water from the three largest Chinese rivers (Xijiang, Huanghe, Changjiang), where the fractionation depends on the degree of weathering in their respective catchments (Wang et al., 2015).

Fractionation of the Mo isotopes has also been recorded in microbiological investigations. The preferential uptake of the lighter isotopes of Mo has been found in both N utilisation and N_2 fixation. The soil bacterium *Azotobacter vinelandii* and freshwater cyanobacterium *Anabaena variabilis* have both been observed to fractionate Mo in the course of N_2 fixation, by up to −1‰ in the δ^{98}Mo ratio between cells and growth media. Microbes could therefore contribute to the isotopic signature of adsorbed Mo in soils, sediments and aquifers (Wasylenki et al., 2007; Zerkle et al., 2011).

At high temperatures, a lack of isotopic fractionation has been noted in mid-ocean ridge rocks of basaltic to rhyolitic composition, having evolved by fractional crystallisation. Icelandic volcanic rocks have a narrow range of δ^{98}Mo compositions (-0.15 ± 0.05‰) (Goto et al., 2015). This evidence supports other studies that have shown a fairly limited range of isotopic compositions and lack of fractionation in igneous rocks from oceanic settings (Goto et al., 2015; Siebert et al., 2003). Greater fractionation has been observed

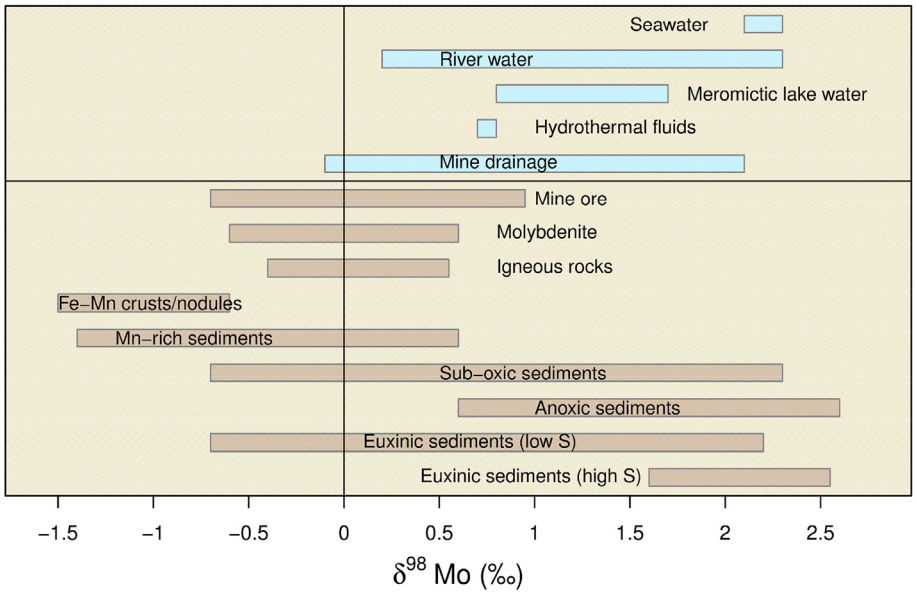

Fig. 8. Range of δ^{98}Mo compositions in documented aqueous (blue) and solid materials (brown), showing fractionation relative to modern seawater. Data are normalised to the NIST SRM 3134 (value + 0.25‰). Data sources: Breillat et al. (2016); Dahl et al. (2010); Goldberg et al. (2013, 2016); Kendall et al. (2011) McManus et al. (2006); Siebert et al. (2006); Skierszkan et al. (2016); Yang et al. (2015a,b); Zerkle et al. (2011).

within island-arc volcanic systems in transition from mafic to silicic compositions. Heavier compositions of dacite (δ^{98}Mo 0.6‰) have been recorded than associated basalt (δ^{98}Mo 0.3‰) in the Aegean arc volcanic system (Voegelin et al., 2014), attributed to fractional crystallisation. The different responses possibly reflect differences in oxygen fugacity and water content of the slab-influenced system compared with the Icelandic mid-ocean ridge system. On the basis of the Aegean data, Voegelin et al. (2014) proposed an average δ^{98}Mo value for the continental crust of +0.3 to +0.4‰, which compares reasonably well with average values found for molybdenite (Greber et al., 2011), taken as a further indicator of crustal compositions. The range also compares reasonably well with Mo isotopic compositions of large rivers (Fig. 8).

The range of Mo isotopic compositions resulting from mass-dependent fractionation has been interpreted extensively in the oceanic and paleoclimate arenas; its use in the environmental and hydrogeological arenas has yet to be explored in detail.

7. Freshwater case studies

7.1. Argentina: Quaternary loess aquifer of the Chaco-Pampean Plain

The Chaco-Pampean Plain of Argentina extends for some 1.2×10^6 km^2 from the Paraguay border to the Patagonian Plateau (Fig. 10). The region is semi-arid to temperate and largely rural, with a strong dependence on groundwater for rural water supply. Regional development is hindered by the poor quality of groundwater resources in the region, which are commonly hard and/or saline with often high concentrations of trace elements (especially the anions/oxyanions As, F, Mo, B, V and U). These render many of the shallow groundwater sources unsuitable for drinking and agricultural use. Trace-element problems have been reported in the provinces of Córdoba, Santa Fe, La Pampa, Buenos Aires, Santiago Del Estero and Tucumán.

The main water-quality problems occur in the Pampa formation, a Plio-Pleistocene loess deposit, dominantly composed of silt with fine sand, which is extensive and in excess of 100 m thick in places. In parts of the plain, the aquifer is underlain by sandy fluvial deposits of the Puelche Formation (Pliocene age), which also form an aquifer where present. The Pampa deposits have an important component of volcanic ash derived from Andean eruptions, which affected the region throughout Cenozoic and Quaternary times. The ash deposits, either disseminated within the loess, or forming distinct layers a few centimetres thick, are typically of rhyolitic composition.

As noted in Section 5.6, Mo concentrations in groundwater from the Pampean aquifer can be extremely high by international standards, reaching up to 7900 μg/L in Córdoba Province (Nicolli et al., 1989), 727 μg/L in the Salí River Basin, Tucumán (Nicolli et al., 2012b), 1907 μg/L in Santiago Del Estero (Bhattacharya et al., 2006) and 990 μg/L in La Pampa (Smedley et al., 2002). Though reducing conditions have been documented in some areas, the shallow groundwaters of the region are overwhelmingly oxic. Groundwater pH is neutral to alkaline (ca. 7.0–8.8).

In La Pampa, the Mo range in pumped groundwaters (2.7–990 μg/L, median 61.5 μg/L, n = 114) was found to be broadly similar to that in porewaters extracted from two cored boreholes: 1–435 μg/L and <2–569 μg/L (Smedley et al., 2002). Under the ambient oxic and alkaline groundwater conditions, dissolved Mo consists of molybdate, MoO_4^{2-} (Fig. 9). Molybdenum concentration shows a weak positive correlation with groundwater pH but better correlations with other anions and oxyanions (HCO_3, As, B, F, V, U), the strongest being with B (r = 0.75) (Fig. 10) (Smedley and Nicolli, 2014).

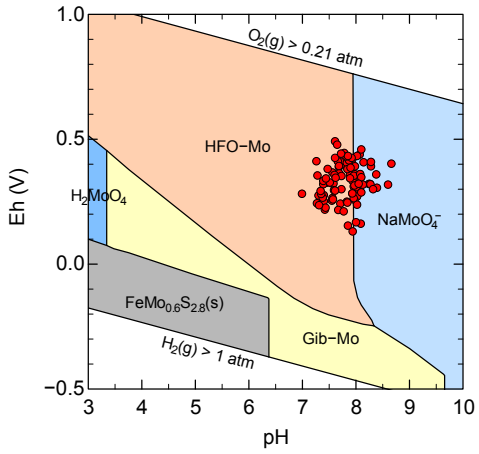

Fig. 9. Eh-pH diagram of the Mo-H_2O system with groundwater samples from the Chaco-Pampean Plain, Argentina superimposed using data from Smedley and Nicolli (2014). This diagram has been calculated using the median quantities of Fe, Al, Mo and S from oxalate-extractions of the sediments, a background electrolyte concentration of 3 mM NaCl and a moisture content of 25 g H_2O/100 g wet sediment. HFO = Hydrous ferric oxide; Gib = Gibbsite.

Rhyolitic ash, from discrete layers in the loess silts of La Pampa, has Mo contents in the range 2–6 mg/kg, slightly higher than the silts themselves which are more typically <1–4 mg/kg (Smedley and Nicolli, 2014). The ash is considered the likely dominant primary source of Mo in the groundwater. Associations are also seen between Mo in the sediments and occurrence of Mn oxide and to a lesser extent, Fe oxides, Al oxides and clays. These together represent possible secondary sources or sinks of labile Mo, although under the alkaline conditions, sorption to oxide and clay surfaces is restricted.

Forty percent of the pumped groundwaters investigated in the Smedley and Nicolli (2014) study have Mo concentrations above the WHO health-based value of 70 μg/L. Similar exceedance percentages are seen in other areas of the Chaco-Pampean Plain. The Chaco-Pampean Plain represents by far the largest high-Mo province that has been documented in the literature, and one of the largest for other potentially harmful anion/oxyanion-forming elements (As, F, V, U, B).

7.2. Jordan: Cretaceous aquifer and oil shale

Groundwater is an important resource in semi-arid northern Jordan. In the Wadi Al Arab area investigated by Al Kuisi et al. (2015), some 500 wells are used to abstract groundwater for drinking and irrigation from Upper Cretaceous (Turonian–Campanian) limestone aquifers, with depths of 100 m to over 1000 m. Groundwater from the aquifers shows a large range of Mo concentrations from 4 to 650 μg/L (Al Kuisi et al., 2015) (Fig. 11). The aquifers are partially unconfined but dip northwards below the Maastrichtian Muwaqqar Chalk Marl, the lowermost unit of which consists of oil-shale deposits some 100 m thick. The Jordanian oil shales are kerogen-rich marine argillaceous limestones with an organic matter content of some 14% (Abed and Amireh, 1983). An overlying Palaeocene limestone aquifer has a hydraulic head lower than that in the Upper Cretaceous units, and as a result of faulting and fractures, the aquifers and intervening oil-shale-bearing aquitard, are concluded to be hydraulically connected, with likely downward flow to the lowermost aquifer (Al Kuisi et al., 2015).

Molybdenum concentrations in the Cretaceous aquifers are relatively high under anoxic conditions (e.g. low dissolved-oxygen concentration: DO; Fig. 12) and show some correlations with

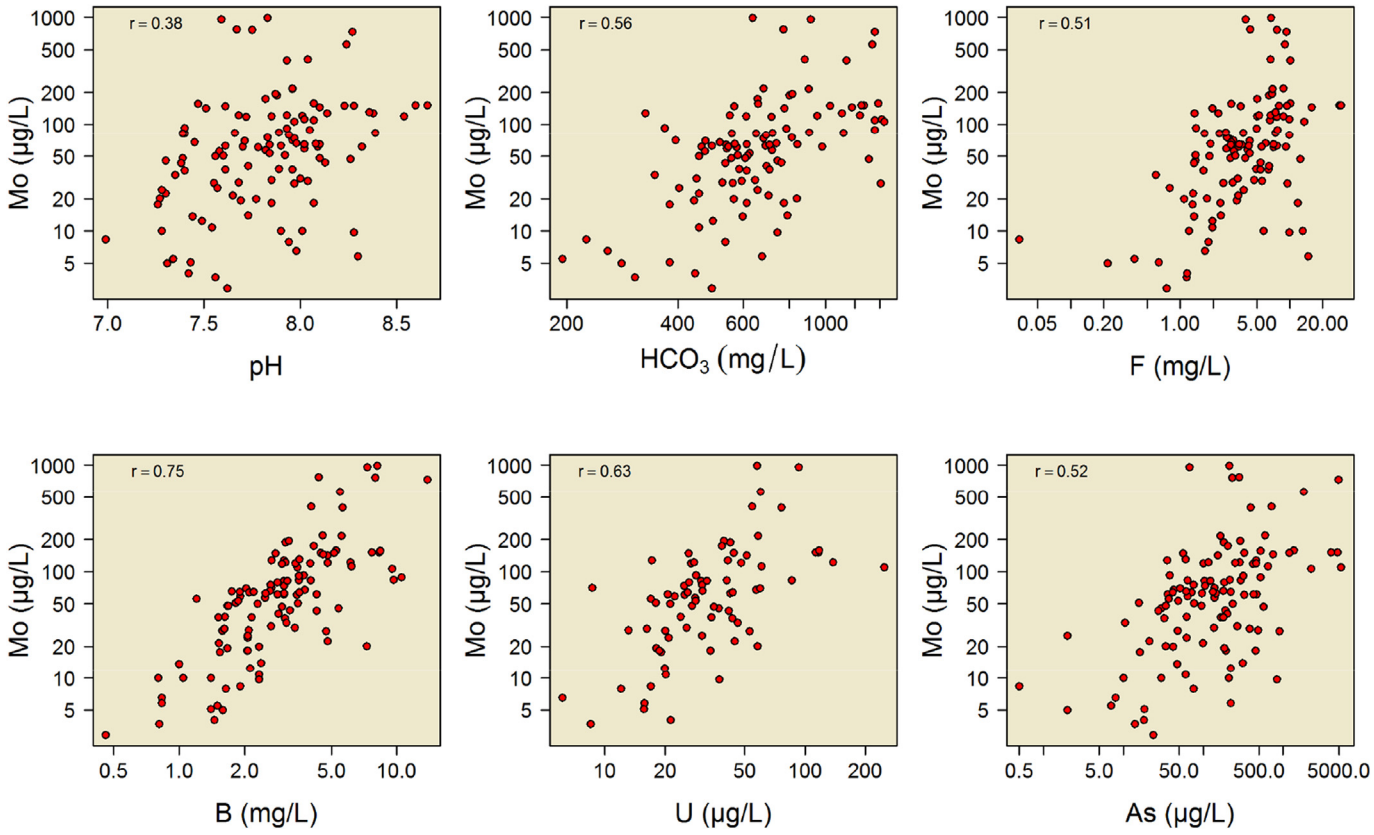

Fig. 10. Variations of Mo with other analytes in groundwater from the Chaco-Pampean Plain, Argentina (Smedley and Nicolli, 2014). Variations show a generally poor correlation between Mo and pH but better positive correlations with other anions and oxyanions.

dissolved SO_4 as well as other trace elements such as Ni, Cr and U. The high concentrations have been attributed largely to oxidation of Mo(IV) derived from oil shales in the overlying aquitard (Al Kuisi et al., 2015). The authors concluded that the dominant source of Mo was organic matter rather than sulphide minerals, although distinguishing the two from the study is difficult. The observed range of SO_4 $\delta^{34}S$ ratios (−27.8 to −23.4‰, mean −24.7‰) is consistent with a SO_4 origin from the oxidation of sulphide minerals (Al Kuisi et al., 2015; Siebert et al., 2014). It is likely that both organic matter and sulphide play a role in Mo mobilisation, either directly or indirectly.

7.3. Qatar: Palaeogene sedimentary rocks

Qatar is an arid country with limited supplies of fresh water and a strong dependence on groundwater for industrial and irrigation use; municipal supply is mostly from seawater desalination (Amer, 2008). The Northern Groundwater Basin in northern Qatar hosts Palaeogene sedimentary aquifers (Rus and Upper Umm Er Rhadouma formations), consisting mostly of limestone with gypsum. The aquifers are up to 150 m thick. Groundwater abstraction generally exceeds recharge and water levels are in serious decline. As a result, coastal aquifers are prone to saline intrusion and soil to salinisation (Kuiper et al., 2015).

A study of shallow groundwater (25–90 m depth) in the Northern Groundwater Basin by Kuiper et al. (2015) found near-neutral to alkaline pHs (6.94–8.22) and often high salinity, with TDS in the range 11–15,000 mg/L and Na and Cl as the dominant solutes in the more saline waters (Fig. 13). Groundwater is oxic with average dissolved-oxygen content of >8 mg/L (B. Shomar, pers. commun., 2016), as supported by distributions of NO_3, Fe and Mn (Kuiper et al., 2015). Concentrations of Mo have been recorded, in the range 1.0–103 µg/L with a median of 24.3 µg/L and mean of 26.9 µg/L (n = 205). Some high concentrations of other oxyanions are also apparent (As, Cr, F, Se, U, V; Fig. 13), with several samples exceeding WHO guideline values for drinking-water quality (Kuiper et al., 2015).

Mobilisation of Mo (as molybdate) and the other anions/oxyanions is likely related to the oxic and neutral to alkaline conditions in the groundwaters. However, a potential impact from hydrocarbon contamination cannot be ruled out. Qatar has important resources of oil and gas and is the largest exporter of liquid natural gas in the world. Hydrocarbon production wells penetrate the main aquifers and produced water from the industry is said to have been discharged into them. Groundwater affected by such contamination has enhanced salinity as well as concentrations of H_2S and CO_2 (Johnsen, 2015). The impact, if any, on Mo mobilisation is so far unclear.

7.4. Ethiopia: East African Rift Valley

Groundwater-quality problems are a well-established feature of the East African Rift Valley and the Main Ethiopian Rift is one of the best-documented areas. High concentrations of fluoride are a particular feature of the Rift Valley groundwaters, but F is commonly accompanied by other anion and oxyanion species such as Mo, As, U and B (Rango et al., 2010). The affected groundwaters are derived from rhyolitic and volcanogenic sedimentary aquifers. Groundwater pH is neutral to alkaline and groundwater is oxic (Rango et al., 2013) with variable total-dissolved-solids contents (TDS 30–860 mg/L). Molybdenum concentrations have been reported in the range 0.53–446 µg/L (n = 25; water wells and cold

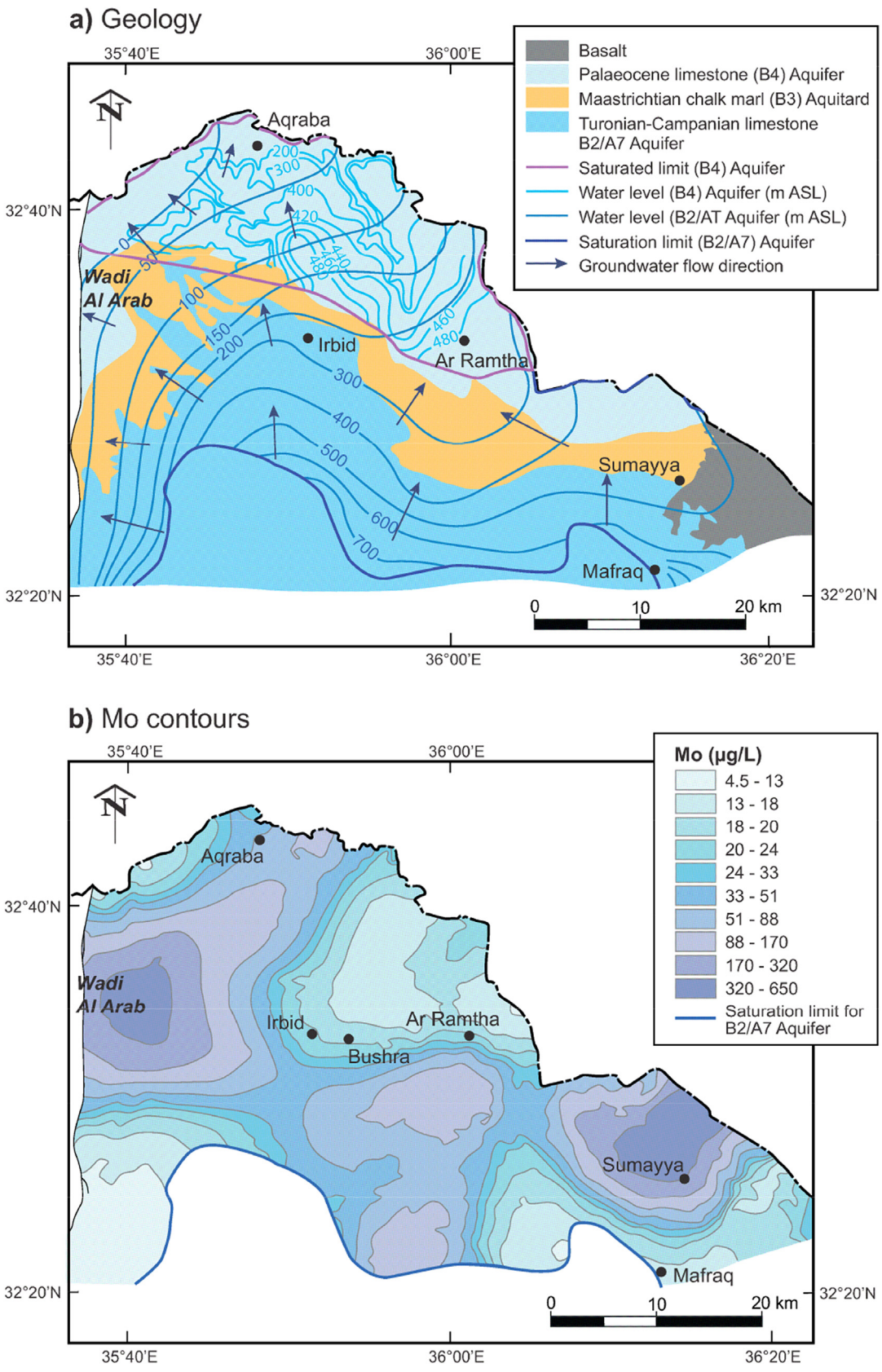

Fig. 11. (a) Regional geology of the Wadi Al Arab area of north-west Jordan; and (b) contour map of Mo distributions in groundwater from the Turonian–Campanian limestone (A2/B7) aquifer (from Al Kuisi et al., 2015).

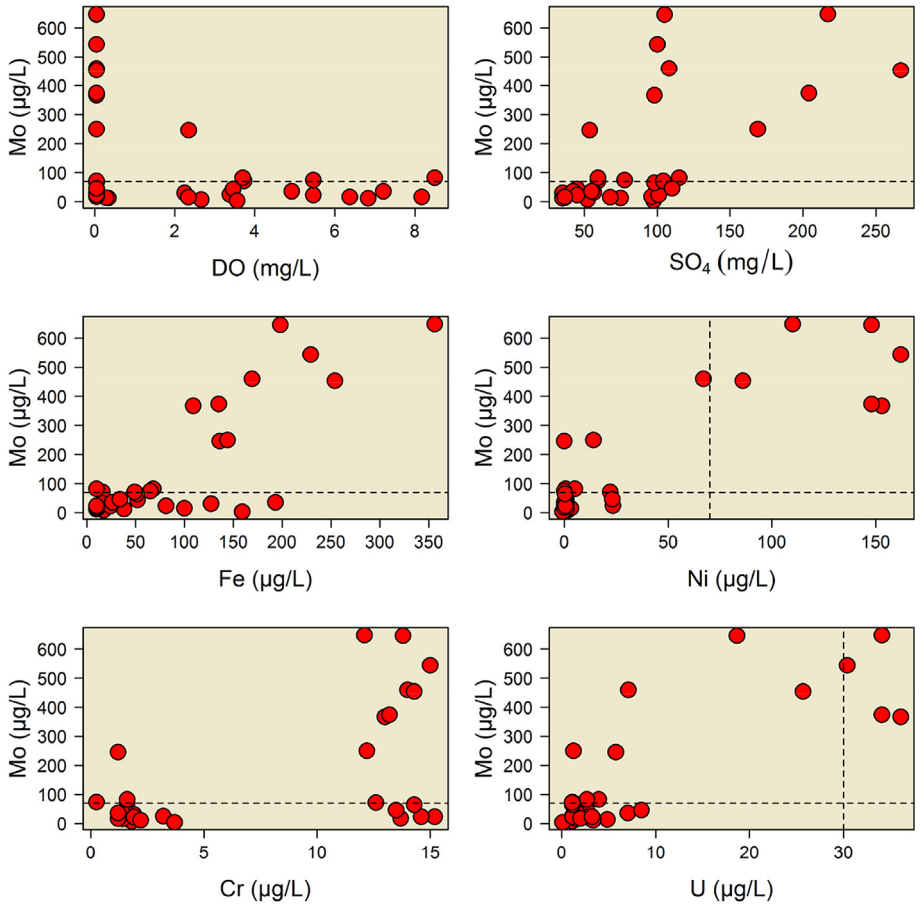

Fig. 12. Variations of Mo with selected other parameters in groundwater from Upper Cretaceous limestone aquifers of northern Jordan (Al Kuisi et al., 2015). Dashed lines are WHO guideline values for drinking water and, for Mo, the WHO health-based value.

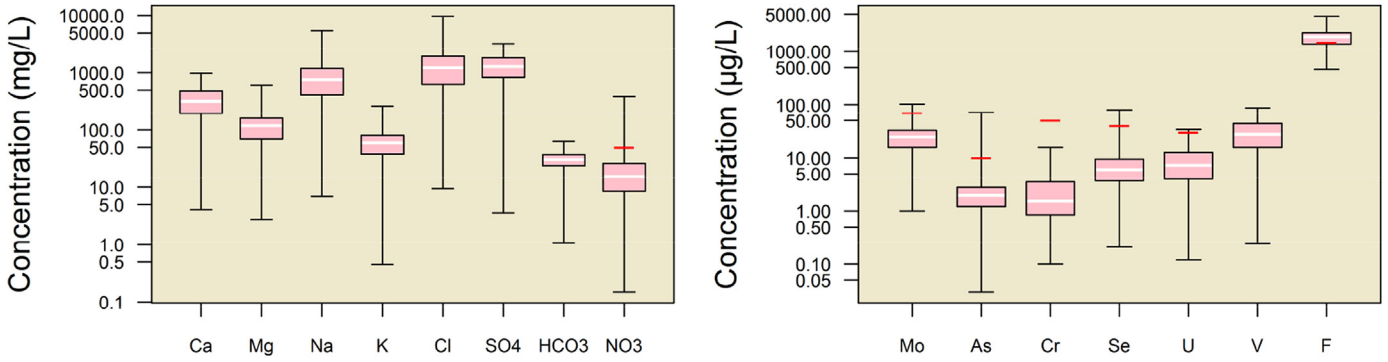

Fig. 13. Box plots showing the compositional variations in groundwater from Palaeogene aquifers of the Northern Groundwater Basin, Qatar. Horizontal red lines indicate WHO guideline values where they exist; for Mo, the red line represents the WHO health-based value. Data are from Kuiper et al. (2015).

springs). Concentrations in the range 30–100 µg/L are not uncommon (Fig. 14). Groundwater Mo correlates well with As (r^2 0.79) (Rango et al., 2010). A source for Mo from the rhyolites and the volcanic ash within the volcanogenic sediments is probable, although molybdate sorption reactions involving clays and metal oxides are also likely to be controlling the spatial variations.

7.5. UK: surface waters of the River Clyde catchment, Glasgow

A regional investigation of stream and river water chemistry in the catchment of the River Clyde, Glasgow, Scotland, carried out as part of the BGS Clyde Urban Super Project (CUSP) (Smedley et al., 2017) has shown some notable spatial variations in Mo as well as other solutes (Fig. 15). The study compiled data for low-order streams, urban tributaries, River Clyde water and estuary water across the catchment. The combined dataset showed a range of Mo concentrations of <0.02–214 µg/L (n = 1891), although only one sample exceeded the WHO health-based value of 70 µg/L and all others were less than 14 µg/L.

Concentrations were generally lowest in the south and along the

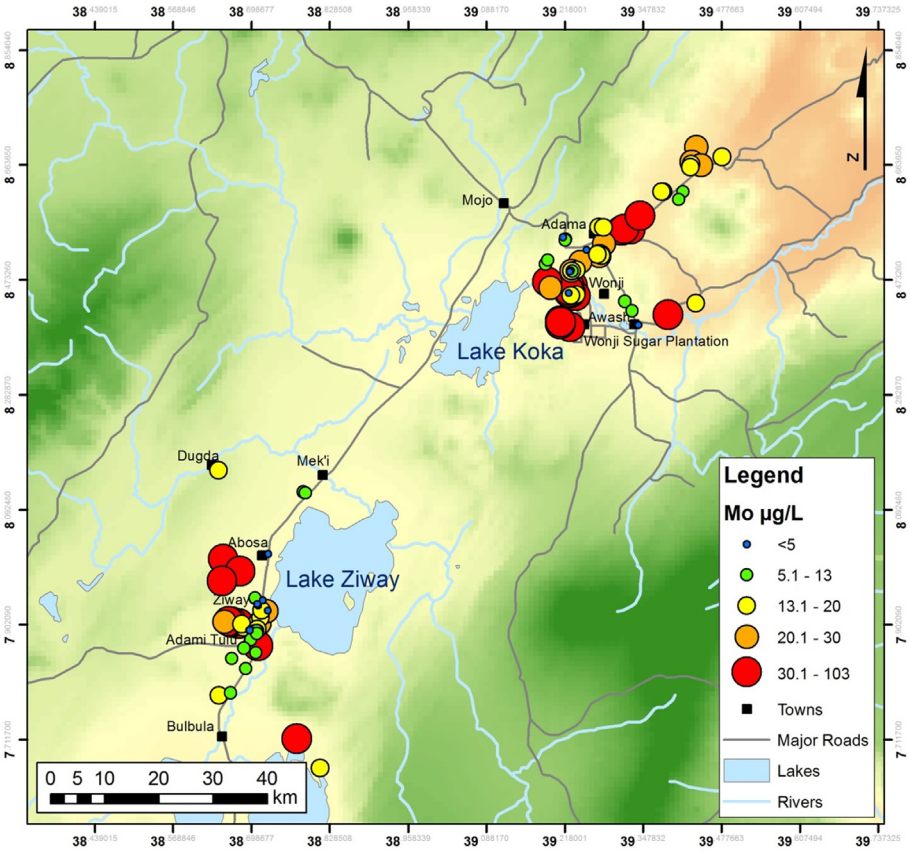

Fig. 14. Spatial variation in Mo concentrations in the Awash area of the Ethiopian Rift Valley (data: BGS, unpublished, 2015).

periphery of the catchment and highest in the central lowland belt corresponding with the urban area of Glasgow (Fig. 15). Categorised by geology, the highest concentrations correspond with streams on glacial till above Scottish Carboniferous largely argillaceous sedimentary rocks (Coal Measures, Strathclyde & Clackmannan Group), which predominate in the lowland urban area. In terms of land-use, highest values are within areas classed as built environment. Relatively high concentrations were found in industrial areas with point-source anomalies occurring locally around some landfill sites.

The largest range and highest concentrations in the catchment occur in streams with pH values of 7.0–8.5 (Smedley et al., 2017). Controls on Mo distributions in water are likely to be a combination of geology (abundance in argillaceous and organic-rich Carboniferous sediments) and urban sources (coal-mining activity, industrial contamination). Relative lows in dissolved Mo from streams around the catchment boundary and from Precambrian metasedimentary rocks may be a combination of lower concentrations in component rock types, greater dilution by rainfall in the upland watershed areas and a greater influence of sorption to mineral surfaces in the stream sediments at lower pH.

7.6. USA: lake stratification, Fayetteville Green Lake, New York

Fayetteville Green Lake, New York, is a 53 m deep meromictic lake that has been the focus of a number of studies for over 100 years. The lake shows a strong stratification in redox conditions and chemistry with depth, with an oxic mixolimnion to 15 m depth, a chemocline over the interval 15–21 m and a more saline euxinic monolimnion from 21 m to 53 m (Fig. 16). A dense population of anoxygenic photosynthetic bacteria corresponding with increased turbidity occurs at around 21 m depth (Havig et al., 2015) in response to the steep gradient in redox conditions. At the chemocline, bacterially-mediated reduction of Mn(IV) and Fe(III) leads to mobilisation of dissolved Mn(II) and thereafter Fe(II). The oxic lakewater system has high SO_4 concentration (1120–1450 mg/L) due to the influence of groundwater flowing through the Silurian gypsum-bearing Vernon Shale, and this constitutes a driver for dissolved Mo stability in the oxic zone and, together with organic matter, for SO_4 reduction beyond the chemocline. Beyond this, Mo concentration decreases by transformations to Mo(VI) thiomolybdate and Mo(IV) oxythiols, possibly with a Mo(V) intermediate step, and ultimately to an Fe or Fe-Mo sulphide mineral phase (e.g. greigite or Helz's mineral) (Dahl et al., 2010; Havig et al., 2015; Helz et al., 2011; Vorlicek et al., 2004). Bacterially-mediated SO_4 reduction in the euxinic bottom waters also immobilises Mn and Fe, Mn mainly in association with Ca-Mn-carbonate, and Fe with sulphide (e.g. amorphous FeS, greigite, mackinawite). The dissolved concentrations of Mn and Fe reduce accordingly. Temporal variation looks to be relatively minor, with similar profiles in November and March (Fig. 16) (Havig et al., 2015).

Similar variations in Mo concentrations with vertical redox and salinity changes are seen in stratified lakes elsewhere, for example Lake Cadagno, Switzerland (Dahl et al., 2010) and the McMurdo Dry Valley Lakes of Antarctica (N. Yang et al., 2015).

7.7. USA: anoxic groundwater, south-east Wisconsin

In Caledonia, WI, USA, high concentrations of Mo have been found in anoxic groundwater from private-supply wells in Quaternary glacial/alluvial till and Ordovician–Silurian dolomite aquifers suspected of having been contaminated by coal ash leachate from a local landfill (Lourigan and Phelps, 2013). The landfill was

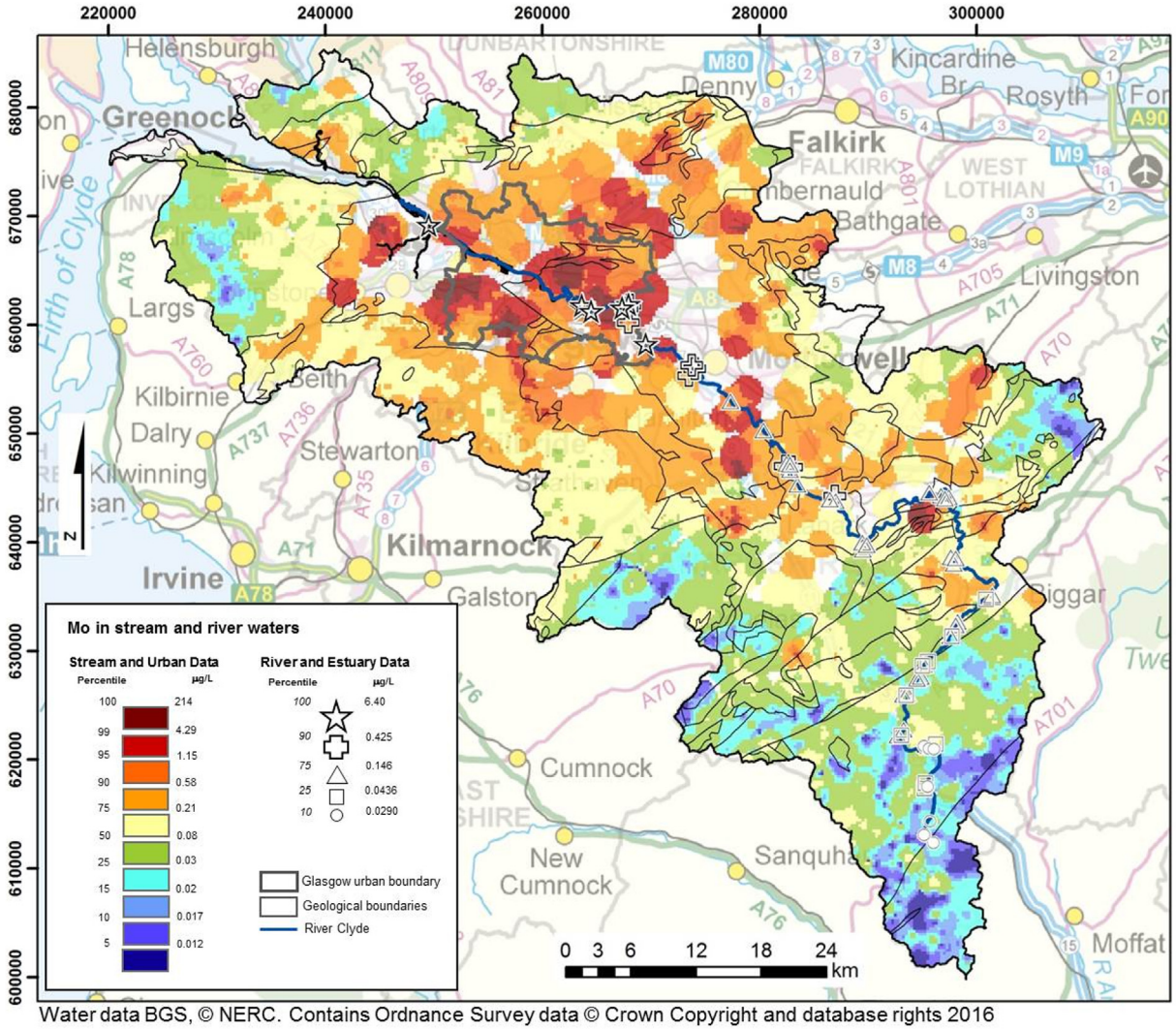

Fig. 15. Distributions of molybdenum in stream and river waters from the Clyde catchment, Glasgow, Scotland (from Smedley et al., 2017). High concentrations are centred around the lowland urban part of the catchment and linked to coal-bearing Carboniferous rocks as well as historical mining and industrial works.

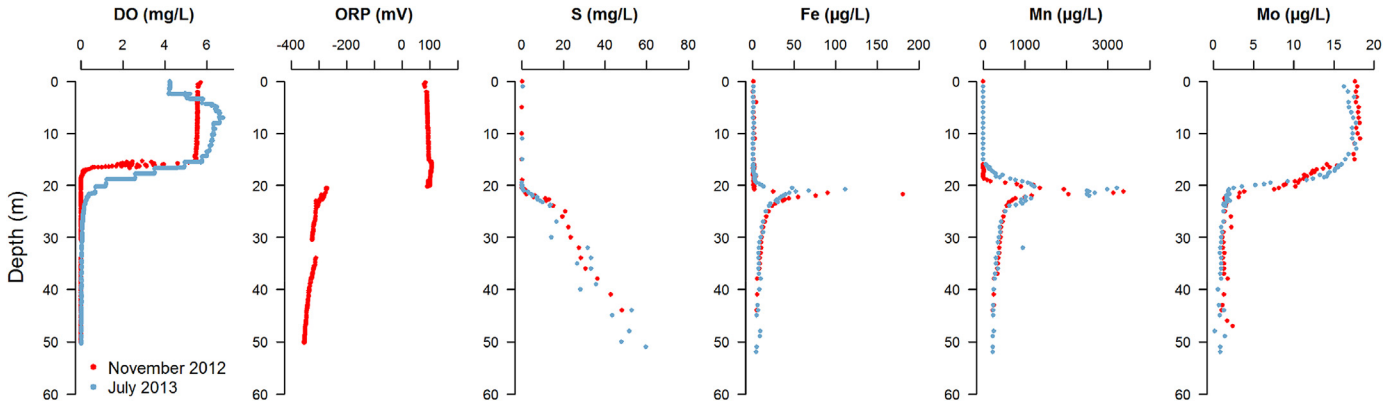

Fig. 16. Profiles of lakewater chemistry, Fayetteville Green Lake, New York, USA, surveyed and sampled in November 2012 and July 2013. DO: dissolved oxygen; ORP: oxidation-reduction potential (data from Havig et al., 2015).

used to dispose of coal ash from the nearby We Energies Oak Creek power plant between 1959 and 1974, and capped in 1990. Of the wells surveyed in the investigation, 44 had groundwater with >40 µg/L, in groundwater from both the till and dolomite aquifers. High groundwater pumping rates from the dolomite have caused downward vertical gradients with flow induced from an overlying shale, the Maquoketa Shale. The shale did not show a large Mo content (1.1–1.3 mg/kg) (Lourigan and Phelps, 2013), though

whether this was a typical grey shale or a weathered black shale having lost Mo is unclear.

Hensel et al. (2015) found that where groundwater had Mo concentrations >40 μg/L, they were tritium-poor (<2 TU) with B concentrations and B and Sr isotopic compositions which suggested against an origin from local coal-ash leachate. The presence of high Mo concentrations in groundwaters at up to 8 km distance, and in one case upgradient of, the landfill, and from a dolomite at 200 m depth, also points to a natural origin being the more likely (Hensel et al., 2015). Subsequent groundwater monitoring in the area has identified elevated Mo concentrations from Oak Creek and Caledonia to the Town of Norway and the City of Muskego, with high values located several kilometres west and south-west of the power plant and landfill. The distribution of high-Mo groundwater has some correlation with the location of an east-west buried valley and a causal relationship is possible.

The Wisconsin Department of Natural Resources (DNR) advises the residents of the Oak Creek–Caledonia area not to drink water with a Mo concentration greater than their interim advisory level of 90 μg/L.

7.8. USA: anoxic mixed groundwater, Florida

In the town of Lithia, FL, USA, groundwater from domestic wells in a limestone aquifer (depth range around 20–60 m below ground level) has concentrations of Mo and As in the ranges 0.3–4740 μg/L and <0.1–371 μg/L respectively (Pichler et al., 2017). These high concentrations occur under anoxic conditions, with a strong negative correlation observed between the two trace elements and dissolved sulphide. The intermediate aquifer system (IAS) is overlain by a relatively oxic superficial aquifer system (SAS, <20 m depth) and underlain by an anoxic Upper Floridan aquifer (UFA, approximate depth range 60–370 m below ground level). All aquifers are limestone and the intermediate and deeper Upper Floridan aquifers contain small amounts of pyrite, as well as organic matter and powellite (Pichler et al., 2017; Pichler and Mozaffari, 2015). The high density of domestic wells in the local area (Fig. 17) was taken to be responsible for increasing aquifer permeability. The presence of groundwater in the intermediate aquifer with chemical and isotopic compositions which are intermediate between those of the upper and lower aquifers was consistent with induced flow and mixing of groundwater both from above and below in the intermediate aquifer (Pichler et al., 2017). A pyrite source for the dissolved Mo was ruled out on the basis of low contents of Mo observed in the pyrite (<100 mg/kg) (Pichler and Mozaffari, 2015); Pichler et al. (2017) favoured organic matter as the likely source.

7.9. Chile: Spence Porphyry Copper Deposit, Atacama Desert

Chile is the largest producer of copper in the world and the Spence Porphyry Copper Deposit contains 400 Mt of 1% copper (Leybourne and Cameron, 2006). The deposit lies along a line of porphyry copper deposits extending some 800 km in a narrow NNE-SSW belt across the Atacama Desert and was emplaced during Cenozoic hydrothermal events associated with subduction and continental arc magmatism. The copper ore is associated with quartz-feldspar porphyry bodies intruded into andesitic volcanic rock; the body is covered completely by Miocene gravels. Supergene alteration took place during the mid-Miocene (Leybourne and Cameron, 2008). Primary ore minerals comprise chalcopyrite, bornite, molybdenite, tennantite and pyrite, and secondary minerals include chalcocite, covellite, anterite, atacamite, brochantite and malachite.

Groundwater in the vicinity of the deposit has very variable salinity, ranging from TDS of 900–7000 mg/L upgradient, to 53,200 mg/L downgradient (Leybourne and Cameron, 2006). Water types are dominated by Na-SO_4 upgradient and Na-Cl downgradient. Concentrations of dissolved Mo in the area lie in the range 2–475 μg/L, being highest within the deposit. In and downgradient of the deposit, Mo concentrations are lowest where pH values are low (<6); Mo is mobile in the groundwaters where pH values are 7 and above because of the lower tendency to sorb to metal oxides in alkaline conditions.

8. Conclusions

8.1. Molybdenum distributions and controls

From the collation of available data, the concentrations of Mo in natural fresh surface waters and groundwaters appear to be usually <10 μg/L and often substantially less. The value for open seawater is fairly uniform at around 10 μg/L but much less in sulphidic bottom waters. Our review has highlighted a number of occurrences with concentrations much higher than 10 μg/L, and the range observed spans some five orders of magnitude, with rare observations in the mg/L range. A number of these studies are reported precisely because the concentrations of Mo found are high. Others are reported because the associated anion/oxyanion (F, As) concentrations are high. It is important to appreciate this when assessing the ranges that are likely to be representative of most natural waters. Large, multi-element geochemical surveys provide more representative statistics. This is evident from large-scale studies such as in the USA where 3063 groundwater samples gave a 10^{th}–90^{th} percentile range of 0.13–4.9 μg/L with a median of 1.0 μg/L (Ayotte et al., 2011), or the UK where the 1735 groundwater samples yielded a 10^{th}-90^{th} percentile range of 0.035–1.80 μg/L with a median of 0.20 μg/L (Smedley et al., 2014a). Similarly low concentrations occur for typical surface waters, 11,600 UK streamwaters having a 10^{th}–90^{th} percentile range of 0.08–2.44 μg/L with a median of 0.57 μg/L (Smedley et al., 2014a). Large-scale studies of Mo are however the exception because of the lack of existing regulations to drive the monitoring and reporting.

There are a number of geological conditions and risk factors that give rise to high Mo concentrations in surface waters and groundwaters. These can be summarised as:

(i) *oxic, alkaline conditions.* Here, Mo is stable in aqueous form as the molybdate species and accumulation of dissolved Mo can occur as a result of reaction with soils and sediments (surface water) or host aquifers (groundwater). Under arid conditions (e.g. Argentina, Qatar), oxic groundwater can persist over greater areas and timescales given a paucity of decaying organic matter in the aquifers. Hot, arid conditions can result in extensive evaporation with further concentration of molybdate in both groundwater and lake environments. In groundwater, oxic and alkaline conditions may not in themselves be sufficient to cause sufficiently high Mo concentrations to pose a health problem in drinking water. However, young aquifers may be more prone especially where secondary minerals are newly-formed (in a geological sense), are poorly-structured and so contain relatively large concentrations of labile Mo. Young volcanogenic aquifers in which sediments contain intermixed felsic volcanic ash appear to be particularly vulnerable. Here, Mo release from the ash has been observed to give rise to exceptionally high dissolved Mo concentrations (e.g. Argentina, Ethiopia) (Rango et al., 2013; Smedley et al., 2002). The Mo content of rhyolitic ash may not be anomalously high but only small mass transfers of Mo are involved in generating Mo

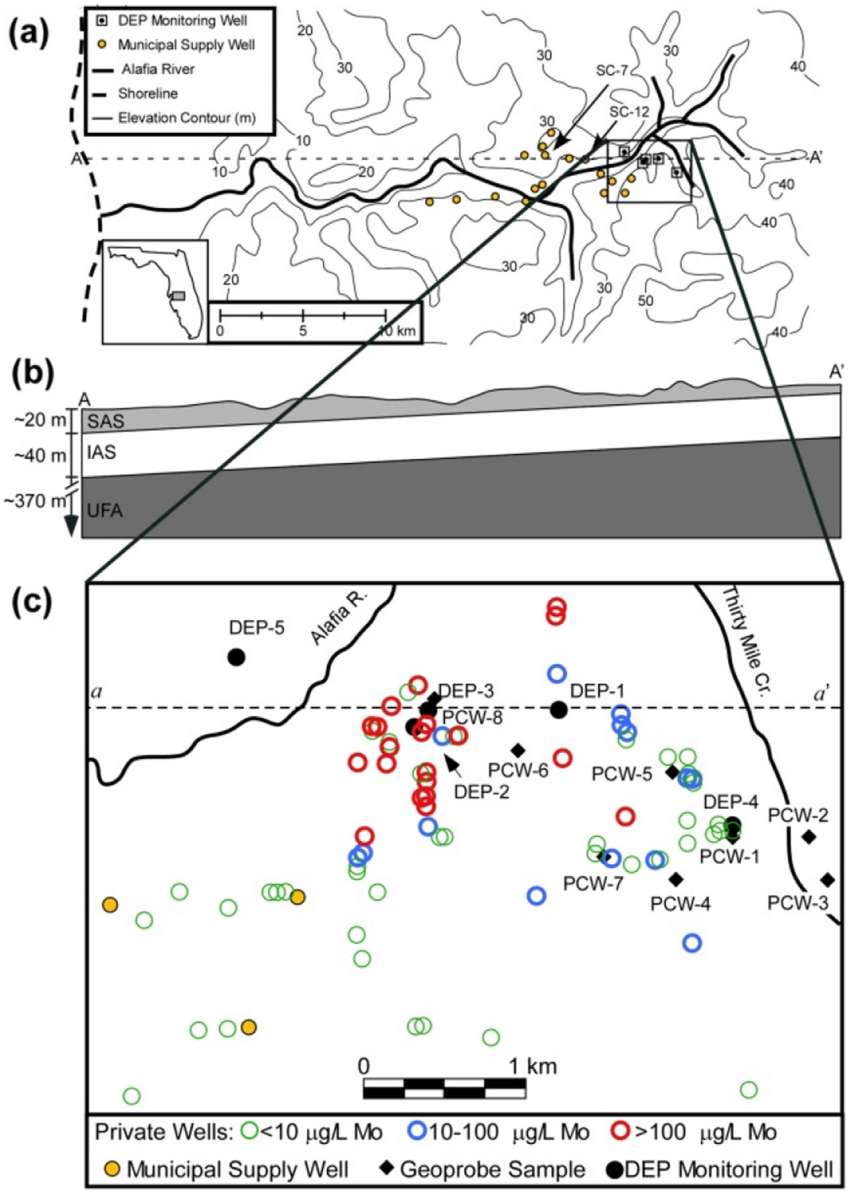

Fig. 17. (a) Map of Lithia area, FL, showing locations of municipal supply wells and DEP (Department of Environmental Protection) monitoring wells, with location in inset, (b) simplified cross section along A-A′, and (c) concentration ranges of Mo in domestic supply wells (from Pichler et al., 2017).

concentrations in the hundreds of µg/L range and so reactivity of the ash is key. A pH > 7.5 is usually required for this.

(ii) *anoxic, non-sulphidic conditions.* There are a large number of case studies that reveal increased concentrations of dissolved Mo under Mn- and Fe-reducing conditions. These occur in both groundwater from confined aquifers and lake waters undergoing vertical transition from oxic to anoxic (non-sulphidic) conditions (e.g. Aquia aquifer, USA; Datong Basin aquifer, China; McMurdo Dry Valley Lakes, Antarctica) (Guo and Wang, 2005; Schlieker et al., 2001; Shimmield and Price, 1986; Vallee, 2009; N. Yang et al., 2015). Most confined aquifers do not yield groundwater with Mo concentrations sufficiently high to cause a problem for drinking water, but a number of aquifers have some representatives with concentrations in the tens to hundreds of µg/L range. Again, young aquifers with newly-formed and reactive mineral surfaces appear to be the most at risk. Aquifers bearing enrichments of organic matter, such as black shale and oil shales can yield elevated concentrations of dissolved Mo if conditions are conducive to the oxidation of organic carbon.

iii) *surface water and groundwater impacted by metal sulphide mining and/or mineralisation.* Here, high concentrations of Mo and other potentially toxic trace elements can arise through sulphide oxidation reactions and the dissolution of secondary molybdate minerals, e.g. Spence deposit, Chile (Leybourne and Cameron, 2008). Molybdenum concentrations in impacted surface waters and groundwaters can be very high but are more likely to be sporadic and local to the area of mineralisation or mining.

In all these cases, the mobility of Mo has some notable overlap with that of a number of other anions/oxyanions, in particular As, and the risk factors outlined above have many notable similarities (Smedley and Kinniburgh, 2002).

8.2. Uncertainties

While the complexity of Mo interactions in natural waters is quite well understood, there are many areas where quantification has been difficult and considerable uncertainty remains. The reduction of Mo concentrations in reducing and euxinic environments has been much studied and is of considerable importance in understanding Mo behaviour in the oceans and in sediments, past and present. There is a large literature on this subject because of the role of molybdenum as a palaeo-redox indicator and its potential to reveal the oxygen status of past atmospheres. However, the precise role of Fe and S in scavenging Mo under these conditions remains unclear – is there some Fe-S-Mo mineral involved or is it more related to surface phenomena, sorption by Fe-S minerals, for example? Analysis of Mo-rich black shales highlights the possible importance of Mo-organic matter interactions, possibly even more so than Mo-S mineral interactions. These are all difficult areas to study and to quantify in a comprehensive way yet without some attempt to do so, it remains difficult to model the interactions in a convincing way. While much can be learnt by observing the variation of molybdenum behaviour in natural environments, advances in fundamental understanding are more likely to arise from studying simpler model systems in the laboratory and in theory.

Thermodynamic databases need to be updated not only in terms of Mo species but also with modern data for allied S species such as the thiomolybdates and polysulphides. Surface speciation is more difficult to characterise but is of undoubted importance – and the Langmuir isotherm which is often used to characterise these interactions is too simplistic to capture all the relevant interactions needed for more general-purpose modelling. At a minimum, it is necessary to capture both the Mo concentration dependence and the pH dependence of adsorption, as well as the redox status of the species involved. Mo is often only one of many trace elements involved and so some grasp of the effect of competition is necessary too. This requires a fundamental insight into the reactions occurring. The type of binding in terms of coordination and oxidation status of Mo is now becoming accessible through EXAFS and XANES and this serves to constrain molecular-based models (Freund et al., 2016; Gustafsson and Tiberg, 2015). But even with these powerful tools available, the precise mechanisms for Mo uptake by black shales has so far proven difficult to pin down (Helz et al., 1996). Instrumental methods involving separation coupled with ICP-MS offer new ways of discriminating different forms of Mo (Vorlicek et al., 2015).

Molecular dynamic simulations based on density functional theory can provide a valuable insight into areas that are difficult to study experimentally and will surely help to constrain future models better. The greater the number of parameters that can be derived from theory, the greater the chance of success in extrapolating to new areas. Interactions in the Mo-Fe-S system need some detailed laboratory studies aimed at separating surface reactions from mineral precipitation and solid-solution reactions. The importance of interactions of Mo with organic matter is evident from field studies but these interactions are poorly understood at a fundamental level and need to be studied in simplified laboratory systems in both oxidising and reducing environments.

The redox behaviour of Mo is critical in many applications and yet the stability of molybdate in strongly-reducing conditions is surprisingly poorly understood. While Mo(V) has been identified in laboratory systems and in the protected environment of enzymes and cofactors (George et al., 1989), its role and even its existence as a free species in natural systems remains to be demonstrated convincingly. Primary thermodynamic data for the reduction of Mo(VI) to Mo(V) date back to the 1950s and need to be revisited using modern instrumental methods and a rigorous thermodynamic approach.

The majority of studies of Mo, including Mo stable isotopes, have involved the study of marine environments. There is scope for applying the same approaches to freshwater and contaminated environments. To the best of our knowledge, no Mo isotopic data are so far available for groundwater. On the basis of the isotopic signatures demonstrated in redox-variable marine and lacustrine settings, significant isotopic fractionation can be anticipated. Whether this proves useful as an indicator of hydrogeochemical processes or as a tracer remains to be seen. More detailed studies of Mo chemistry in high-Mo areas, as outlined in our Case Studies, might showcase the element's behaviour in a relatively accessible and useful way.

8.3. Implications for drinking water and drinking-water guidelines

This review concludes that most natural waters which are candidates for drinking-water supply have low concentrations of Mo, usually well below the WHO health-based value of 70 μg/L. However, a notable minority have more, and some appreciably more, than this health-based value. The WHO 2011 guidelines removed the 70 μg/L concentration as a formal guideline value on the grounds that such concentrations were unlikely to be found in drinking water. While this is mostly true, the observed exceptions are perhaps sufficiently common to deserve extra scrutiny in certain risk areas in order to ensure safeguarding of health. The Wisconsin Department of Natural Resources has shown sufficient concern to promulgate a Health Advisory Level for Mo in drinking water of 90 μg/L.

Measurement of Mo in drinking water would therefore seem a prudent endeavour, at least at a reconnaissance level, to gain a better appreciation of the concentrations occurring. This is particularly the case in areas with the risk factors outlined in Section 8.1. Areas deemed ‘at-risk’ for As may well be similarly ‘at-risk’ for Mo, albeit the concentrations of As that lead to toxicity are much lower (10 μg/L). The WHO health-based value for Mo is well within the analytical range of a number of analytical methods and the marginal cost of data collection should be low if a multi-element technique such as ICP-MS is used.

Acknowledgements

We are greatly indebted to Thomas Pichler, Anthony Chappaz, Tais Dahl and two anonymous reviewers for the effort and care that they took in reviewing our original submission, for correcting our mistakes and misunderstandings and for providing many suggestions for improving the manuscript. This paper reflects their generosity. We also thank George Helz, Lee Cronin and Regina Lohmayer for answering our queries and John Mahoney for helpful discussions. Thanks are also due to Gill Tyson and Jenny Bearcock for help with some of the figures and the BGS library staff for their help with finding references. This research did not receive any specific grant from funding agencies in the public, commercial, or not-for-profit sectors, although open access has been provided through a Natural Environment Research Council block grant.

References

Abed, A., Amireh, B., 1983. Petrography and geochemistry of some Jordanian oil shales from north Jordan. J. Pet. Geol. 5, 261–274. http://dx.doi.org/10.1111/j.1747-5457.1983.tb00571.x.

Abed, A.M., Arouri, Z., Amiereh, D.S., Al-Hawari, Z., 2009. Characterization and genesis of some Jordanian oil shales. Dirasat Pure Sci. 36, 7–17.

Abed, A.M., Jaber, O., Alkuisi, M., Sadaqah, R., 2016. Rare earth elements and uranium geochemistry in the Al-Kora phosphorite province, Late Cretaceous, northwestern Jordan. Arab. J. Geosci. 9 http://dx.doi.org/10.1007/s12517-015-2135-6.

Adams, J.F., 1997. Yield responses to molybdenum by field and horticultural crops. In: Gupta, U.C. (Ed.), Molybdenum in Agriculture. Cambridge University Press, Cambridge, pp. 182–201.

Agusa, T., Kunito, T., Fujihara, J., Kubota, R., Minh, T.B., Trang, P.T.K., Iwata, H., Subramanian, A., Viet, P.H., Tanabe, S., 2006. Contamination by arsenic and other trace elements in tube-well water and its risk assessment to humans in Hanoi, Vietnam. Environ. Pollut. 139, 95–106. http://dx.doi.org/10.1016/j.envpol.2005.04.033.

Ahmed, M.J., Haque, M.E., 2002. A rapid spectrophotometric method for the determination of molybdenum in industrial, environmental, biological and soil samples using 5,7-Dibromo-8-hydroxyquinoline. Anal. Sci. 18, 433–439. http://dx.doi.org/10.2116/analsci.18.433.

Al Kuisi, M., Al-Hwaiti, M., Mashal, K., Abed, A.M., 2015. Spatial distribution patterns of molybdenum (Mo) concentrations in potable groundwater in Northern Jordan. Environ. Monit. Assess. 187, 148. http://dx.doi.org/10.1007/s10661-015-4264-5.

Albéric, P., Voillier, E., Jézéquel, D., Grosbois, C., Michard, G., 2000. Interactions between trace elements and dissolved organic matter in the stagnant anoxic deep layer of a meromictic lake. Limnol. Oceanogr. 45, 1088–1096. http://dx.doi.org/10.4319/lo.2000.45.5.1088.

Al-Dalama, K., Aravind, B., Stanislaus, A., 2005. Influence of complexing agents on the adsorption of molybdate and nickel ions on alumina. Appl. Catal. A Gen. 296, 49–53. http://dx.doi.org/10.1016/j.apcata.2005.07.041.

Algeo, T.J., Lyons, T.W., 2006. Mo-total organic carbon covariation in modern anoxic marine environments: implications for analysis of paleoredox and paleohydrographic conditions. Paleoceanography 21.

Alpers, C.N., Taylor, H.E., Domagalski, J.L., 2000. Metals Transport in the Sacramento River, California, 1996-1997. Volume 1: Methods and Data. Water-Resources Investigations Report No. 99–4286. USGS.

Amer, K.M., 2008. Groundwater resources sustainability in Qatar: problems and perspectives. In: Groundwater for Sustainable Development: Problems, Perspectives and Challenges. CRC Press, pp. 25–37.

Anbar, A.D., Knoll, A.H., 2002. Proterozoic ocean chemistry and evolution: a bioinorganic bridge? Science 297, 1137. http://dx.doi.org/10.1126/science.1069651.

Anbar, A.D., 2004. Molybdenum stable isotopes: observations, interpretations and directions. In: Johnson, C.M., Beard, B.L., Albarede, F. (Eds.), Geochemistry of Non-traditional Stable Isotopes, pp. 429–454.

Anbar, A.D., Duan, Y., Lyons, T.W., Arnold, G.L., Kendall, B., Creaser, R.A., Kaufman, A.J., Gordon, G.W., Scott, C., Garvin, J., Buick, R., 2007. A whiff of oxygen before the great oxidation event? Science 317, 1903–1906. http://dx.doi.org/10.1126/science.1140325.

Anbar, A.D., Gordon, G.W., 2008. Redox renaissance. Geology 36, 271–272. http://dx.doi.org/10.1130/focus032008.1.

Ander, E.L., 2009. Quality Control of Regional Geochemical Stream Water Samples Collected in 2005 in Northern Ireland for the Tellus Project (No. CR/06/200N). British Geological Survey, Keyworth, Nottingham.

Arai, Y., 2010. X-ray absorption spectroscopic investigation of molybdenum multinuclear sorption mechanism at the goethite-water interface. Environ. Sci. Technol. 44, 8491–8496. http://dx.doi.org/10.1021/es101270g.

Archer, C., Vance, D., 2008. The isotopic signature of the global riverine molybdenum flux and anoxia in the ancient oceans. Nat. Geosci. 1, 597–600. http://dx.doi.org/10.1038/ngeo282.

Ardakani, O.H., Chappaz, A., Sanei, H., Mayer, B., 2016. Effect of thermal maturity on remobilization of molybdenum in black shales. Earth Planet. Sci. Lett. 449, 311–320. http://dx.doi.org/10.1016/j.epsl.2016.06.004.

Ardau, C., Frau, F., Dore, E., Lattanzi, P., 2012. Molybdate sorption by Zn-Al sulphate layered double hydroxides. Appl. Clay Sci. 65–66, 128–133. http://dx.doi.org/10.1016/j.clay.2012.05.005.

Arnórsson, S., Ívarsson, G., 1985. Molybdenum in Icelandic geothermal waters. Contrib. Mineral. Petrol 90, 179–189. http://dx.doi.org/10.1007/BF00378259.

Arnórsson, S., Oskarsson, N., 2007. Molybdenum and tungsten in volcanic rocks and in surface and <100°C ground waters in Iceland. Geochim. Cosmochim. Acta 71, 284–304. http://dx.doi.org/10.1016/j.gca.2006.09.030.

Asael, D., Tissot, F.L.H., Reinhard, C.T., Rouxel, O., Dauphas, N., Lyons, T.W., Ponzevera, E., Liorzou, C., Chéron, S., 2013. Coupled molybdenum, iron and uranium stable isotopes as oceanic paleoredox proxies during the Paleoproterozoic Shunga event. Chem. Geol. 362, 193–210. http://dx.doi.org/10.1016/j.chemgeo.2013.08.003.

Ayotte, J.D., Gronberg, J.A.M., Apodaca, L.E., 2011. Trace Elements and Radon in Groundwater Across the United States, 1992-2003. Scientific Investigations Report No. 2011–5059. United States Geological Survey.

Azrieli-Tal, I., Matthews, A., Bar-Matthews, M., Almogi-Labin, A., Vance, D., Archer, C., Teutsch, N., 2014. Evidence from molybdenum and iron isotopes and molybdenum–uranium covariation for sulphidic bottom waters during Eastern Mediterranean sapropel S1 formation. Earth Planet. Sci. Lett. 393, 231–242. http://dx.doi.org/10.1016/j.epsl.2014.02.054.

Balandis, V.A., Zamana, L.V., Ptitsyn, A.B., 2005. Chemical characteristics of natural waters: dependence on the geologic structure of the Uronai ore unit, eastern Transbaikalia. Russ. Geol. Geophys. 46, 645–651.

Balistrieri, L., Murray, J., 1982. The surface chemistry of δMnO_2 in major ion sea water. Geochim. Cosmochim. Acta 46, 1041–1052.

Balistrieri, L.S., Chao, T.T., 1990. Adsorption of selenium by amorphous iron oxyhydroxide and manganese dioxide. Geochim. Cosmochim. Acta 54, 739–751. http://dx.doi.org/10.1016/0016-7037(90)90369-V.

Barałkiewicz, D., Siepak, J., 1997. Determination of trace amounts of molybdenum in water samples by graphite furnace atomic absorption spectrometry with multiple injections and cool down step. Anal. Chim. Acta 353, 85–89. http://dx.doi.org/10.1016/S0003-2670(97)00379-6.

Barling, J., Anbar, A.D.D., 2004. Molybdenum isotope fractionation during adsorption by manganese oxides. Earth Planet. Sci. Lett. 217, 315–329. http://dx.doi.org/10.1016/S0012-821X(03)00608-3.

Barling, J., Arnold, G.L., Anbar, A.D., 2001. Natural mass-dependent variations in the isotopic composition of molybdenum. Earth Planet. Sci. Lett. 193, 447–457. http://dx.doi.org/10.1016/S0012-821X(01)00514-3.

Barrow, N.J., 1970. Comparison of the adsorption of molybdate, sulfate and phosphate by soils. Soil Sci. 109, 282–288.

Baston, G.M., Hunter, F.M.I., Heath, T.G., 1988. Summary of Additions and Amendments to Data in the HATCHES Chemical Thermodynamic Database 2002 to 2007 (No. SA/ENV-0934). Serco for United Kingdom Nirex Limited. Didcot, Oxfordshire, UK.

Beck, M., Dellwig, O., Schnetger, B., Brumsack, H.-J., 2008. Cycling of trace metals (Mn, Fe, Mo, U, V, Cr) in deep pore waters of intertidal flat sediments. Geochim. Cosmochim. Acta 72, 2822–2840. http://dx.doi.org/10.1016/j.gca.2008.04.013.

Bellenger, J.P., Wichard, T., Kustka, A.B., Kraepiel, A.M.L., 2008. Uptake of molybdenum and vanadium by a nitrogen-fixing soil bacterium using siderophores. Nat. Geosci. 1, 243–246. http://dx.doi.org/10.1038/ngeo161.

Bennett, B., Dudas, M.J., 2003. Release of arsenic and molybdenum by reductive dissolution of iron oxides in a soil with enriched levels of native arsenic. J. Environ. Eng. Sci. 2, 265–272.

Berrang, P.G.G., Grill, E.V.V., 1974. The effect of manganese oxide scavenging on molybdenum in Saanich Inlet, British Columbia. Mar. Chem. 2, 125–148. http://dx.doi.org/10.1016/0304-4203(74)90033-4.

Bertine, K.K., Turekian, K.K., 1973. Molybdenum in marine deposits. Geochim. Cosmochim. Acta 37, 1415–1434. http://dx.doi.org/10.1016/0016-7037(73)90080-X.

Bertoni, F.A., Medeot, A.C., González, J.C., Sala, L.F., Bellú, S.E., 2015. Application of green seaweed biomass for Mo^{VI} sorption from contaminated waters. Kinetic, thermodynamic and continuous sorption studies. J. Colloid Interface Sci. 446, 122–132. http://dx.doi.org/10.1016/j.jcis.2015.01.033.

Bettinelli, M., Baffi, C., Beone, G.M., Spezia, S., 2000. Soils and sediments analysis by spectroscopic techniques part II: determination of trace elements by ICP-MS. At. Spectrosc. 21, 60–70.

BGS, 2006. Regional Geochemistry of the Humber-Trent Region: Stream Sediment, Soil and Stream Water. British Geological Survey, Keyworth, Nottingham.

BGS, 1999. Regional Geochemistry: Stream Water, Wales. British Geological Survey, Keyworth, Nottingham.

BGS and DPHE, 2001. Arsenic Contamination of Groundwater in Bangladesh. British Geological Survey Report No. WC/00/019. British Geological Survey, Keyworth, Nottingham.

Bhattacharya, P., Claesson, M., Bundschuh, J., Sracek, O., Fagerberg, J., Jacks, G., Martin, R.A., Storniolo, A., del, R., Thir, J.M., 2006. Distribution and mobility of arsenic in the Río Dulce alluvial aquifers in Santiago del Estero Province, Argentina. Sci. Total Environ. 358, 97–120. http://dx.doi.org/10.1016/j.scitotenv.2005.04.048.

Bibak, A., Borggard, O.K., 1994. Molybdenum adsorption by aluminum and iron-oxides and humic-acid. Soil Sci. 158, 323–328.

Biswas, K.C., Woodards, N.A., Xu, H., Barton, L.L., 2009. Reduction of molybdate by sulfate-reducing bacteria. BioMetals 22, 131–139. http://dx.doi.org/10.1007/s10534-008-9198-8.

Blanc, P., Lassin, A., Piantone, P., Azaroual, M., Jacquemet, N., Fabbri, A., Gaucher, E.C., 2012. Thermoddem: a geochemical database focused on low temperature water/rock interactions and waste materials. Appl. Geochem 27, 2107–2116. http://dx.doi.org/10.1016/j.apgeochem.2012.06.002.

Blowes, D.W., Ptacek, C.J., Jambor, J.L., Weisener, C.G., 2004. The geochemistry of acid mine drainage. In: Lollar, B.S. (Ed.), Treatise on Geochemistry. Elsevier, Amsterdam, pp. 149–204.

Borg, S., Liu, W., Etschmann, B., Tian, Y., Brugger, J., 2012. An XAS study of molybdenum speciation in hydrothermal chloride solutions from 25–385 °C and 600 bar. Geochim. Cosmochim. Acta 92, 292–307. http://dx.doi.org/10.1016/j.gca.2012.06.001.

Bostick, B.C., Fendorf, S., Helz, G.R., 2003. Differential adsorption of molybdate and tetrathiomolybdate on pyrite (FeS_2). Environ. Sci. Technol. 37, 285–291.

Bourikas, K., Hiemstra, T., Van Riemsdijk, W.H., 2001. Adsorption of molybdate monomers and polymers on titania with a multisite approach. J. Phys. Chem. B 105, 2393–2403. http://dx.doi.org/10.1021/jp002267q.

Bradford, G.R., Bakhtar, D., Westcot, D., 1990. Uranium, vanadium, and molybdenum in saline waters of California (USA). J. Environ. Qual. 19, 105–108.

Bradford, G.R., Change, A.C., Page, A.L., Bakhtar, D., Frampton, J.A., Wright, H., 1996. Background Concentrations of Trace and Major Elements in California Soils (Kearney Foundation of Soil Science Special Report). University of California, California, USA.

Breillat, N., Guerrot, C., Marcoux, E., Négrel, P., 2016. A new global database of $\delta^{98}Mo$ in molybdenites: a literature review and new data. J. Geochem. Explor 161, 1–15. http://dx.doi.org/10.1016/j.gexplo.2015.07.019.

Brendler, V., Vahle, A., Arnold, T., Bernhard, G., Fanghänel, T., 2003. RES3T-Rossendorf expert system for surface and sorption thermodynamics. J. Contam. Hydrol. 61, 281–291. http://dx.doi.org/10.1016/S0169-7722(02)00129-8.

Brennan, R.F., Bolland, M.D.A., Bowden, J.W., 2004. Potassium deficiency, and molybdenum deficiency and aluminium toxicity due to soil acidification, have become problems for cropping sandy soils in south-western Australia. Aust. J.

Exp. Agric. 44, 1031–1039.
Brinza, L., Benning, L.G., Statham, P.J., 2008. Adsorption studies of Mo and V onto ferrihydrite. Mineral. Mag. 72, 385–388. http://dx.doi.org/10.1180/minmag.2008.072.1.385.
Bruland, K.W., Middag, R., Lohan, M.C., 2014. Controls of trace metals in seawater. In: Holland, H.D., Turekian, K.K. (Eds.), Treatise on Geochemistry. Elsevier, pp. 19–51.
Brumsack, H.J., 2006. The trace metal content of recent organic carbon-rich sediments: implications for Cretaceous black shale formation. Palaeogeogr. Palaeoclimatol. Palaeoecol. 232, 344–361. http://dx.doi.org/10.1016/j.palaeo.2005.05.011.
Burgess, B.K., Lowe, D.J., 1996. Mechanism of molybdenum nitrogenase. Chem. Rev. 96, 2983–3012. http://dx.doi.org/10.1021/cr950055x.
Calvert, S.E., Pedersen, T.F., 1993. Geochemistry of Recent oxic and anoxic marine sediments: implications for the geological record. Mar. Geol. 113, 67–88. http://dx.doi.org/10.1016/0025-3227(93)90150-T.
Campbell, M.R., 1923. The Twentymile Park District of the Yampa Coal Field, United States Geological Survey Bulletin 748. Government Printing Office.
Campillo, N., Lopez-Garcia, I., Viñas, P., Arnau-Jerez, I., Hernandez-Cordoba, M., 2002. Determination of vanadium, molybdenum and chromium in soils, sediments and sludges by electrothermal atomic absorption spectrometry with slurry sample introduction. J. Anal. At. Spectrom. 17, 1429.
Chaillou, G., Schäfer, J., Blanc, G., Anschutz, P., 2008. Mobility of Mo, U, As, and Sb within modern turbidites. Mar. Geol. 254, 171–179. http://dx.doi.org/10.1016/j.margeo.2008.06.002.
Chapelle, W., Meglen, R.R., Moure-Eraso, R., Solomons, C.C., Tsongas, T.A., Walravens, P.A., Winston, P.W., 1979. Human Health Effects of Molybdenum in Drinking Water. The US Environmental Protection Agency, Cincinatti, USA.
Chappaz, A., Gobeil, C., Tessier, A., 2008. Geochemical and anthropogenic enrichments of Mo in sediments from perennially oxic and seasonally anoxic lakes in Eastern Canada. Geochim. Cosmochim. Acta 72, 170–184. http://dx.doi.org/10.1016/j.gca.2007.10.014.
Chappaz, A., Lyons, T.W., Gordon, G.W., Anbar, A.D., 2012. Isotopic fingerprints of anthropogenic molybdenum in lake sediments. Environ. Sci. Technol. 46, 10934–10940. http://dx.doi.org/10.1021/es3019379.
Chappaz, A., Lyons, T.W., Gregory, D.D., Reinhard, C.T., Gill, B.C., Li, C., Large, R.R., 2014. Does pyrite act as an important host for molybdenum in modern and ancient euxinic sediments? Geochim. Cosmochim. Acta 126, 112–122.
Chen, Z.G., Zhu, L., Zhang, T.Y., Liu, J.B., Han, Y.L., 2008. A novel and selective assay for the quantitative analysis of molybdenum(VI) at nanogram level by resonance light scattering quenching technique. Spectrochim. Acta. A. Mol. Biomol. Spectrosc. 70, 290–296. http://dx.doi.org/10.1016/j.saa.2007.07.048.
Cheng, W.C., Luthra, N.P., 1988. NMR study of the adsorption of phosphomolybdates on alumina. J. Catal. 109, 163–169. http://dx.doi.org/10.1016/0021-9517(88)90194-7.
Clarke, F.W., 1924. The data of geochemistry. In: United States Geological Survey Bulletin 770, fifth ed. Government Printing Office, Washington.
Clarke, N.J., Laurie, S.H., 1980. The copper-molybdenum antagonism in ruminants. I. The formation of thiomolybdates in animal rumen. J. Inorg. Biochem. 12, 37–43. http://dx.doi.org/10.1016/S0162-0134(00)80041-0.
Coetsiers, M., Walraevens, K., 2009. The Neogene aquifer, Flanders, Belgium. In: Natural Groundwater Quality. Blackwell Publishing, pp. 263–286.
Collier, R.W., 1985. Molybdenum in the northeast Pacific Ocean. Limnol. Oceanogr. 30, 1351–1354. http://dx.doi.org/10.2307/2836491.
Condesso de Melo, M.T., Marques da Silva, M.A., 2009. The Aveiro Quaternary and Cretaceous aquifers, Portugal. In: Natural Groundwater Quality. Blackwell Publishing, pp. 233–262.
Conlan, M.J., Mayer, K.U., Blaskovich, R., Beckie, R.D., 2012. Solubility controls for molybdenum in neutral rock drainage. Geochem. Explor. Environ. Anal. 12, 21–32.
Contreras, R., Fogg, T.R., Chasteen, N.D., Gaudette, H.E., Lyons, W.B., 1978. Molybdenum in pore waters of anoxic marine sediments by electron paramagnetic resonance spectroscopy. Mar. Chem. 6, 365–373. http://dx.doi.org/10.1016/0304-4203(78)90017-8.
Crusius, J., Calvert, S., Pedersen, T., Sage, D., 1996. Rhenium and molybdenum enrichments in sediments as indicators of oxic, suboxic and sulfidic conditions of deposition. Earth Planet. Sci. Lett. 145, 65–78. http://dx.doi.org/10.1016/s0012-821x(96)00204-x.
Cruywagen, J.J., 1999. Protonation, oligomerization, and condensation reactions of vanadate(V), molybdate(VI), and tungstate(VI). In: Sykes, A.G. (Ed.), Advances in Inorganic Chemistry. Academic Press, pp. 127–182.
Cruywagen, J.J., Draaijer, A.G., Heyns, J.B.B., Rohwer, E.A., 2002. Molybdenum(VI) equilibria in different ionic media. Formation constants and thermodynamic quantities. Inorg. Chim. Acta 331, 322–329. http://dx.doi.org/10.1016/S0020-1693(02)00700-4.
Cruywagen, J.J., Heyns, J.B.B., 1987. Equilibria and UV spectra of mono- and polynuclear molybdenum(VI) species. Inorg. Chem. 26, 2569–2572. http://dx.doi.org/10.1021/ic00263a003.
Cutter, G.A., Kluckhohn, R.S., 1999. The cycling of particulate carbon, nitrogen, sulfur, and sulfur species (iron monosulfide, pyrite, and organic sulfur) in the water columns of Framvaren Fjord and the Black Sea. Mar. Chem. 67 http://dx.doi.org/10.1016/S0304-4203(99)00056-0.
Dahl, T.W., Anbar, A.D., Gordon, G.W., Rosing, M.T., Frei, R., Canfield, D.E., 2010. The behavior of molybdenum and its isotopes across the chemocline and in the sediments of sulfidic Lake Cadagno, Switzerland. Geochim. Cosmochim. Acta 74, 144–163. http://dx.doi.org/10.1016/j.gca.2009.09.018.
Dahl, T.W., Chappaz, A., Fitts, J.P., Lyons, T.W., 2013a. Molybdenum reduction in a sulfidic lake: evidence from X-ray absorption fine-structure spectroscopy and implications for the Mo paleoproxy. Geochim. Cosmochim. Acta 103, 213–231. http://dx.doi.org/10.1016/j.gca.2012.10.058.
Dahl, T.W., Chappaz, A., Hoek, J., McKenzie, C.J., Svane, S., Canfield, D.E., 2016. Evidence of molybdenum association with particulate organic matter under sulfidic conditions. Geobiology. http://dx.doi.org/10.1111/gbi.12220 n/a-n/a.
Dahl, T.W., Ruhl, M., Hammarlund, E.U., Canfield, D.E., Rosing, M.T., Bjerrum, C.J., 2013b. Tracing euxinia by molybdenum concentrations in sediments using handheld X-ray fluorescence spectroscopy (HHXRF). Chem. Geol. 360–361, 241–251. http://dx.doi.org/10.1016/j.chemgeo.2013.10.022.
Dalai, T.K., Nishimura, K., Nozaki, Y., 2005. Geochemistry of molybdenum in the Chao Phraya River estuary, Thailand: role of suboxic diagenesis and porewater transport. Chem. Geol. 218, 189–202. http://dx.doi.org/10.1016/j.chemgeo.2005.01.002.
Das, A.K., Chakraborty, R., Cervera, M.L., de la Guardia, M., 2007. A review on molybdenum determination in solid geological samples. Talanta 71, 987–1000.
Das, S., Essilfie-Dughan, J., Hendry, M.J., 2016. Sequestration of molybdate during transformation of 2-line ferrihydrite under alkaline conditions. Appl. Geochem 73, 70–80. http://dx.doi.org/10.1016/j.apgeochem.2016.08.003.
Davison, W., 1991. The solubility of iron sulphides in synthetic and natural waters at ambient temperature. Aquat. Sci. 53, 309–329. http://dx.doi.org/10.1007/BF00877139.
Dellwig, O., Beck, M., Lemke, A., Lunau, M., Kolditz, K., Schnetger, B., Brumsack, H.-J., 2007. Non-conservative behaviour of molybdenum in coastal waters: coupling geochemical, biological, and sedimentological processes. Geochim. Cosmochim. Acta 71, 2745–2761. http://dx.doi.org/10.1016/j.gca.2007.03.014.
Denison, F.H., Garnier-Laplace, J., 2005. The effects of database parameter uncertainty on uranium(VI) equilibrium calculations. Geochim. Cosmochim. Acta 69, 2183–2191. http://dx.doi.org/10.1016/j.gca.2004.09.033.
Diwakar, J., Johnston, S.G., Burton, E.D., Shrestha, S.D., 2015. Arsenic mobilization in an alluvial aquifer of the Terai region, Nepal. J. Hydrol. Reg. Stud. 4 (Part A), 59–79. http://dx.doi.org/10.1016/j.ejrh.2014.10.001.
Dold, B., Fontboté, L., 2001. Element cycling and secondary mineralogy in porphyry copper tailings as a function of climate, primary mineralogy, and mineral processing. J. Geochem. Explor 74, 3–55. http://dx.doi.org/10.1016/S0375-6742(01)00174-1.
Domagalski, J.L., Eugster, H.P., Jones, B.F., 1990. Trace metal geochemistry of Walker, Mono, and Great Salt lakes. In: Spencer, R.J., Chou, I.-M. (Eds.), Fluid-Mineral Interactions: a Tribute to H. P. Eugster. Special Publication No. 2. The Geochemical Society, pp. 315–353.
Edmonds, T.E., 1980. The differential pulse polarographic determination of molybdenum in nitrate media. Anal. Chim. Acta 116, 323–333. http://dx.doi.org/10.1016/S0003-2670(01)95212-2.
Ehrlich, H.L., 1996. Geomicrobiology. Dekker, New York.
Elbaz-Poulichet, F., Seidel, J.L., Casiot, C., Tusseau-Vuillemin, M.H., 2006. Short-term variability of dissolved trace element concentrations in the Marne and Seine rivers near Paris. Sci. Total Environ. 367, 278–287.
Emerson, S.R., Huested, S.S., 1991. Ocean anoxia and the concentrations of molybdenum and vanadium in seawater. Mar. Chem. 34, 177–196. http://dx.doi.org/10.1016/0304-4203(91)90002-E.
Ensafi, A., 2002. Simultaneous voltammetric determination of molybdenum and copper by adsorption cathodic differential pulse stripping method using a principal component artificial neural network. Talanta 57, 785–793. http://dx.doi.org/10.1016/S0039-9140(02)00103-0.
ENSR, 2007. Town of Pines Groundwater Superfund Site Chemical Analysis Data. ENSR Consulting. https://quicksilver.epa.gov/work/05/919282.pdf.
Erickson, B.E., Helz, G.R., 2000. Molybdenum(VI) speciation in sulfidic waters:: stability and lability of thiomolybdates. Geochim. Cosmochim. Acta 64, 1149–1158. http://dx.doi.org/10.1016/S0016-7037(99)00423-8.
Essilfie-Dughan, J., Pickering, I.J., Hendry, M.J., George, G.N., Kotzer, T., 2011. Molybdenum speciation in uranium mine tailings using x-ray absorption spectroscopy. Environ. Sci. Technol. 45, 455–460. http://dx.doi.org/10.1021/es102954b.
Essington, M.E., Huntington, G.S., 1990. Formation of Calcium and Magnesium Molybdate Complexes in Dilute Aqueous Solutions and Evaluation of Powellite Solubility in Spent Oil Shale. Western Research Institute, Laramie, Wyoming.
Expert Group on Vitamins and Minerals, 2003. Risk Assessment: Molybdenum. http://www.food.gov.uk/multimedia/pdfs/evm_molybdenum.pdf.
Feldman, P.R., Rosenboom, J.W., Saray, M., Navuth, P., Samnang, C., Iddings, S., 2007. Assessment of the chemical quality of drinking water in Cambodia. J. Water Health 5, 101–106.
Ferreira, S.L.C., Dos Santos, H.C., Campos, R.C., 2003. The determination of molybdenum in water and biological samples by graphite furnace atomic spectrometry after polyurethane foam column separation and preconcentration. Talanta 61, 789–795. http://dx.doi.org/10.1016/S0039-9140(03)00378-3.
Firdaus, L.M., Norisuye, K., Nakagawa, Y., Nakatsuka, S., Sohrin, Y., 2008. Dissolved and labile particulate Zr, Hf, Nb, Ta, Mo and W in the western North Pacific Ocean. J. Oceanogr. 64, 247–257. http://dx.doi.org/10.1007/s10872-008-0019-z.
Food and Nutrition Board, Institute of Medicine, 2001. Chapter 11: molybdenum. In: Dietary Reference Intakes for Vitamin A, Vitamin K, Arsenic, Boron, Chromium, Copper, Iodine, Iron, Manganese, Molybdenum, Nickel, Silicon, Vanadium, and Zinc. National Academy Press, Washington DC, USA, pp. 420–441.
Freund, C., Wishard, A., Brenner, R., Sobel, M., Mizelle, J., Kim, A., Meyer, D.A.,

Morford, J.L., 2016. The effect of a thiol-containing organic molecule on molybdenum adsorption onto pyrite. Geochim. Cosmochim. Acta 174, 222–235. http://dx.doi.org/10.1016/j.gca.2015.11.015.
Freymuth, H., Vils, F., Willbold, M., Taylor, R.N., Elliott, T., 2015. Molybdenum mobility and isotopic fractionation during subduction at the Mariana arc. Earth Planet. Sci. Lett. 432, 176–186. http://dx.doi.org/10.1016/j.epsl.2015.10.006.
Gaillardet, J., Viers, J., Dupré, B., 2014. 7.7-Trace elements in river waters. In: Holland, H.D., Turekian, K.K. (Eds.), Treatise on Geochemistry, second ed. Elsevier, Oxford, pp. 195–235.
George, G.N., Kipke, C.A., Prince, R.C., Sunde, R.A., Enemark, J.H., Cramer, S.P., 1989. Structure of the active site of sulfite oxidase. X-ray absorption spectroscopy of the molybdenum(IV), molybdenum(V), and molybdenum(VI) oxidation states. Biochem. 28, 5075–5080.
Ghiasvand, A.R., Shadabi, S., Mohagheghzadeh, E., Hashemi, P., 2005. Homogeneous liquid-liquid extraction method for the selective separation and preconcentration of ultra trace molybdenum. Talanta 66, 912–916. http://dx.doi.org/10.1016/j.talanta.2004.12.041.
Giffaut, E., Grivé, M., Blanc, P., Vieillard, P., Colàs, E., Gailhanou, H., Gaboreau, S., Marty, N., Madé, B., Duro, L., 2014. Andra thermodynamic database for performance assessment: ThermoChimie. Appl. Geochem 49, 225–236. http://dx.doi.org/10.1016/j.apgeochem.2014.05.007.
Glass, J.B., Chappaz, A., Eustis, B., Heyvaert, A.C., Waetjen, D.P., Hartnett, H.E., Anbar, A.D., 2013. Molybdenum geochemistry in a seasonally dysoxic Mo-limited lacustrine ecosystem. Geochim. Cosmochim. Acta 114, 204–219. http://dx.doi.org/10.1016/j.gca.2013.03.023.
Goldberg, K., Humayun, M., 2016. Geochemical paleoredox indicators in organic-rich shales of the Irati Formation, Permian of the Paraná Basin, southern Brazil. Braz. J. Geol. 46, 377–393.
Goldberg, S., 2009. Influence of soil solution salinity on molybdenum adsorption by soils. Soil Sci. 174, 9–13. http://dx.doi.org/10.1097/SS.0b013e318203aec5.
Goldberg, S., Forster, H.S., 1998. Factors affecting molybdenum adsorption by soils and minerals. Soil Sci. 163, 109–114.
Goldberg, S., Forster, H.S., Godfrey, C.L., 1996. Molybdenum adsorption on oxides, clay minerals, and soils. Soil Sci. Soc. Am. J. 60, 425–432. http://dx.doi.org/10.2136/sssaj1996.03615995006000020013x.
Goldberg, S., Johnston, C.T., Suarez, D.L., Lesch, L.M., 2008. Mechanism of molybdenum adsorption on soils and soil minerals evaluated using vibrational spectroscopy and surface complexation modeling. In: Barnett, M.O., Kent, D.B. (Eds.), Developments in Earth & Environmental Sciences. Elsevier, pp. 235–266.
Goldberg, S., Sposito, G., 1984. A chemical model of phosphate adsorption by soils: I. Reference oxide Minerals. Soil Sci. Soc. Am. J. 48, 772–778. http://dx.doi.org/10.2136/sssaj1984.03615995004800040015x.
Goldberg, S., Su, C., Forster, H.S., 1998. Sorption of molybdenum on oxides, clay minerals, and soils. In: Jenne, E.A. (Ed.), Adsorption of Metals by Geomedia. Academic Press, pp. 401–426.
Goldberg, T., Archer, C., Vance, D., Poulton, S.W., 2009. Mo isotope fractionation during adsorption to Fe (oxyhydr)oxides. Geochim. Cosmochim. Acta 73, 6502–6516. http://dx.doi.org/10.1016/j.gca.2009.08.004.
Goldberg, T., Archer, C., Vance, D., Thamdrup, B., McAnena, A., Poulton, S.W., 2012. Controls on Mo isotope fractionations in a Mn-rich anoxic marine sediment, Gullmar Fjord, Sweden. Chem. Geol. 296–297, 73–82. http://dx.doi.org/10.1016/j.chemgeo.2011.12.020.
Goldberg, T., Gordon, G., Izon, G., Archer, C., Pearce, C.R., McManus, J., Anbar, A.D., Rehkaemper, M., 2013. Resolution of inter-laboratory discrepancies in Mo isotope data: an intercalibration. J. Anal. At. Spectrom. 28, 724–735. http://dx.doi.org/10.1039/c3ja30375f.
Goldberg, T., Poulton, S.W., Wagner, T., Kolonic, S.F., Rehkämper, M., 2016. Molybdenum drawdown during cretaceous oceanic anoxic event 2. Earth Planet. Sci. Lett. 440, 81–91. http://dx.doi.org/10.1016/j.epsl.2016.02.006.
Goodman, B.A., Cheshire, M.V., 1982. Reduction of molybdate by soil organic matter: EPR evidence for formation of both Mo(V) and Mo(III). Nature 299, 618–620. http://dx.doi.org/10.1038/299618a0.
Goto, K.T., Shimoda, G., Anbar, A.D., Gordon, G.W., Harigane, Y., Senda, R., Suzuki, K., 2015. Molybdenum isotopes in hydrothermal manganese crust from the Ryukyu arc system: implications for the source of molybdenum. Mar. Geol. 369, 91–99. http://dx.doi.org/10.1016/j.margeo.2015.08.007.
Gould, L., Kendall, N.R., 2011. Role of the rumen in copper and thiomolybdate absorption. Nutr. Res. Rev. 24, 176–182. http://dx.doi.org/10.1017/S0954422411000059.
Gouzerh, P., Che, M., 2006. From Scheele and Berzelius to Müller: polyoxometalates (POMs) revisited and the “missing link” between the bottom up and top down approaches. L'actualité Chim. 298, 9–22.
Grauer, R., 1997. Chapter IV: solubility limitations: an “old Timer's” view. In: Grenthe, Ingmar, Puigdomenech, Ignasi (Eds.), Modelling in Aquatic Chemistry. OECD Publications, pp. 131–152.
Greber, N.D., Hofmann, B.A., Voegelin, A.R., Villa, I.M., Naegler, T.F., 2011. Mo isotope composition in Mo-rich high- and low-T hydrothermal systems from the Swiss Alps. Geochim. Cosmochim. Acta 75, 6600–6609. http://dx.doi.org/10.1016/j.gca.2011.08.034.
Greber, N.D., Mäder, U., Nägler, T.F., 2015. Experimental dissolution of molybdenum-sulphides at low oxygen concentrations: a first-order approximation of late Archean atmospheric conditions. Earth Space Sci. 2, 173–180. http://dx.doi.org/10.1002/2014EA000059.
Gregory, D.D., Large, R.R., Halpin, J.A., Baturina, E.L., Lyons, T.W., Wu, S., Danyushevsky, L., Sack, P.J., Chappaz, A., Maslennikov, V.V., et al., 2015. Trace element content of sedimentary pyrite in black shales. Econ. Geol. 110, 1389–1410.
Grenthe, I., Mompean, F., Spahiu, K., Wanner, H., 2013. Guidelines for the Extrapolation to Zero Ionic Strength. OECD Nuclear Energy Agency, Data Bank, Issy-les-Moulineaux, France.
Guan, D.-X., Williams, P.N., Luo, J., Zheng, J.-L., Xu, H.-C., Cai, C., Ma, L.Q., 2015. Novel precipitated zirconia-based DGT technique for high-resolution imaging of oxyanions in waters and sediments. Environ. Sci. Technol. 49, 3653–3661. http://dx.doi.org/10.1021/es505424m.
Guo, H.M., Wang, Y.X., 2005. Geochemical characteristics of shallow groundwater in Datong basin, northwestern China. J. Geochem. Explor 87, 109–120. http://dx.doi.org/10.1016/j.gexplo.2005.08.002.
Gupta, U.C., 1997. Symptoms of molybdenum deficiency and toxicity in crops. In: Molybdenum in Agriculture. Cambridge University Press, Cambridge, pp. 160–181.
Gustafsson, J.P., 2003. Modelling molybdate and tungstate adsorption to ferrihydrite. Chem. Geol. 200, 105–115. http://dx.doi.org/10.1016/S0009-2541(03)00161-X.
Gustafsson, J.P., Tiberg, C., 2015. Molybdenum binding to soil constituents in acid soils: an XAS and modelling study. Chem. Geol. 417, 279–288. http://dx.doi.org/10.1016/j.chemgeo.2015.10.016.
Hale, K.L., McGrath, S.P., Lombi, E., Stack, S.M., Terry, N., Pickering, I.J., George, G.N., Pilon-Smits, E.A., 2001. Molybdenum sequestration in *Brassica* species. A role for anthocyanins? Plant Physiol. 126, 1391–1402.
Hall, G.E.M., Jefferson, C.W., Michel, F.A., 1988. Determination of W and Mo in natural spring waters by ICP-AES (inductively coupled plasma atomic emission spectrometry) and ICP-MS (inductively coupled plasma mass spectrometry): application to south Nahanni river area, N.W.T. Can. J. Geochem. Explor 30, 63–84. http://dx.doi.org/10.1016/0375-6742(88)90050-7.
Hall, G.E.M., Pelchat, J.-C., de Silva, K.N., 1987. Determination of low concentrations of tungsten and molybdenum in geological materials using inductively coupled plasma atomic emission spectrometry with pre-concentration on activated charcoal. Analyst 112, 631–635. http://dx.doi.org/10.1039/AN9871200631.
Harita, Y., Hori, T., Sugiyama, M., 2005. Release of trace oxyanions from littoral sediments and suspended particles induced by pH increase in the epilimnion of lakes. Limnol. Oceanogr. 50, 636–645.
Harrison, W.J., Pevear, D.R., Lindahl, P.C., 1973. Trace elements in pyrites of the Green River Formation Oil shales, Wyoming, Utah, and Colorado. In: Geochemical, Biogeochemical and Sedimentological Studies of the Green River Formation, Wyoming, Utah and Colorado. U.S. Geological Survey Bulletin 1973 A-G, pp. D1–D23.
Havig, J.R., McCormick, M.L., Hamilton, T.L., Kump, L.R., 2015. The behavior of biologically important trace elements across the oxic/euxinic transition of meromictic Fayetteville Green Lake, New York, USA. Geochim. Cosmochim. Acta 165, 389–406. http://dx.doi.org/10.1016/j.gca.2015.06.024.
Healy, T.W., Herring, A., Fuerstenau, D., 1966. The effect of crystal structure on the surface properties of a series of manganese dioxides. J. Colloid Interface Sci. 21, 435–444.
Helz, G.R., 2014. Activity of zero-valent sulfur in sulfidic natural waters. Geochem. Trans. 15, 13. http://dx.doi.org/10.1186/s12932-014-0013-x.
Helz, G.R., Bura-Nakić, E., Mikac, N., Ciglenečki, I., 2011. New model for molybdenum behavior in euxinic waters. Chem. Geol. 284, 323–332. http://dx.doi.org/10.1016/j.chemgeo.2011.03.012.
Helz, G.R., Erickson, B.E., 2011. Extraordinary stability of copper(I)–tetrathiomolybdate complexes: possible implications for aquatic ecosystems. Environ. Toxicol. Chem. 30, 97–102. http://dx.doi.org/10.1002/etc.379.
Helz, G.R., Erickson, B.E., Vorlicek, T.P., 2014. Stabilities of thiomolybdate complexes of iron; implications for retention of essential trace elements (Fe, Cu, Mo) in sulfidic waters. Metallomics 6, 1131–1140. http://dx.doi.org/10.1039/C3MT00217A.
Helz, G.R., Miller, C.V., Charnock, J.M., Mosselmans, J.F.W., Pattrick, R.A.D., Garner, C.D., Vaughan, D.J., 1996. Mechanism of molybdenum removal from the sea and its concentration in black shales: EXAFS evidence. Geochim. Cosmochim. Acta 60, 3631–3642.
Helz, G.R., Vorlicek, T.P., Kahn, M.D., 2004. Molybdenum scavenging by iron monosulfide. Environ. Sci. Technol. 38, 4263–4268.
Hensel, B.R., Jansen, T.A., Muehlfeld, T.C., 2015. Groundwater forensics to evaluate molybdenum concentrations near a CCR landfill, in: World of Coal Ash. Presented at the World of Coal Ash (WOCA), Nashville, TN, USA, p. 14 pp.
Hewitt, E.J., 1956. Symptoms of molybdenum deficiency in plants. Soil Sci. 81, 159–171.
Hille, R., 1996. The mononuclear molybdenum enzymes. Chem. Rev. 96, 2757–2816. http://dx.doi.org/10.1021/cr950061t.
Hodge, V.F., Johannesson, K.H., Stetzenbach, K.J., 1996. Rhenium, molybdenum, and uranium in groundwater from the southern Great Basin, USA: evidence for conservative behavior. Geochim. Cosmochim. Acta 60, 3197–3214.
Horton, F.W., Laney, F.B., 1916. Molybdenum: its ores and thier concentration, with a discussion of markets, prices and uses. Bur. Mines Bull. 111, 15–16.
Hu, Z., Gao, S., 2008. Upper crustal abundances of trace elements: a revision and update. Chem. Geol. 253, 205–221. http://dx.doi.org/10.1016/j.chemgeo.2008.05.010.
Huang, P.M., Iskandar, I.K. (Eds.), 1999. Soils and Groundwater Pollution and Remediation: Asia, Africa, and Oceania. CRC Press, Boca Raton.
Imperial College, 1978. The Wolfson Geochemical Atlas of England and Wales. Clarendon Press, Oxford.

Jarrell, W.M., Page, A.L., Elseewi, A.A., 1980. Molybdenum in the environment. Residue Rev. 7, 41–43.
Johannesson, K.H., Lyons, W.B., Graham, E.Y., Welch, K.A., 2000. Oxyanion concentrations in eastern Sierra Nevada rivers - 3. Boron, molybdenum, vanadium, and tungsten. Aquat. Geochem 6, 19–46. http://dx.doi.org/10.1023/a:1009622219482.
Johnsen, R., 2015. Corrosion challenges for the oil and gas industry in the State of Qatar. In: Karaman, I., Arroyave, R., Masad, E. (Eds.), TMS Middle East - Mediterranean Materials Congress on Energy and Infrastructure Systems. Wiley & Sons, New Jersey, pp. 3–12.
Johnson, C.C., Breward, N., Ander, E.L., Ault, L., 2005. G-BASE: baseline geochemical mapping of Great Britain and Northern Ireland. Geochem. Explor. Environ. Anal. 5, 347–357. http://dx.doi.org/10.1144/1467-7873/05-070.
Jones, L.H.P., 1957. The solubility of molybdenum in simplified systems and aqueous soil suspensions. J. Soil Sci. 8, 313–327. http://dx.doi.org/10.1111/j.1365-2389.1957.tb01891.x.
Kaback, D.S., Runnells, D.D., 1980. Geochemistry of molybdenum in some stream sediments and waters. Geochim. Cosmochim. Acta 44, 447–456. http://dx.doi.org/10.1016/0016-7037(80)90043-5.
Kargar, M., Khorasani, N., Karami, M., Rafiee, G.-R., Naseh, R., 2011. Study of aluminum, copper and molybdenum pollution in groundwater sources surrounding (Miduk) Shahr-E-Babak Copper Complex Tailings Dam. World Acad. Sci. Eng. Technol. 52, 412–416.
Karimian, N., Cox, F.R., 1978. Adsorption and extractability of molybdenum in relation to some chemical properties of soil. Soil Sci. Soc. Am. J. 42, 757–761.
Kashiwabara, T., Takahashi, Y., Marcus, M.A., Uruga, T., Tanida, H., Terada, Y., Usui, A., 2013. Tungsten species in natural ferromanganese oxides related to its different behavior from molybdenum in oxic ocean. Geochim. Cosmochim. Acta 106, 364–378. http://dx.doi.org/10.1016/j.gca.2012.12.026.
Kashiwabara, T., Takahashi, Y., Tanimizu, M., Usui, A., 2011. Molecular-scale mechanisms of distribution and isotopic fractionation of molybdenum between seawater and ferromanganese oxides. Geochim. Cosmochim. Acta 75, 5762–5784. http://dx.doi.org/10.1016/j.gca.2011.07.022.
Kawakubo, S., Hashi, S., Iwatsuki, M., 2001. Physicochemical speciation of molybdenum in rain water. Water Res. 35, 2489–2495. http://dx.doi.org/10.1016/S0043-1354(00)00520-0.
Kendall, B., Dahl, T.W., Anbar, A.D., 2017. The stable isotope geochemistry of molybdenum. Rev. Mineral. Geochem 82, 683–732.
Kendall, B., Gordon, G.W., Poulton, S.W., Anbar, A.D., 2011. Molybdenum isotope constraints on the extent of late Paleoproterozoic ocean euxinia. Earth Planet. Sci. Lett. 307, 450–460. http://dx.doi.org/10.1016/j.epsl.2011.05.019.
Kendall, B., Komiya, T., Lyons, T.W., Bates, S.M., Gordon, G.W., Romaniello, S.J., Jiang, G., Creaser, R.A., Xiao, S., McFadden, K., Sawaki, Y., Tahata, M., Shu, D., Han, J., Li, Y., Chu, X., Anbar, A.D., 2015. Uranium and molybdenum isotope evidence for an episode of widespread ocean oxygenation during the late Ediacaran Period. Geochim. Cosmochim. Acta 156, 173–193. http://dx.doi.org/10.1016/j.gca.2015.02.025.
Khan, S.H., Berg, C.M.G.V.D., 1989. The determination of molybdenum in estuarine waters using cathodic stripping voltammetry. Mar. Chem. 27, 31–42. http://dx.doi.org/10.1016/0304-4203(89)90026-1.
Kinniburgh, D.G., Cooper, D.M., 2004. Predominance and mineral stability diagrams revisited. Environ. Sci. Technol. 38, 3641–3648. http://dx.doi.org/10.1021/es034927l.
Kinniburgh, D.G., Syers, J.K., Jackson, M.L., 1975. Specific adsorption of trace amounts of calcium and strontium by hydrous oxide of iron and aluminum. Soil Sci. Soc. Am. Proc. 39, 464–470.
Kuhn, T., Bostick, B.C., Koschinsky, A., Halbach, P., Fendorf, S., 2003. Enrichment of Mo in hydrothermal Mn precipitates: possible Mo sources, formation process and phase associations. Chem. Geol. 199, 29–43. http://dx.doi.org/10.1016/S0009-2541(03)00054-8.
Kuiper, N., Rowell, C., Shomar, B., 2015. High levels of molybdenum in Qatar's groundwater and potential impacts. J. Geochem. Explor 150, 16–24. http://dx.doi.org/10.1016/j.gexplo.2014.12.009.
Lang, F., Kaupenjohann, M., 2003. Immobilisation of molybdate by iron oxides: effects of organic coatings. Geoderma 113, 31–46. http://dx.doi.org/10.1016/s0016-7061(02)00314-2.
Lazaridis, N.K., Jekel, M., Zouboulis, A.I., 2003. Removal of Cr(VI), Mo(VI), and V(V) ions from single metal aqueous solutions by sorption or nanofiltration. Sep. Sci. Technol. 38, 2201–2219.
Leech, A.F., Thornton, I., 1987. Trace elements in soils and pasture herbage on farms with bovine hypocupraemia. J. Agric. Sci. 108, 591–597.
Leybourne, M.I., 1998. Hydrogeochemical, isotopic, and rare earth element evidence for contrasting water–rock interactions at two undisturbed Zn–Pb massive sulphide deposits, Bathurst mining Camp, N.B. Can. J. Geochem. Explor 64, 237–261.
Leybourne, M.I., Cameron, E.M., 2008. Source, transport, and fate of rhenium, selenium, molybdenum, arsenic, and copper in groundwater associated with porphyry-Cu deposits, Atacama Desert, Chile. Chem. Geol. 247, 208–228. http://dx.doi.org/10.1016/j.chemgeo.2007.10.017. ISSN 0009–2541.
Leybourne, M.I., Cameron, E.M., 2006. Composition of groundwaters associated with porphyry-Cu deposits, Atacama Desert, Chile: elemental and isotopic constraints on water sources and water–rock reactions. Geochim. Cosmochim. Acta 70, 1616–1635. http://dx.doi.org/10.1016/j.gca.2005.12.003.
Li, C., Love, G.D., Lyons, T.W., Fike, D.A., Sessions, A.L., Chu, X., 2010. A stratified redox model for the Ediacaran ocean. Science 328, 80. http://dx.doi.org/10.1126/science.1182369.
Linnik, P.N., Ignatenko, I.I., 2015. Molybdenum in natural surface waters: content and forms of occurrence (a review). Hydrobiol. J. 51, 80–103.
Lister, T.R., Flight, D.M.A., Patton, M.A.G., Smyth, D., 2007. Molybdenum in stream sediments (XRF). 1:250,000 scale map. Reg. Geochem. Ser. Geol. Surv. North. Irel.
Liu, T., Diemann, E., Li, H., Dress, A.W.M., Müller, Achim, 2003. Self-assembly in aqueous solution of wheel-shaped Mo154 oxide clusters into vesicles. Nature 426, 59–62.
Lourigan, J., Phelps, W., 2013. Caledonia Groundwater Molybdenum Investigation Southeast Wisconsin. Wisconsin Department of Natural Resources.
Ludington, B.S., Plumlee, G.S., 2009. Climax-type porphyry molybdenum deposits. U. S. Geol. Survey 1215, 1–16.
Luong, E.T., Houk, R.S., Serfass, R.S., 1997. Chromatographic isolation of molybdenum from human blood plasma and determination by inductively coupled plasma mass spectrometry with isotope dilution. J. Anal. At. Spectrom. 12, 703–708. http://dx.doi.org/10.1039/A608265C.
Luthra, N.P., Cheng, W.C., 1987. Molybdenum-95 NMR study of the adsorption of molybdates on alumina. J. Catal. 107, 154–160. http://dx.doi.org/10.1016/0021-9517(87)90280-6.
Lyons, T.W., Reinhard, C.T., Planavsky, N.J., 2014. The rise of oxygen in Earth's early ocean and atmosphere. Nature 506, 307–315.
Lyons, T.W., Werne, J.P., Hollander, D.J., Murray, R., 2003. Contrasting sulfur geochemistry and Fe/Al and Mo/Al ratios across the last oxic-to-anoxic transition in the Cariaco Basin, Venezuela. Chem. Geol. 195, 131–157. http://dx.doi.org/10.1016/S0009-2541(02)00392-3.
Ma, W., Sha, X., Gao, L., Cheng, Z., Meng, F., Cai, J., Tan, D., Wang, R., 2015. Effect of iron oxide nanocluster on enhanced removal of molybdate from surface water and pilot scale test. Colloids Surf. Physicochem. Eng. Asp. 478, 45–53. http://dx.doi.org/10.1016/j.colsurfa.2015.03.032.
Machkova, M., Velikov, B., Dimitrov, D., Neykov, N., Neytchev, P., 2009. Quality status of the Upper Thracian Plio-Quaternary aquifer, south Bulgaria. In: Natural Groundwater Quality. Blackwell Publishing, pp. 391–403.
Magyar, B., Moor, H.C., Sigg, L., 1993. Vertical distribution and transport of molybdenum in a lake with a seasonally anoxic hypolimnion. Limnol. Oceanogr. 38, 521–531.
Manning, B.A., Goldberg, S., 1996. Modeling competitive adsorption of arsenate with phosphate and molybdate on oxide minerals. Soil Sci. Soc. Am. J. 60, 121–131.
Mansouri, A.I., Mirzaei, M., Afzali, D., Ganjavie, F., 2011. Catalytic spectrophotometric determination of Mo(VI) in water samples using 4-amino-3-hydroxy-naphthalene sulfonic acid. Arab. J. Chem. http://dx.doi.org/10.1016/j.arabjc.2011.12.009.
Marie, L., Pernet-Coudrier, B., Waeles, M., Gabon, M., Riso, R., 2015. Dynamics and sources of reduced sulfur, humic substances and dissolved organic carbon in a temperate river system affected by agricultural practices. Sci. Total Environ. 537, 23–32. http://dx.doi.org/10.1016/j.scitotenv.2015.07.089.
Marks, J.A., Perakis, S.S., King, E.K., Pett-Ridge, J., 2015. Soil organic matter regulates molybdenum storage and mobility in forests. Biogeochemistry 125, 167–183. http://dx.doi.org/10.1007/s10533-015-0121-4.
Matern, K., Mansfeldt, T., 2015. Molybdate adsorption by birnessite. Appl. Clay Sci. 108, 78–83. http://dx.doi.org/10.1016/j.clay.2015.01.024.
McKenzie, R.M., 1983. The adsorption of molybdenum on oxide surfaces. Aust. J. Soil Res. 21, 500–513. http://dx.doi.org/10.1071/SR9830505.
McManus, J., Berelson, W.M., Severmann, S., Poulson, R.L., Hammond, D.E., Klinkhammer, G.P., Holm, C., 2006. Molybdenum and uranium geochemistry in continental margin sediments: paleoproxy potential. Geochim. Cosmochim. Acta 70, 4643–4662.
Mendel, R.R., 2007. Biology of the molybdenum cofactor. J. Exp. Bot. 2289–2296. http://dx.doi.org/10.1093/jxb/erm024.
Miedaner, M.M., Weerasooriya, R., Tobschall, H.J., 2011. Molybdate interactions with gibbsite surfaces examined by macroscopic and cluster modeling. J. Geol. Soc. 14, 11–19.
Miller, C.A., Peucker-Ehrenbrink, B., Walker, B.D., Marcantonio, F., 2011. Re-assessing the surface cycling of molybdenum and rhenium. Geochim. Cosmochim. Acta 75, 7146–7179.
Misch, D., Gross, D., Huang, Q., Zaccarini, F., Sachsenhofer, R.F., 2016. Light and trace element composition of Carboniferous coals from the Donets Basin (Ukraine): an electron microprobe study. Int. J. Coal Geol. http://dx.doi.org/10.1016/j.coal.2016.06.004.
Mitchell, P.C.H., 1966. Oxo-species of molybdenum-(V) and -(VI). Q. Rev. Chem. Soc. 20, 103–118. http://dx.doi.org/10.1039/QR9662000103.
Mohajerin, T.J., Helz, G.R., Johannesson, K.H., 2016. Tungsten–molybdenum fractionation in estuarine environments. Geochim. Cosmochim. Acta 177, 105–119. http://dx.doi.org/10.1016/j.gca.2015.12.030.
Morford, J.L., Emerson, S.R., Breckel, E.J., Kim, S.H., 2005. Diagenesis of oxyanions (V, U, Re, and Mo) in pore waters and sediments from a continental margin. Geochim. Cosmochim. Acta 69, 5021–5032. http://dx.doi.org/10.1016/j.gca.2005.05.015.
Morford, J.L., Martin, W.R., Kalnejais, L.H., François, R., Bothner, M., Karle, I.-M., 2007. Insights on geochemical cycling of U, Re and Mo from seasonal sampling in Boston Harbor, Massachusetts, USA. Geochim. Cosmochim. Acta 71, 895–917. http://dx.doi.org/10.1016/j.gca.2006.10.016.
Morrison, S.J., Mushovic, P.S., Niesen, P.L., 2006. Early breakthrough of molybdenum and uranium in a permeable reactive barrier. Environ. Sci. Technol. 40,

2018–2024.
Morrison, S.J., Spangler, R.R., 1992. Extraction of uranium and molybdenum from aqueous-solutions - a survey of industrial materials for use in chemical barriers for uranium mill tailings remediation. Environ. Sci. Technol. 26, 1922–1931. http://dx.doi.org/10.1021/es00034a007.
Mortvedt, J.J., 1997. Sources and methods for molybdenum fertilization of crops. In: Molybdenum in Agriculture. Cambridge University Press, Cambridge, pp. 171–181.
Müller, A., Serain, C., 2000. Soluble Molybdenum Blues "des Pudels Kern". Acc. Chem. Res. 33, 2–10. http://dx.doi.org/10.1021/ar9601510.
Nagai, Y., Yokoyama, T., 2014. Chemical separation of Mo and W from terrestrial and extraterrestrial samples via anion exchange chromatography. Anal. Chem. 86, 4856–4863. http://dx.doi.org/10.1021/ac404223t.
Nägler, T.F., Anbar, A.D., Archer, C., Goldberg, T., Gordon, G.W., Greber, N.D., Siebert, C., Sohrin, Y., Vance, D., 2014. Proposal for an international molybdenum isotope measurement standard and data representation. Geostand. Geoanal. Res. 38, 149–151. http://dx.doi.org/10.1111/j.1751-908X.2013.00275.x.
Nägler, T.F.F., Neubert, N., Böttcher, M.E.E., Dellwig, O., Schnetger, B., 2011. Molybdenum isotope fractionation in pelagic euxinia: evidence from the modern Black and Baltic Seas. Chem. Geol. 289, 1–11. http://dx.doi.org/10.1016/j.chemgeo.2011.07.001.
Nakamura, I., Miras, H.N., Fujiwara, A., Fujibayashi, M., Song, Y.-F., Cronin, L., Tsunashima, R., 2015. Investigating the formation of "molybdenum blues" with gel electrophoresis and mass spectrometry. J. Am. Chem. Soc. 137, 6524–6530. http://dx.doi.org/10.1021/ja512758j.
National Academy of Sciences, 1989. Recommended Dietary Allowances, tenth ed. National Academy Press, Washington DC.
Nduna, M.K., Lewis, A.E., Nortier, P., 2014. A model for the zeta potential of copper sulphide. Colloids Surf. Physicochem. Eng. Asp. 441, 643–652. http://dx.doi.org/10.1016/j.colsurfa.2013.10.024.
Neal, C., Davies, H., 2003. Water quality fluxes for eastern UK rivers entering the North Sea: a summary of information from the Land Ocean Interaction Study (LOIS). Sci. Total Environ. 314, 821–882. http://dx.doi.org/10.1016/S0048-9697(03)00086-X.
Neal, C., Jarvie, H.P., Williams, R.J., Pinder, L.C.V.C.V., Collett, G.D., Neal, M., Bhardwaj, L.C., 2000a. The water quality of the Great Ouse. Sci. Total Environ. 251/252, 423–440. http://dx.doi.org/10.1016/S0048-9697(00)00420-4.
Neal, C., Neal, M., Ryland, G.P., Jeffery, H.A., Harrow, M., Hill, S., Smith, C.J., 1994. Chemical variations in near surface drainage water for an acidic spruce forested UK upland area subjected to timber harvesting: inferences on cation exchange processes in the soil. Sci. Total Environ. 154, 47–61.
Neal, C., Reynolds, B., Wilkinson, J., Hill, T., Neal, M., Hill, S., Harrow, M., 1998. The impacts of conifer harvesting on runoff water quality: a regional survey for Wales. Hydrol. Earth Syst. Sci. 2, 323–344.
Neal, C., Robson, A.J., 2000. A summary of river water quality data collected within the Land-Ocean interaction study: core data for eastern UK rivers draining the North Sea. Sci. Total Environ. 251/252, 585–665. http://dx.doi.org/10.1016/S0048-9697(00)00397-1.
Neal, C., Williams, R.J., Neal, M., Bhardwaj, L.C., Wickham, H., Harrow, M., Hill, L.K., 2000b. The water quality of the River Thames at a rural site downstream of Oxford. Sci. Total Environ. 251–252, 441–457. http://dx.doi.org/10.1016/S0048-9697(00)00398-3.
Neubert, N., Nägler, T.F., Böttcher, M.E., 2008. Sulfidity controls molybdenum isotope fractionation into euxinic sediments: evidence from the modern Black Sea. Geology 36, 775–778. http://dx.doi.org/10.1130/G24959A.1.
Nicolli, H.B., Bundschuh, J., Blanco, M., del, C., Tujchneider, O.C., Panarello, H.O., Dapeña, C., Rusansky, J.E., 2012a. Arsenic and associated trace-elements in groundwater from the Chaco-Pampean plain, Argentina: results from 100 years of research. Sci. Total Environ. 429, 36–56. http://dx.doi.org/10.1016/j.scitotenv.2012.04.048.
Nicolli, H.B., García, J.W., Falcón, C.M., Smedley, P.L., 2012b. Mobilization of arsenic and other trace elements of health concern in groundwater from the Salí River Basin, Tucumán Province, Argentina. Environ. Geochem. Health 34, 251–262. http://dx.doi.org/10.1007/s10653-011-9429-8.
Nicolli, H.B., Suriano, J.M., Gomez Peral, M.A., Ferpozzi, L.H., Baleani, O.A., 1989. Groundwater contamination with arsenic and other trace elements in an area of the pampa, province of Córdoba, Argentina. Environ. Geol. Water Sci. 14, 3–16. http://dx.doi.org/10.1007/BF01740581.
Nicolli, H.B., Tineo, A., Falcón, C.M., García, J.W., Merino, M.H., Etchichury, M.C., Alonso, M.S., Tofalo, O.R., 2008. Arsenic hydrogeochemistry in groundwater from the Burruyacú basin, Tucumán province, Argentina. In: Bundschuh, J., Armienta, M.A., Birkle, P., Bhattacharya, P., Matschullat, J., Mukherjee, A.B. (Eds.), Natural Arsenic in Groundwaters of Latin America, Arsenic in the Environment. CRC Press, Boca Raton, pp. 47–59.
Noordmann, J., Weyer, S., Montoya-Pino, C., Dellwig, O., Neubert, N., Eckert, S., Paetzel, M., Böttcher, M.E., 2015. Uranium and molybdenum isotope systematics in modern euxinic basins: case studies from the central Baltic Sea and the Kyllaren fjord (Norway). Chem. Geol. 396, 182–195. http://dx.doi.org/10.1016/j.chemgeo.2014.12.012.
Nordstrom, D.K., 2015. Baseline and premining geochemical characterization of mined sites. Appl. Geochem 57, 17–34. http://dx.doi.org/10.1016/j.apgeochem.2014.12.010.
Och, L.M., Shields-Zhou, G.A., Poulton, S.W., Manning, C., Thirlwall, M.F., Li, D., Chen, X., Ling, H., Osborn, T., Cremonese, L., 2013. Redox changes in early Cambrian black shales at Xiaotan section, Yunnan Province, south China. Precambrian Res. 225, 166–189. http://dx.doi.org/10.1016/j.precamres.2011.10.005.
Olson, G.J., Clark, T.R., 2008. Bioleaching of molybdenite. Hydrometallurgy 93, 10–15. http://dx.doi.org/10.1016/j.hydromet.2008.02.013.
Ono, S., Kaufman, A.J., Farquhar, J., Sumner, D.Y., Beukes, N.J., 2009. Lithofacies control on multiple-sulfur isotope records and Neoarchean sulfur cycles. Precambrian Res. 169, 58–67. http://dx.doi.org/10.1016/j.precamres.2008.10.013.
Oyerinde, O.F., Weeks, C.L., Anbar, A.D., Spiro, T.G., 2008. Solution structure of molybdic acid from Raman spectroscopy and DFT analysis. Inorg. Chim. Acta 361, 1000–1007. http://dx.doi.org/10.1016/j.ica.2007.06.025.
Paces, T., Corcho Alvarado, J.A., Herrmann, Z., Kodes, V., Muzak, J., Novák, J., Purtschert, R., Remenarova, D., Valecka, J., 2009. The Cenomanian and Turonian aquifers of the Bohemian Cretaceous Basin, Czech Republic. In: Edmunds, W.M., Shand, P. (Eds.), Natural Groundwater Quality. Blackwell Publishing, pp. 372–390.
Panther, J.G., Stewart, R.R., Teasdale, P.R., Bennett, W.W., Welsh, D.T., Zhao, H., 2013. Titanium dioxide-based DGT for measuring dissolved As(V), V(V), Sb(V), Mo(VI) and W(VI) in water. Talanta 105, 80–86.
Parkhurst, D.L., Appelo, C.A.J., 2013. Description of Input and Examples for PHREEQC Version 3–A Computer Program for Speciation, Batch-reaction, One-dimensional Transport, and Inverse Geochemical Calculations, Techniques and Methods. U.S. Geological Survey Techniques and Methods book 6, chap. A43, pp. 497.
Parnell, J., Brolly, C., Spinks, S., Bowden, S., 2016. Selenium enrichment in Carboniferous Shales, Britain and Ireland: problem or opportunity for shale gas extraction? Appl. Geochem 66, 82–87. http://dx.doi.org/10.1016/j.apgeochem.2015.12.008.
Parnell, J., Lindgren, P., 2016. Anomalous supply of bioessential molybdenum in mid-Proterozoic surface environments. Precambrian Res. 275, 100–104. http://dx.doi.org/10.1016/j.precamres.2015.12.016.
Parnell, J., Spinks, S., Andrews, S., Thayalan, W., Bowden, S., 2015. High Molybdenum availability for evolution in a Mesoproterozoic lacustrine environment. Nat. Commun. 6, 6996.
Pelit, L., Kocak, S., Pelit, F.O., Turkmen, H., Ertas, F.N., 2013. A spectrophotometric method for determination of molybdenum in water samples by using pyrogallol red and a water soluble ionic liquid. Anal. Methods 5, 5792–5798. http://dx.doi.org/10.1039/C3AY40772A.
Pichler, T., Mozaffari, A., 2015. Distribution and mobility of geogenic molybdenum and arsenic in a limestone aquifer matrix. Appl. Geochem 63, 623–633. http://dx.doi.org/10.1016/j.apgeochem.2015.08.006.
Pichler, T., Renshaw, C.E., Sültenfuß, J., 2017. Geogenic As and Mo groundwater contamination caused by an abundance of domestic supply wells. Appl. Geochem 77, 68–79. http://dx.doi.org/10.1016/j.apgeochem.2016.03.002.
Pietruszka, A.J., Walker, R.J., Candela, P.A., 2006. Determination of mass-dependent molybdenum isotopic variations by MC-ICP-MS: an evaluation of matrix effects. Chem. Geol. 225, 121–136.
Popov, S.I., Stafilov, T., Sajn, R., Tanaselia, C., Baceva, K., 2014. Applying of factor analyses for determination of trace elements distribution in water from river Vardar and its tributaries, Macedonia/Greece. Sci. World J. http://dx.doi.org/10.1155/2014/809253.
Prieto, M., Astilleros, J.M., Fernández-Díaz, L., 2013. Environmental remediation by crystallization of solid solutions. Elements 9, 195–201. http://dx.doi.org/10.2113/gselements.9.3.195.
Rahaman, W., Singh, S.K., Raghav, S., 2010. Dissolved Mo and U in rivers and estuaries of India: implication to geochemistry of redox sensitive elements and their marine budgets. Chem. Geol. 278, 160–172. http://dx.doi.org/10.1016/j.chemgeo.2010.09.009.
Rango, T., Bianchini, G., Beccaluva, L., Tassinari, R., 2010. Geochemistry and water quality assessment of central Main Ethiopian Rift natural waters with emphasis on source and occurrence of fluoride and arsenic. J. Afr. Earth Sci. 57, 479–491. http://dx.doi.org/10.1016/j.jafrearsci.2009.12.005.
Rango, T., Vengosh, A., Dwyer, G., Bianchini, G., 2013. Mobilization of arsenic and other naturally occurring contaminants in groundwater of the Main Ethiopian Rift aquifers. Water Res. 47, 5801–5818. http://dx.doi.org/10.1016/j.watres.2013.07.002.
Rawlins, B.G., McGrath, S.P., Scheib, A.J., Breward, N., Cave, M., Lister, T.R., Ingham, M., Gowing, C., Carter, S., 2012. The Advanced Soil Geochemical Atlas of England and Wales. British Geological Survey, Keyworth, Nottingham. http://www.bgs.ac.uk/gbase/advsoilatlasEW.html.
Reddy, K.J., Wang, L., Lindsay, W.L., 1990. Molybdenum Supplement to Technical Bulletin 134: Selection of Standard Free Energies of Formation for Use in Soil Chemistry. Colorado State University.
Reimann, C., Bjorvatn, K., Frengstad, B., Melaku, Z., Tekle-Haimanot, R., Siewers, U., 2003. Drinking water quality in the Ethiopian section of the East African Rift Valley I - data and health aspects. Sci. Total Environ. 311, 65–80. http://dx.doi.org/10.1016/s0048-9697(03)00137-2.
Reimann, C., de Caritat, P., 1998. Chemical Elements in the Environment. Factsheets for the Geochemist and Environmental Scientist. Springer-Verlag, Berlin.
Reisenauer, H.M., Tabikh, A.A., Stout, P.R., 1962. Molybdenum reactions with soils and the hydrous oxides of iron, aluminum, and titanium. Soil Sci. Soc. Am. J. 26 http://dx.doi.org/10.2136/sssaj1962.03615995002600010007x.
Rietra, R.P.J., Hiemstra, T., van Riemsdijk, W.H., 1999. The relationship between molecular structure and ion adsorption on variable charge minerals. Geochim. Cosmochim. Acta 63, 3009–3015. http://dx.doi.org/10.1016/S0016-7037(99)00228-8.

Robertson, F., 1989. Arsenic in groundwater under oxidizing conditions, south-west United-States. Environ. Geochem. Health 11, 171–185. http://dx.doi.org/10.1007/BF01758668.

Rodriguez-Freire, L., Avasarala, S., Ali, A.-M.S., Agnew, D., Hoover, J.H., Artyushkova, K., Latta, D.E., Peterson, E.J., Lewis, J., Crossey, L.J., Brearley, A.J., Cerrato, J.M., 2016. Post gold King mine spill investigation of metal stability in water and sediments of the Animas River watershed. Environ. Sci. Technol. 50, 11539–11548. http://dx.doi.org/10.1021/acs.est.6b03092.

Romaniello, S.J., Herrmann, A.D., Anbar, A.D., 2016. Syndepositional diagenetic control of molybdenum isotope variations in carbonate sediments from the Bahamas. Chem. Geol. 438, 84–90. http://dx.doi.org/10.1016/j.chemgeo.2016.05.019.

Rowland, H.A.L., Omoregie, E.O., Millot, R., Jimenez, C., Mertens, J., Baciu, C., Hug, S.J., Berg, M., 2011. Geochemistry and arsenic behaviour in groundwater resources of the Pannonian Basin (Hungary and Romania). Appl. Geochem 26, 1–17. http://dx.doi.org/10.1016/j.apgeochem.2010.10.006.

Ryden, J.C., Syers, J.K., Tillman, R.W., 1987. Inorganic anion sorption and interactions with phosphate sorption by hydrous ferric oxide gel. J. Soil Sci. 38, 211–217. http://dx.doi.org/10.1111/j.1365-2389.1987.tb02138.x.

Salminen, R. (Ed.), 2005. Geochemical Atlas of Europe, Part 1: Background Information, Methodology and Maps. Geological Survey of Finland, Otamedia Oy, Espoo.

Sánchez España, J., González Toril, E., López Pamo, E., Amils, R., Diez Ercilla, M., Santofimia Pastor, E., San Martín-Úriz, P., 2008. Biogeochemistry of a hyperacidic and ultraconcentrated pyrite leachate in San Telmo mine (Iberian Pyrite Belt, Spain). Water. Air. Soil Pollut. 194, 243–257. http://dx.doi.org/10.1007/s11270-008-9713-0.

Saripalli, K.P., McGrail, B.P., Girvin, D.C., 2002. Adsorption of molybdenum on to anatase from dilute aqueous solutions. Appl. Geochem 17, 649–656. http://dx.doi.org/10.1016/S0883-2927(01)00127-5.

Scheiderich, K., Helz, G.R., Walker, R.J., 2010. Century-long record of Mo isotopic composition in sediments of a seasonally anoxic estuary (Chesapeake Bay). Earth Planet. Sci. Lett. 289, 189–197. http://dx.doi.org/10.1016/j.epsl.2009.11.008.

Schettler, G., Oberhänsli, H., Stulina, G., Mavlonov, A.A., Naumann, R., 2013. Hydrochemical water evolution in the aral Sea Basin. Part I: unconfined groundwater of the Amu Darya Delta – interactions with surface waters. J. Hydrol. 495, 267–284. http://dx.doi.org/10.1016/j.jhydrol.2013.03.044.

Schlieker, M., Schuring, J., Hencke, J., Schulz, H.D., 2001. The influence of redox processes on trace element mobility in a sandy aquifer–an experimental approach. J. Geochem. Explor 73, 167–179.

Schneider, A.B., Koschinsky, A., Kiprotich, J., Poehle, S., do Nascimento, P.C., 2016. An experimental study on the mixing behavior of Ti, Zr, V and Mo in the Elbe, Rhine and Weser estuaries. Estuar. Coast. Shelf Sci. 170, 34–44. http://dx.doi.org/10.1016/j.ecss.2015.12.002.

Schwarz, G., Mendel, R.R., Ribbe, M.W., 2009. Molybdenum cofactors, enzymes and pathways. Nature 460, 839–847. http://dx.doi.org/10.1038/nature08302.

Scott, C., Lyons, T., Bekker, A., Shen, Y., Poulton, S., Chu, X., Anbar, A., 2008. Tracing the stepwise oxygenation of the Proterozoic ocean. Nature 452, 456–459.

Scott, C., Lyons, T.W., 2012. Contrasting molybdenum cycling and isotopic properties in euxinic versus non-euxinic sediments and sedimentary rocks: Refining the paleoproxies. Chem. Geol. 324–325, 19–27. http://dx.doi.org/10.1016/j.chemgeo.2012.05.012.

Seal II, R.R., 2012. Geologic and environmental characteristics of porphyry copper deposits with emphasis on potential future development in the Bristol Bay watershed, Alaska, in: An Assessment Of Potential Mining Impacts On Salmon Ecosystems Of Bristol Bay, Alaska.

Shen, X.Y., Du, G.Z., Li, H., 2006. Studies of a naturally occurring molybdenum-induced copper deficiency in the yak. Vet. J. 171, 352–357.

Shimmield, G.B., Price, N.B., 1986. The behaviour of molybdenum and manganese during early sediment diagenesis — offshore Baja California, Mexico. Mar. Chem. 19, 261–280. http://dx.doi.org/10.1016/0304-4203(86)90027-7.

Shiva, A.H., Bennett, W.W., Welsh, D.T., Teasdale, P.R., 2016. In situ evaluation of DGT techniques for measurement of trace metals in estuarine waters: a comparison of four binding layers with open and restricted diffusive layers. Environ. Sci. Process. Impacts 18, 51–63. http://dx.doi.org/10.1039/c5em00550g.

Shukor, M., Rahman, M., Suhaili, Z., Shamaan, N., Syed, M., 2010. Hexavalent molybdenum reduction to Mo-blue by Acinetobacter calcoaceticus. Folia Microbiol. (Praha) 55, 137–143.

Siebert, C., McManus, J., Bice, A., Poulson, R., Berelson, W.M., 2006. Molybdenum isotope signatures in continental margin marine sediments. Earth Planet. Sci. Lett. 241, 723–733. http://dx.doi.org/10.1016/j.epsl.2005.11.010.

Siebert, C., Moller, P., Geyer, S., Kraushaar, S., Dulski, P., Guttman, J., Subah, A., Rodiger, T., 2014. Thermal waters in the Lower Yarmouk Gorge and their relation to surrounding aquifers. Chem. Erde 74, 425–441.

Siebert, C., Nägler, T.F., von Blanckenburg, F., Kramers, J.D., 2003. Molybdenum isotope records as a potential new proxy for paleoceanography. Earth Planet. Sci. Lett. 211, 159–171. http://dx.doi.org/10.1016/S0012-821X(03)00189-4.

Siebert, C., Pett-Ridge, J., Opfergelt, S., Guicharnaud, R., Halliday, A., Burton, K., 2015. Molybdenum isotope fractionation in soils: influence of redox conditions, organic matter, and atmospheric inputs. Geochim. Cosmochim. Acta 162, 1–24.

Skierszkan, E.K., Mayer, K.U., Weis, D., Beckie, R.D., 2016. Molybdenum and zinc stable isotope variation in mining waste rock drainage and waste rock at the Antamina mine. Peru. Sci. Total Environ. 550, 103–113. http://dx.doi.org/10.1016/j.scitotenv.2016.01.053.

Slomp, C.P., Gaast, S.J.V., der, Raaphorst, W.V., 1996. Phosphorus binding by poorly crystalline iron oxides in North Sea sediments. Mar. Chem. 52, 55–73. http://dx.doi.org/10.1016/0304-4203(95)00078-X.

Smedley, P., Edmunds, W., 2002. Redox patterns and trace-element behavior in the East Midlands Triassic sandstone aquifer, UK. Ground Water 40, 44–58. http://dx.doi.org/10.1111/j.1745-6584.2002.tb02490.x.

Smedley, P.L., Cooper, D.M., Ander, E.L., Milne, C.J., Lapworth, D.J., 2014a. Occurrence of molybdenum in British surface water and groundwater: distributions, controls and implications for water supply. Appl. Geochem 40, 144–154. http://dx.doi.org/10.1016/j.apgeochem.2013.03.014.

Smedley, P.L., Cooper, D.M., Lapworth, D.J., 2014b. Molybdenum distributions and variability in drinking water from England and Wales. Environ. Monit. Assess. 186, 6403–6416.

Smedley, P.L., Kinniburgh, D.G., 2002. A review of the source, behaviour and distribution of arsenic in natural waters. Appl. Geochem 17, 517–568.

Smedley, P.L., Kinniburgh, D.G., Macdonald, D.M.J., Nicolli, H.B., Barros, A.J., Tullio, J.O., Pearce, J.M., Alonso, M.S., 2005. Arsenic associations in sediments from the loess aquifer of La Pampa, Argentina. Appl. Geochem 20, 989–1016.

Smedley, P.L., Knudsen, J., Maiga, D., 2007. Arsenic in groundwater from mineralised Proterozoic basement rocks of Burkina Faso. Appl. Geochem 22, 1074–1092. http://dx.doi.org/10.1016/j.apgeochem.2007.01.001.

Smedley, P.L., Nicolli, H.B., 2014. Molybdenum distributions and controls in groundwater from the Pampean aquifer of La Pampa Province, Argentina. In: Viswanathan, S.S., Lopatin, S.I. (Eds.), Molybdenum and its Compounds: Applications, Electrochemical Properties and Geological Implications. Nova Publishers, USA, pp. 399–416.

Smedley, P.L., Nicolli, H.B., Macdonald, D.M.J., Barros, A.J., Tullio, J.O., 2002. Hydrogeochemistry of arsenic and other inorganic constituents in groundwaters from La Pampa, Argentina. Appl. Geochem 17, 259–284. http://dx.doi.org/10.1016/S0883-2927(01)00082-8.

Smedley, P.L., Zhang, M., Zhang, G., Luo, Z., 2003. Mobilisation of arsenic and other trace elements in fluviolacustrine aquifers of the Huhhot Basin, Inner Mongolia. Appl. Geochem 18, 1453–1477. http://dx.doi.org/10.1016/S0883-2927(03)00062-3.

Smedley, P.L., Bearcock, J.M., Fordyce, F.M., Everett, P.A., Chenery, S., Ellen, R., 2017. Stream Water Geochemical Atlas of the Clyde Basin (No. OR/16/015). British Geological Survey, Keyworth, Nottingham.

Smyth, D., 2007. Methods Used in the Tellus Geochemical Mapping of Northern Ireland, Open Report OR/07/022. British Geological Survey, Keyworth.

Sohrin, Y., Isshiki, K., Kuwamoto, T., Nakayama, E., 1987. Tungsten in north Pacific waters. Mar. Chem. 22, 95–103. http://dx.doi.org/10.1016/0304-4203(87)90051-x.

Spanos, N., Matralis, H.K., Kordulis, C., Lycourghiotis, A., 1992. Molybdenum-oxo species deposited on titania by adsorption: mechanism of the adsorption and characterization of the calcined samples. J. Catal. 136, 432–445. http://dx.doi.org/10.1016/0021-9517(92)90074-R.

Spanos, N., Vordonis, L., Kordulis, C., Koutsoukos, P.G., Lycourghiotis, A., 1990. Molybdenum-oxo species deposited on alumina by adsorption. II. Regulation of the surface MoVI concentration by control of the protonated surface hydroxyls. J. Catal. 124, 315–323. http://dx.doi.org/10.1016/0021-9517(90)90180-R.

Spence, J.T., Heydanek, M., 1967. Formation and dimerization of molybdenum(V) monomer in aqueous solution. Inorg. Chem. 6, 1489–1492. http://dx.doi.org/10.1021/ic50054a013.

Stensvold, K.A., 2012. Distribution and Variation of Arsenic in Wisconsin Surface Soils, with Data on Other Trace Elements. Scientific Investigations Report 2011-5202. U.S. Geological Survey.

Stiefel, E.I., 1996. Molybdenum bolsters the bioinorganic brigade. Science 272, 1599–1600.

Stiefel, E.I., 1977. The coordination and bioinorganic chemistry of molybdenum. In: Lippiard, Stephen J. (Ed.), Progress in Inorganic Chemistry, vol. 22. John Wiley & Sons Inc, New York, pp. 1–224.

Suttle, N.F., 1991. The interactions between copper, molybdenum, and sulfur in ruminant nutrition. Annu. Rev. Nutr. 11, 121–140.

Taylor, H.E., Antweiler, R.C., Roth, D.A., Alpers, C.N., Dileanis, P., 2012. Selected trace elements in the Sacramento River, California: occurrence and distribution. Arch. Environ. Contam. Toxicol. 62, 557–569. http://dx.doi.org/10.1007/s00244-011-9738-z.

Taylor, S.R., 1964. Abundance of chemical elements in the continental crust: a new table. Geochim. Cosmochim. Acta 1273–1285.

Thomson, I., Thornton, I., Webb, J.S., 1972. Molybdenum in black shales and the incidence of bovine hypocuprosis. J. Sci. Food Agric. 23, 879–891. http://dx.doi.org/10.1002/jsfa.2740230709.

Thornton, I., Webb, J.S., 1979. Geochemistry and health in the United Kingdom. Philos. Trans. R. Soc. Lond. B. Biol. Sci. 288, 151–168.

Titley, S.R., 1963. Some behavioral aspects of molybdenum in the supergene environment. AIME Trans. 226, 199–204.

Tribovillard, N., Riboulleau, A., Lyons, T., Baudin, F.O., 2004. Enhanced trapping of molybdenum by sulfurized marine organic matter of marine origin in Mesozoic limestones and shales. Chem. Geol. 213, 385–401. http://dx.doi.org/10.1016/j.chemgeo.2004.08.011.

Tucker, M.D., Barton, L.L., Thomson, B.M., 1998. Reduction of Cr, Mo, Se and U by *Desulfovibrio desulfuricans* immobilized in polyacrylamide gels. J. Ind. Microbiol. Biotechnol. 20, 13–19. http://dx.doi.org/10.1038/sj.jim.2900472.

Tucker, M.D., Barton, L.L., Thomson, B.M., 1997. Reduction and immobilization of molybdenum by *Desulfovibrio desulfuricans*. J. Environ. Qual. 26, 1146–1152.

http://dx.doi.org/10.2134/jeq1997.00472425002600040029x.
Vallee, T.I., 2009. Geochemistry of Molybdenum in the Aquia Aquifer, Maryland, USA. University of Texas at Arlington.
Ventura, G.T., Gall, L., Siebert, C., Prytulak, J., Szatmari, P., Hürlimann, M., Halliday, A.N., 2015. The stable isotope composition of vanadium, nickel, and molybdenum in crude oils. Appl. Geochem 59, 104–117.
Verbinnen, B., Block, C., Hannes, D., Lievens, P., Vaclavikova, M., Stefusova, K., Gallios, G., Vandecasteele, C., 2012. Removal of molybdate anions from water by adsorption on zeolite-supported magnetite. Water Environ. Res. 84, 753–760. http://dx.doi.org/10.2175/106143012X13373550427318.
Villalobos, M., Toner, B., Bargar, J., Sposito, G., 2003. Characterization of the manganese oxide produced by *Pseudomonas putida* strain MnB1. Geochim. Cosmochim. Acta 67, 2649–2662.
Vistoso, E., Theng, B.K.G., Bolan, N.S., Parfitt, R.L., Mora, M.L., 2012. Competitive sorption of molybdate and phosphate in Andisols. J. Soil Sci. Plant Nutr. 12, 59–72.
Vlek, P.L.G., Lindsay, W.L., 1977. Thermodynamic stability and solubility of molybdenum minerals in soils. Soil Sci. Soc. Am. J. 41, 42–46. http://dx.doi.org/10.2136/sssaj1977.03615995004100010016x.
Voegelin, A.R., Nägler, T.F., Pettke, T., Neubert, N., Steinmann, M., Pourret, O., Villa, I.M., 2012. The impact of igneous bedrock weathering on the Mo isotopic composition of stream waters: natural samples and laboratory experiments. Geochim. Cosmochim. Acta 86, 150–165. http://dx.doi.org/10.1016/j.gca.2012.02.029.
Voegelin, A.R., Pettke, T., Greber, N.D., Niederhäusern, B., von, Nägler, T.F., 2014. Magma differentiation fractionates Mo isotope ratios: evidence from the Kos plateau tuff (Aegean arc). Lithos 190–191, 440–448. http://doi.org/10.1016/j.lithos.2013.12.016.
Voegelin, A.R.A., Nägler, T.F.T., Samankassou, E., Villa, I.I.M., 2009. Molybdenum isotopic composition of modern and Carboniferous carbonates. Chem. Geol. 265, 488–498. http://dx.doi.org/10.1016/j.chemgeo.2009.05.015.
Voigt, W., Brendler, V., Marsh, K., Rarey, R., Wanner, H., Gaune-Escard, M., Cloke, P., Vercouter, T., Bastrakov, E., Hagemann, S., 2007. Quality assurance in thermodynamic databases for performance assessment studies in waste disposal. Pure Appl. Chem. 79, 883–894.
Vorlicek, T.P., Chappaz, A., Groskreutz, L.M., Young, N., Lyons, T.W., 2015. A new analytical approach to determining Mo and Re speciation in sulfidic waters. Chem. Geol. 403, 52–57. http://dx.doi.org/10.1016/j.chemgeo.2015.03.003.
Vorlicek, T.P., Helz, G.R., 2002. Catalysis by mineral surfaces: implications for Mo geochemistry in anoxic environments. Geochim. Cosmochim. Acta 66, 3679–3692.
Vorlicek, T.P., Kahn, M.D., Kasuya, Y., Helz, G.R., 2004. Capture of molybdenum in pyrite-forming sediments: role of ligand-induced reduction by polysulfides. Geochim. Cosmochim. Acta 68, 547–556.
Waheed, S., Ahmad, S., Rahman, A., Qureshi, I.H., 2001. Antarctic marine sediments as fingerprints of pollution migration. J. Radioanal. Nucl. Chem. 250, 97–107.
Wahl, B., Reichmann, D., Niks, D., Krompholz, N., Havemeyer, A., Clement, B., Messerschmidt, T., Rothkegel, M., Biester, H., Hille, R., Mendel, R.R., Bittner, F., 2010. Biochemical and spectroscopic characterization of the human mitochondrial amidoxime reducing components hmARC-1 and hmARC-2 suggests the existence of a new molybdenum enzyme family in eukaryotes. J. Biol. Chem. 26, 37847–37859.
Wang, D., 2012. Redox chemistry of molybdenum in natural waters and its involvement in biological evolution. Front. Microbiol. 3, 18–24. http://dx.doi.org/10.3389/fmicb.2012.00427.
Wang, D., Aller, R.C., Sañudo-Wilhelmy, S.A., 2009. A new method for the quantification of different redox-species of molybdenum (V and VI) in seawater. Mar. Chem. 113, 250–256. http://dx.doi.org/10.1016/j.marchem.2009.02.007.
Wang, D.L., Aller, R.C., Sanudo-Wilhelmy, S.A., 2011. Redox speciation and early diagenetic behavior of dissolved molybdenum in sulfidic muds. Mar. Chem. 125, 101–107. http://dx.doi.org/10.1016/j.marchem.2011.03.002.
Wang, F., Tessier, A., 2009. Zero-valent sulfur and metal speciation in sediment porewaters of freshwater lakes. Env. Sci. Technol. 43 http://dx.doi.org/10.1021/es8034973.
Wang, P., Wilson, L.L., Wesolowski, D.J., Rosenqvist, J., Anderko, A., 2010. Solution chemistry of Mo(III) and Mo(IV): thermodynamic foundation for modeling localized corrosion. Corros. Sci. 52, 1625–1634. http://dx.doi.org/10.1016/j.corsci.2010.01.032.
Wang, Z., Ma, J., Li, J., Wei, G., Chen, X., Deng, W., Xie, L., Lu, W., Zou, L., 2015. Chemical weathering controls on variations in the molybdenum isotopic composition of river water: evidence from large rivers in China. Chem. Geol. 410, 201–212. http://dx.doi.org/10.1016/j.chemgeo.2015.06.022.
Wasylenki, L.E., Anbar, A.D., Liermann, L.J., Mathur, R., Gordon, G.W., Brantley, S.L., 2007. Isotope fractionation during microbial metal uptake measured by MC-ICP-MS. J. Anal. At. Spectrom. 22, 905–910. http://dx.doi.org/10.1039/b705476a.
Wasylenki, L.E., Rolfe, B.A., Weeks, C.L., Spiro, T.G., Anbar, A.D., 2008. Experimental investigation of the effects of temperature and ionic strength on Mo isotope fractionation during adsorption to manganese oxides. Geochim. Cosmochim. Acta 72, 5997–6005. http://dx.doi.org/10.1016/j.gca.2008.08.027.
Wasylenki, L.E., Weeks, C.L., Bargar, J.R., Spiro, T.G., Hein, J.R., Anbar, A.D., 2011. The molecular mechanism of Mo isotope fractionation during adsorption to birnessite. Geochim. Cosmochim. Acta 75, 5019–5031. http://dx.doi.org/10.1016/j.gca.2011.06.020.
Wedepohl, K., 1995. The composition of the continental crust. Geochim. Cosmochim. Acta 59, 1217–1232.
Wen, H., Fan, H., Zhang, Y., Cloquet, C., Carignan, J., 2015. Reconstruction of early Cambrian ocean chemistry from Mo isotopes. Geochim. Cosmochim. Acta 164, 1–16. http://dx.doi.org/10.1016/j.gca.2015.05.008.
WHO, 2011a. Molybdenum in Drinking Water: Background Document for Development of WHO Guidelines for Drinking-water Quality (WHO/SDE/WSH/03.04/11/Rev/1). World Health Organization, Geneva, Switzerland.
WHO, 2011b. Guidelines for Drinking-water Quality, fourth ed. World Health Organization, Geneva.
Wichard, T., Mishra, B., Myneni, S.C.B., Bellenger, J.-P.P., Kraepiel, A.M.L., 2009. Storage and bioavailability of molybdenum in soils increased by organic matter complexation. Nat. Geosci. 2, 625–629. http://dx.doi.org/10.1038/ngeo589.
Wieser, M.E., Laeter, J.R.D., Varner, M.D., 2007. Isotope fractionation studies of molybdenum. Int. J. Mass Spectrom. 265, 40–48. http://dx.doi.org/10.1016/j.ijms.2007.05.010.
Wilde, P., Lyons, T.W., Quinby-Hunt, M.S., 2004. Organic carbon proxies in black shales: molybdenum. Chem. Geol. 206, 167–176.
Wilkinson, D.J., 2015. The Geochemistry of Eclogites from Western Norway: Implications from High-precision Whole-rock and Rutile Analyses (PhD). University of Edinburgh, Edinburgh.
Wirth, S.B., Gilli, A., Niemann, H., Dahl, T.W., Ravasi, D., Sax, N., Hamann, Y., Peduzzi, R., Peduzzi, S., Tonolla, M., Lehmann, M.F., Anselmetti, F.S., 2013. Combining sedimentological, trace metal (Mn, Mo) and molecular evidence for reconstructing past water-column redox conditions: the example of meromictic Lake Cadagno (Swiss Alps). Geochim. Cosmochim. Acta 120, 220–238. http://dx.doi.org/10.1016/j.gca.2013.06.017.
Worsham, E.A., Walker, R.J., Bermingham, K.R., 2016. High-precision molybdenum isotope analysis by negative thermal ionization mass spectrometry. Int. J. Mass Spectrom. 407, 51–61. http://dx.doi.org/10.1016/j.ijms.2016.06.005.
Wu, C.H., Kuo, C.Y., Lin, C.F., Lo, S.L., 2002. Modeling competitive adsorption of molybdate, sulfate, selenate, and selenite using a Freundlich-type multicomponent isotherm. Chemosphere 47, 283–292. http://dx.doi.org/10.1016/s0045-6535(01)00217-x.
Xu, N., Braida, W., Christodoulatos, C., Chen, J., 2013. A review of molybdenum adsorption in soils/bed sediments: speciation, mechanism, and model applications. Soil Sediment. Contam. Int. J. 22, 912–929. http://dx.doi.org/10.1080/15320383.2013.770438.
Xu, N., Christodoulatos, C., Braida, W., 2006a. Adsorption of molybdate and tetrathiomolybdate onto pyrite and goethite: effect of pH and competitive anions. Chemosphere 62, 1726–1735. http://dx.doi.org/10.1016/j.chemosphere.2005.06.025.
Xu, N., Christodoulatos, C., Braida, W., 2006b. Modeling the competitive effect of phosphate, sulfate, silicate, and tungstate anions on the adsorption of molybdate onto goethite. Chemosphere 64, 1325–1333.
Yang, J., Siebert, C., Barling, J., Savage, P., Liang, Y.-H., Halliday, A.N., 2015. Absence of molybdenum isotope fractionation during magmatic differentiation at Hekla volcano, Iceland. Geochim. Cosmochim. Acta 162, 126–136. http://dx.doi.org/10.1016/j.gca.2015.04.011.
Yang, N., Welch, K.A., Mohajerin, T.J., Telfeyan, K., Chevis, D.A., Grimm, D.A., Lyons, W.B., White, C.D., Johannesson, K.H., 2015. Comparison of arsenic and molybdenum geochemistry in meromictic lakes of the McMurdo Dry valleys, Antarctica: implications for oxyanion-forming trace element behavior in permanently stratified lakes. Chem. Geol. 404, 110–125. http://dx.doi.org/10.1016/j.chemgeo.2015.03.029.
Zerkle, A.L., Scheiderich, K., Maresca, J.A., Liermann, L.J., Brantley, S.L., 2011. Molybdenum isotope fractionation by cyanobacterial assimilation during nitrate utilization and N_2 fixation. Geobiology 9, 94–106. http://dx.doi.org/10.1111/j.1472-4669.2010.00262.x.
Zhang, M., Reardon, E.J., 2003. Removal of B, Cr, Mo, and Se from wastewater by incorporation into hydrocalumite and ettringite. Environ. Sci. Technol. 37, 2947–2952.
Zhang, P.C., Sparks, D.L., 1989. Kinetics and mechanisms of molybdate adsorption-desorption at the goethite-water interface using pressure-jump relaxation. Soil Sci. Soc. Am. J. 53, 1028–1034.
Zhang, X., Ma, J., Lu, X., Huangfu, X., Zou, J., 2015. High efficient removal of molybdenum from water by $Fe_2(SO_4)_3$: effects of pH and affecting factors in the presence of co-existing background constituents. J. Hazard. Mater 300, 823–829. http://dx.doi.org/10.1016/j.jhazmat.2015.08.026.
Zhao, J.M., Feng, Z., Huggins, F.E., Shah, N., Huffman, G.P., Wender, I., 1994. Role of molybdenum at the iron oxide surface. J. Catal. 148, 194–197. http://dx.doi.org/10.1006/jcat.1994.1200.
Zhao, Z., Liu, J., Xia, W., Cao, C., Chen, X., Li, H., 2010. Surface complexation modeling of soluble molybdenum adsorption by Mn_3O_4. J. Chem. Technol. Biotechnol. 85, 121–126. http://dx.doi.org/10.1002/jctb.2275.
Zhao, Z., Pei, J., Zhang, X., Zhou, X., 1990. Adsorptive stripping voltammetry determination of molybdenum(VI) in water and soil. Talanta 37, 1007–1010. http://dx.doi.org/10.1016/0039-9140(90)80141-2.
Zheng, Y., Anderson, R.F., van Geen, A., Kuwabara, J., 2000a. Authigenic molybdenum formation in marine sediments: a link to pore water sulfide in the Santa Barbara Basin. Geochim. Cosmochim. Acta 64, 4165–4178. http://dx.doi.org/10.1016/s0016-7037(00)00495-6.
Zheng, Y., van Geen, A., Anderson, R.F., Gardner, J.V., Dean, W.E., 2000b. Intensification of the northeast Pacific oxygen minimum zone during the Bolling-Allerod warm period. Paleoceanography 15, 528–536. http://dx.doi.org/10.1029/1999pa000473.